

THE AUBORUS FORMATION

OF THE

BETHANIE DISTRICT

SOUTH WEST AFRICA

BY

R. McG. MILLER

1969

Thesis submitted in fulfilment of the requirements
of the degree of M.Sc, University of Cape Town

The copyright of this thesis vests in the author. No quotation from it or information derived from it is to be published without full acknowledgement of the source. The thesis is to be used for private study or non-commercial research purposes only.

Published by the University of Cape Town (UCT) in terms of the non-exclusive license granted to UCT by the author.

CONTENTS

	<u>Page</u>
ABSTRACT	
I. INTRODUCTION	1
II. TOPOGRAPHY	3
III. GENERAL STRATIGRAPHY	5
IV. STRUCTURE	8
1) General	8
2) Folding and Faulting	8
3) Joints	10
4) Pebble Fractures	11
V. SEDIMENTARY PETROGRAPHY	12
1) The Conglomerate	12
a) The Pebbles	14
b) The Matrix	16
2) The Sandstone	17
a) Microscopic Characteristics	18
b) Heavy mineral content	23
3) Sedimentary Structures	27
a) Cross-bedding and parting lineation	27
b) Ripple marks	31
c) Other structures	32
VI. THE SHAPE AND NATURE OF THE BASIN	34
VII. THE PROBLEM OF THE RED COLOUR	37
1) The Occurrence of Decoloration	40
VIII. THE CONDITIONS OF DEPOSITION	45
IX. SUMMARY	48
X. ACKNOWLEDGEMENTS	50
XI. REFERENCES	51

ABSTRACT

A study of the southerly occurrence of Auborus sediments revealed a basal conglomerate varying in thickness from 100 ft. to 3300 ft. and lying unconformably on an undulating base of lavas and sediments of the Sinclair Formation. This is overlain by variable thicknesses of sandstone which contain a few interbedded conglomerate bands, most of which are wedge-shaped. Intercalated grit is present in both the sandstone and the conglomerate zones. Shale occurs in the north-west where the sediments reach a thickness of 8500 ft. Nama sediments overlie the formation unconformably.

Deposition, after rapid erosion and decay, took place under warm humid conditions into a shallow, slowly subsiding, intracratonic basin. Inward dipping edges were produced by contemporaneous subsidence.

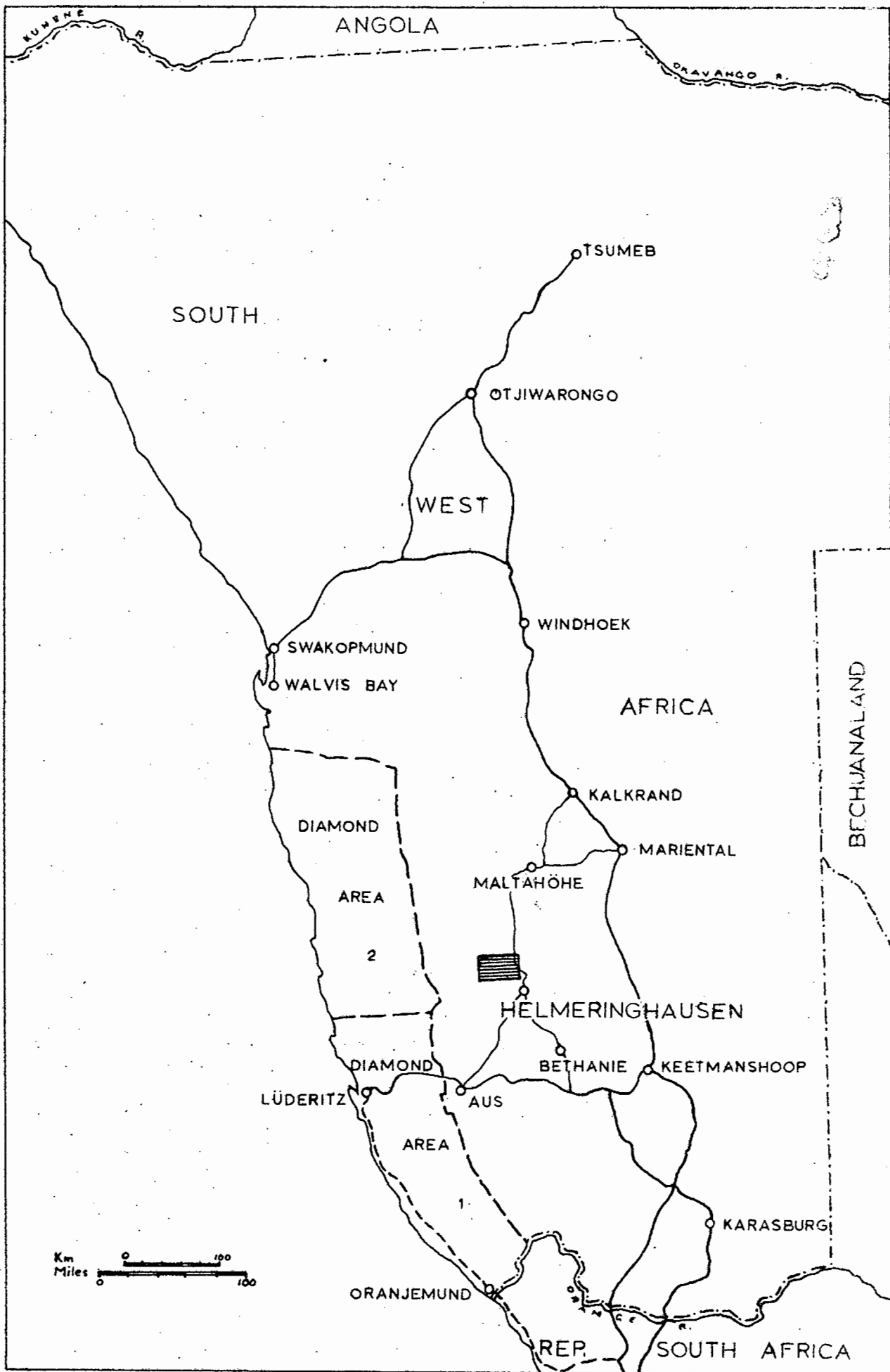
Vertical post-depositional movements in the central section folded the beds of the whole succession in the west into vertical and overturned positions. Block faulting that followed had a meridional trend and elevated this central section. Roughly north-trending faulting has displaced the contact in the south-east, and two later sets of east-west faults occur in the north-east. Diagonal, release and tension joints were revealed by measurement. Fracture planes in conglomerate pebbles apparently show no relationship to nearby faults.

Pebble, cobble and boulder conglomerates contain a great variety of rock types, which have mostly been identified as coming from nearby southerly sources. A matrix is always present. The sandstone is a uniform red colour, very fine-grained, well sorted, very well compacted and is feldspathic and arkosic in character. Rock fragments are ubiquitous. The colouring matter is intergranular, crystalline hematite.

Feldspars and biotite show various stages of alteration. A little recrystallization of quartz has taken place. The main heavy minerals are ore (largely specularite), garnet, epidote, zoisite, clinozoisite, mica, monazite, zircon and tourmaline. Zircon has been classified on colour, roundness, inclusions and zoning; tourmaline on colour, roundness and inclusions.

Bedding in the sandstone is from thin to laminated. The commonest sedimentary structures are cross-beds, mud cracks and clay-pellet impressions. Other features are ripple marks, parting lineations, flute casts and rain prints.

The red colour was probably produced in the source area. Diagenetic processes have produced spots of decoloration; and some joints show decoloration. Chemical analyses have been made of the red beds and a decolored spot.



LOCATION MAP OF AREA

I - INTRODUCTION

Helmeringhausen is a small settlement some 300 miles by road south of Windhoek, South West Africa. Approximately 20 miles north-west of Helmeringhausen are two areas underlain by sediments of the Auborus Formation which form the subject of this study; areas occupied by similar sediments farther north as far as the Zaris Mountains were not studied. The Auborus Formation is composed entirely of sediments: fine-grained sandstone with intercalated shale and conglomerate overlies a basal conglomerate. All the sediments are uniformly red in colour and form a basin-shaped outcrop with fairly gentle dips inward towards the centre. The basal conglomerate occurs throughout and grades upwards, by an increase in the number of sandstone lenses, into the overlying fine-grained sandstone. Wedge-shaped conglomerate bands occur higher up in this sandstone but none is very extensive. In the north-western section deep red shale occurs. This exhibits many ripple-marked bedding planes. Elsewhere sedimentary structures are locally abundant.

The present-day outcrop is in the form of two parallel north-south bands each between six and ten miles apart. North-south block faulting in the central portion has caused the elevation and removal by erosion of the up-faulted sediments, and has produced local steeply dipping beds in the two lateral portions. Prior to deformation the Auborus basin was probably pear-shaped but somewhat irregular with indentations on the farm Aubures (C5) and possibly Blutputz Ost (G2) as well. The axis was north-trending and the apex was in the north.

Reconnaissance work was done on the sediments by Beetz in 1922. He described the occurrences briefly, referring them to the Auborus Series of the "Konkip Formation", in which formation he also included the underlying Kunjas and Sinclair Formations. For the most part it is on the lavas of this latter formation that the Auborus sediments rest unconformably. On the farms Dabis (I7, J7, 8) and Guperas (H6) they rest on lavas and sediments of the Guperas Series of the Sinclair Formation. Detailed mapping does not favour the inclusion of the Auborus sediments in one large formation with the underlying Sinclair Formation, due to the distinct unconformity below its basal conglomerate.

Typical outcrops occur on the farm Aubures (B6, C6, C7) and the formation takes its name from this farm although the spelling of the name has changed slightly.

The study of the Auborus sediments adjacent to Helmeringhausen was undertaken as part of the programme of work being done by the Precambrian Research Unit of the University of Cape Town. The aim was to map the formation in detail, the extent of the outcrops, the units present, to find out if there was any contemporaneous or post-sedimentary igneous activity and to determine the extent of structural deformation that had taken place.

II - TOPOGRAPHY

Much of the area shown on the geological map is part of the drainage system of the Konkiep River which has its source just east of Grosskopf (D7). Most of the tributaries to this river have easterly or southerly courses. Grosskopf itself (D7), rising to a height of 1978 m., is the highest point on a very high and rugged watershed that trends roughly north-south and is elevated in many places 1000 ft. and more above the river valleys just to the west. These form two drainage systems, one with mainly westerly courses through the farm Sinclair Mine (A6) and the other, through the farm Ginas (B1, 2, C1, 2), with mainly north-westerly courses. Together with these two and the Konkiep there is a fourth drainage system which flows north and rises on the farm Blutputz Ost (G2). West of the watershed just mentioned variously trending mountain ranges alternate with long, narrow, low-lying pediments. The latter join up with others farther west of the area on Sinclair Mine and farther north-west on Ginas to form larger pediments which as they extend westward, cut through the bounding mountain ranges. One such mountain range is that bearing the Trigonometrical beacons Auramberg (B3) and Hahnenkamm (C4). (Plate 1).

The central north-south portion of the area that is underlain by pre-Auborus rocks has a rugged topography in the northern half but it is only undulating in the southern half with Aruab, 1922 m, (E6) and Gaugaub, 1796m, (H7) the two highest peaks. Ganaams, 1920m, (E3) is the highest point in the northern half.

In the eastern outcrop much of the Auborus Formation is obscured by gently dipping sediments of the Nama System. On the farm Guperas (H5) the Kuibis quartzite is nearly 1200 ft. above the valley floors but on the eastern boundary of this section it has not been exposed by erosion. Eastwards from Guperas, overlying Schwarzkalk beds appear which, in turn, are succeeded by Schwarzrand beds still farther east. These form the Saraus mountain (J5) and the Schwarzrand erosion scarp just to the east of the area. However, the topography is, for the most part, flat where Nama sediments occur. In this section, in contrast to the western outcrop, there is no great change in the relief of the Auborus sediments.



Plate 1
Looking NW from Ganaams across the farm Ginas. The pediment on the left passes through the mountain ranges in the NW. Aurborus sandstone outcrops in the middle distance.

The Auborus sediments in their western outcrop form, for the most part, very mountainous country in which the layering of the sandstone shows up well, the very highest mountains such as Grosskopf (D7) and its neighbours have gently easterly dipping caps of Kuibis quartzite five to ten feet thick. Both the conglomerate and sandstone of the Auborus Formation form positive and negative features and there is no indication that either one is more resistant to erosion than the other. On the farms Sinclair Mine (A5, 6, 7), part of Aubures (B6) and part of Ginas (B1, 2, C3), the sediments have all been eroded down to pediment surfaces covered with sandstone and conglomerate pebble rubble which obscures a large portion of the outcrop.

Besides the numerous farm roads, two main roads pass through the area, one northward from Helmeringhausen to Maltahöhe and Windhoek and the other north-westward to Walvis Bay.

III - GENERAL STRATIGRAPHY

The basal conglomerate is the only zone that is present everywhere. It rests unconformably on an undulating surface of older lavas and sediments of the Sinclair Formation, and red quartz porphyries intrusive into this formation. Its thickness is very variable and reaches a maximum of 3300 ft. on the farm Saraus (H3) and a minimum of 100 ft. on Ginas (C3). Small depressions in the pre-Auborus surface are filled with breccias which are followed very closely by angular and subangular conglomerate. The breccias and first few conglomeratic beds are usually composed of fragments and pebbles of the immediately underlying rocks but their composition becomes very variable within 10-20 ft. of the base. Sandstone overlies the basal conglomerate.

The sandstone that follows the basal conglomerate on Saraus (I6) is repeated on Guperas (H5) by folding, but lenses out northwards under the Nama sediments. It is overlain sharply on Guperas (H5) by a conglomerate which thus merges in the north with the basal conglomerate. Another sandstone, out-cropping on Guperas (G5, H5), overlies this conglomerate and contains conglomerate beds that pinch and swell very noticeably.

West of the Aruab homestead a local lense-shaped conglomerate band (D6) is interbedded in the sandstone. This thins towards the east and west. Four conglomerate beds in the sandstone on Ganaams (C4, D2,3,4) also show this thinning towards their extremities but have a more easily detectable wedge shape. Below the lowest of these conglomerate beds west of Ganaams beacon (E3) is a succession of fine-grained sandstone which rests on deep red shale with intercalated siltstone. Between the two bands of conglomerate here siltstone beds occur intercalated with grit and very fine-grained sandstone, but above the upper conglomerate only siltstone is found. Shale also occurs along the synclinal fold axis as it passes across the Ganaams-Aruab farm boundary (D4). This is probably the same as that on Ganaams and has the same deep red colour.

On the farms Barby, Naus and Aubures, in contrast to the other areas of outcrop, no conglomerate occurs above the basal conglomerate. There are gritty zones, however, which do have pebbles scattered in them and occasional boulders up to one foot and more in diameter.

Towards the top of all the conglomerate beds the interbedded sandstone lenses increase in number and lateral persistence until they outnumber the conglomerate beds. The sandstone units usually now become thicker than the conglomerate beds, which in turn tend to become lensoid in shape, while the pebble size decreases to average sizes between one and four inches. In this way the conglomerate grades upwards into the overlying sandstone. The change takes place over a thicknesses of approximately 100 ft.

The most common sedimentary structures in the sandstone are cross-beds. Many bedding-plane surfaces are also marked by compressed clay pellets and there are rare parting lineation markings. Scour and fill structures can occasionally be found in grit and small pebble conglomerate, and rare channel deposits in the conglomerate.

The sections AA-FF (Figures 1 and 2) show a greater thickness of sediments in the northern regions of both outcrops due in the east to thicker conglomerate and in the west to thicker sandstone. The thickness in FF totals 5,100 ft. with two sandstone and two conglomerate bands, and in EE 5,300 ft. with one sandstone and one conglomerate. In sections DD and CC of basal conglomerate and overlying sandstone and BB of basal conglomerate and overlying sandstone with interbedded conglomerate, the respective thicknesses are 3,500, 5,250 and 6,400 ft. AA gives a value of 8,300 ft. which reaches 8,500 ft. in the sandstone overlying the upper conglomerate just to the north of the section (G1). This is the deepest part of the Auborus basin.

The eastern outcrop dips for the most part fairly gently westward. An asymmetrical north-south trending fold on Saraus (I6), which fades out northwards, has possibly been caused by a fault with a similar trend on Dabis (J7). Five other faults subparallel to this one have displaced the contact between the basal conglomerate and the pre-Auborus rocks (I7, J7, 8). Where the southern edge of the outcrop is unaffected by faulting the beds dip northward (I7). At the northern limit of outcrop dips are southerly (C2). Just west of Guperas beacon (G5), north-south block faulting has turned the Auborus beds up sharply along the bounding fault. In the north there are two later sets of east-west faults which cut both Auborus and Nama sediments (G3, H2).

Fig. 1. Vertical sections scale 1" = 6300' Notations as for map

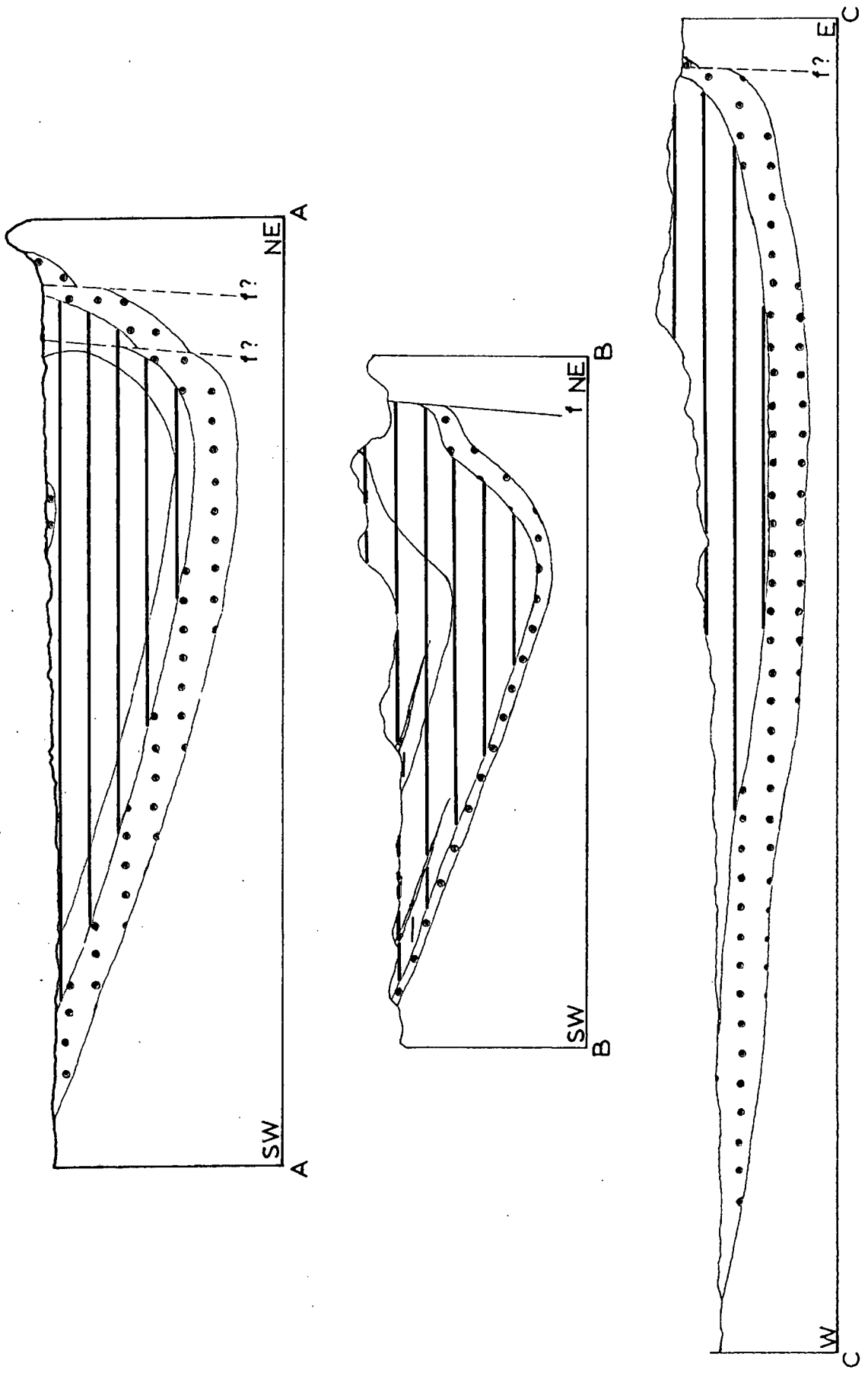
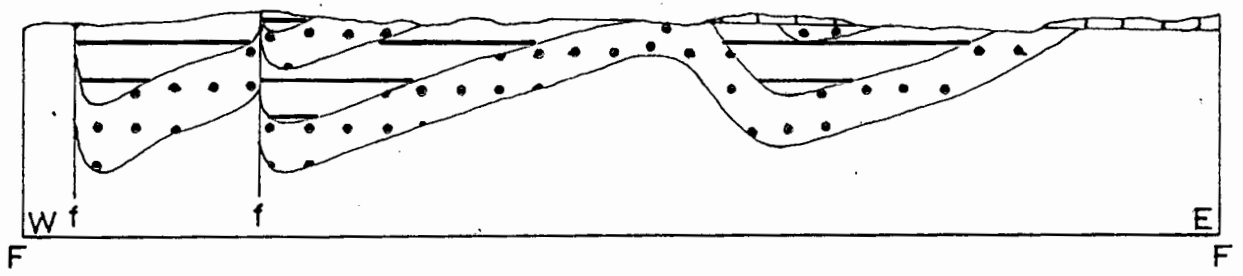
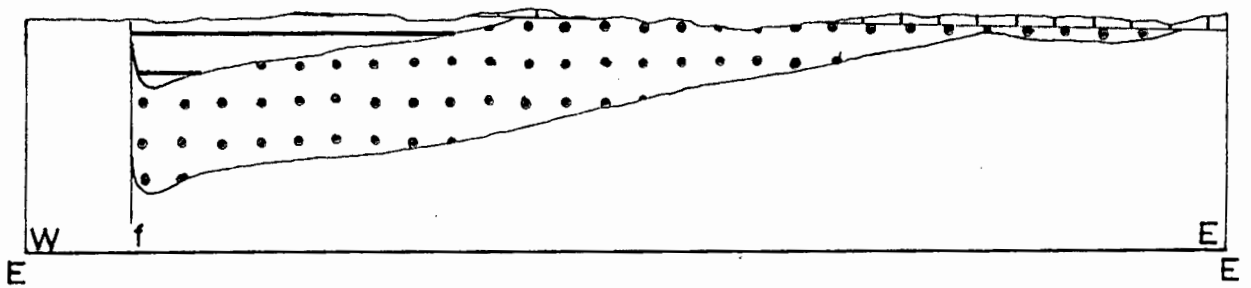
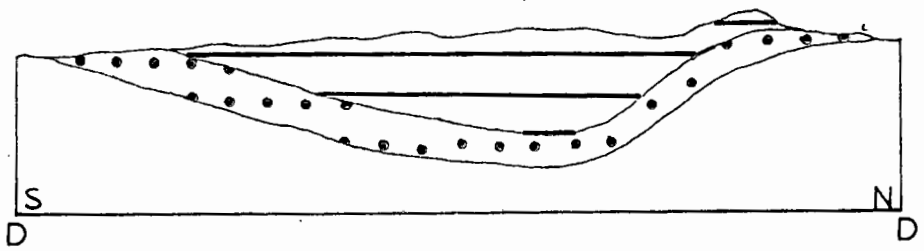


Fig. 2. Vertical sections, scale 1" = 6300'

Notations as for map



The western outcrop is bounded on its eastern edge by the block-faulted zone. This has tilted up the Auborus beds near it very steeply. The thickness of these steeply dipping beds is variable. On Ganaams the whole sequence has near vertical dips with overturning in places. On the western extremity of this outcrop dips are away from the basal conglomerate, mostly gentle but steep on Aubures (A6). Dips are also steep on part of Barby (E8). The synclinal axis in this section and the synclinal and anticlinal axes in the eastern section undulate slightly with a maximum plunge of 5°.

After deformation of the Auborus sediments a long period of erosion resulted in the development of an almost perfect peneplain. It was on this that the Kuibis quartzite of the Nama System was deposited. Only on Chamchawib (I2,3) and the northern portion of Saraus (H3, 4, I3,4) was the evenness of this pre-Nama peneplain broken. Here a few small undulating hills of Auborus conglomerate protrude through the Kuibis quartzite and immediately underlie beds of the Schwarzkalk Series. The Kuibis quartzite dips gently away from these hills where it abuts on them.

Small occurrences of copper are found scattered through the area in the basic lavas of the Sinclair Formation. These are either in the form of vein deposits or of zones a few feet across where copper minerals are concentrated. The largest vein deposit occurs on the farm Sinclair Mine (A6) and has been the scene of sporadic mining activity. Malachite, azurite, bornite and chalcocite were the minerals observed.

IV - STRUCTURE

(1) General

The Auborus basin was only once subjected to large deformational forces. These forces produced north-south block faulting in the centre of the basin and resulted in the disruption of the general basin structure. What now remains after erosion are essentially the two edges of this former basin represented by two parallel belts of Auborus sediments one on either side of a central horst consisting of rocks of the Sinclair Formation.

(2) Folding and Faulting

Figure 3 gives an indication of the general dip of strata in the eastern section. On the whole dips are low and westward, away from the limit of outcrop which is mostly below Nama sediments. Most readings cluster around 10° but some are as much as 40° and 60° . The strike is mainly northerly but swings round to north-east in the south and to east in the north, giving the basin shape of the strata. Dips become a little steeper towards the bounding fault in the west, and close to the fault the beds are sharply up-turned into a vertical position. Sub-parallel faults in the south show, in all cases but one, a relative southward displacement of their eastern sides. Asymmetrical folds just to the north of two of these faults have apparently been caused by the same tectonic forces and their trends follow very closely those of the faults. It is probable that the forces were too great in the south for folding alone to occur. As the effect of the forces decreased northwards only asymmetrical folds formed which, still farther northward, disappear altogether. The western limbs of these folds dip more steeply than the eastern limbs and the general asymmetry is indicated plainly by Figure 3. The dip values of the western limbs cluster about 36° . The fold axes plunge gently north and south and have a maximum dip of 5° . These plunges were probably produced by the same forces that produced the folding.

Large-scale normal faulting in the west, with a throw of at least 5000 ft., has cut off the whole of the Auborus

Formation. Small faults striking due east are of later formation; it is difficult to see the movement on the most southerly of these, but that in the north has its down-throw side to the south. A third set of faults, striking east-northeast, cuts both the earlier sets, and the most northerly one has a throw to the south of about 1,200 ft. There has been a little post-Nama movement on all the faults with a maximum of between 10 and 20 ft. on the north south fault bounding this sector, and on the most northerly east-striking fault.

Figure 4 gives the general dip pattern of the strata in the western outcrop. It is pinched to a width of only two miles on Aruab (D6) but swells north and south of this. The dips are away from the basal unconformity: roughly eastwards on Sinclair Mine (A6), Aruab (D5, 6), Ganaams (C4, D5), Ginas (C3), southerly on Aubures (C6), northerly on Naus (C8, D8), and northerly and westerly on Barby (E8, 9). The greatest values occur around the edges but decrease inwards. The outcrop is thus basin-shaped again, though a little irregular. Nearly the whole of the eastern edge of this outcrop is bounded by a normal fault which has its greatest throw of about 1,800 ft. on central Aruab (E5). The base of the formation is exposed in the southern portion of Aruab (D7) and on Barby (E8) but a small corner between these two areas is cut off by a normal fault with north-westerly strike. Both these faults have down-throw sides to the west. There is again a general asymmetry in this outcrop, as there is in the eastern outcrop. The contrast in asymmetry is shown by comparison of Figures 3 and 4.

In the western section there is a very noticeable decrease in the dip of the strata as one moves from the base of the formation towards the centre of the basin. This indicates that subsidence was contemporaneous with deposition so that the lowermost beds became more steeply inclined as sedimentation progressed. This must have applied to the whole basin of deposition but the present day attitudes of the strata in the eastern section do not show this at all clearly.

The main processes of deformation, however, followed the completion of deposition and possibly lithification too. Figure 5 shows the main forces involved.

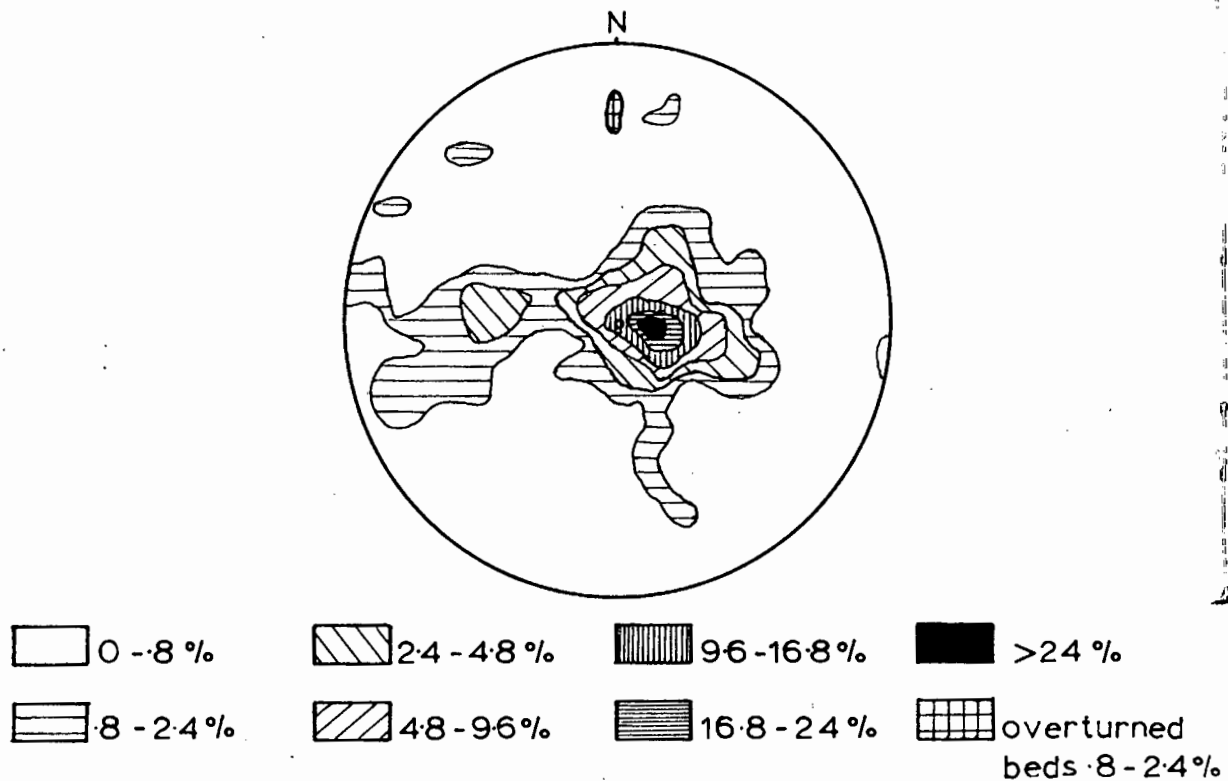


Fig. 3. 128 poles of bedding planes in the eastern outcrop of Auborus sediments. Lower hemisphere of Schmidt net.

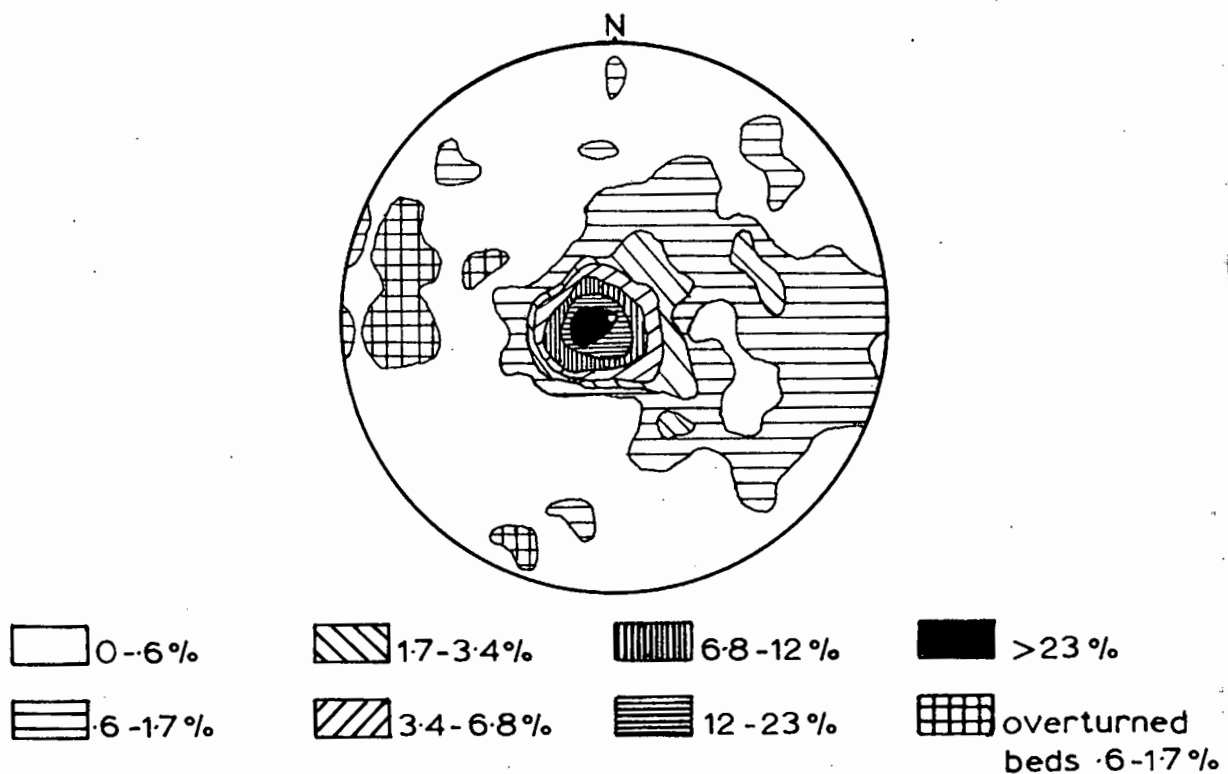


Fig. 4. 175 poles of bedding planes in the western outcrop of Auborus sediments. Lower hemisphere of Schmidt net.

North-south block faulting in the centre of the basin elevated the whole of the central portion in the form of a horst. Erosion later removed all the Auborus sediments that were thus uplifted. The eastern bounding fault of this horst has cut the sediments off very sharply. However, on Aruab and Ganaams the same forces that caused the faulting there were probably responsible, in the early stages, for the folding of virtually the whole succession into vertical and overturned positions (Plate 2). The step faulting in the south-east was probably contemporaneous with the block faulting. There may have been slight tilting from the west and east to produce the gentle inward dips of the uppermost beds.

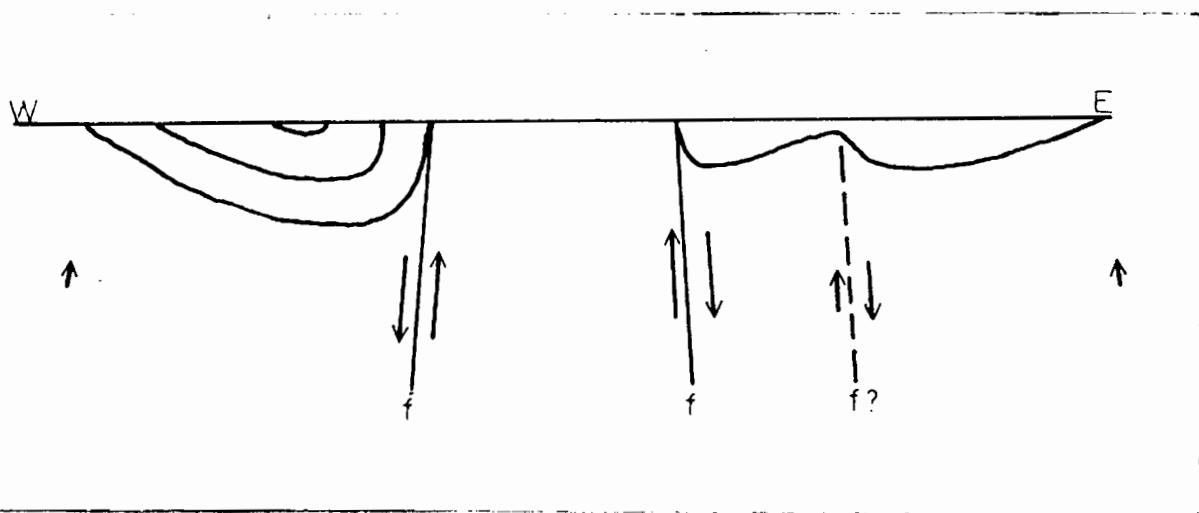


Fig. 5. Diagrammatic representation of the deformed Auborus basin. Length of arrows indicates relative amounts of movement.

Petrofabric work on samples of sandstone did not reveal any alignment of the c-axes of quartz grains.

(3) Joints

Joints are numerous and well formed throughout the sandstone and this formation is noted for the quantity of water it carries. The conglomerate is rarely jointed. Landscape and aerial photographs show up the joints well and often grass is concentrated along them. In some cases tall thorn trees grow along parts of the larger joints. This is shown up well by the aerial photographs of Aubures where one release joint can be traced for nearly three miles. The joint planes are generally between six inches and three feet apart (Plates 38 and 59).

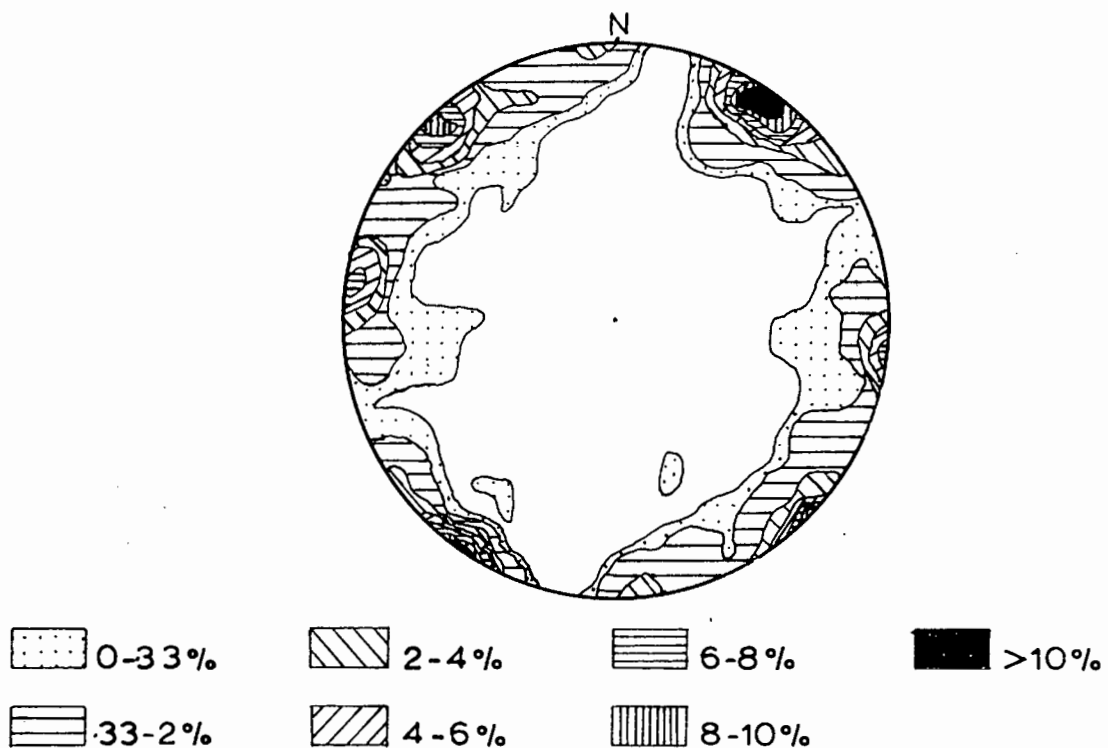


Fig. 6. 300 poles of joint planes plotted on a Schmidt equal-area net. Lower hemisphere.

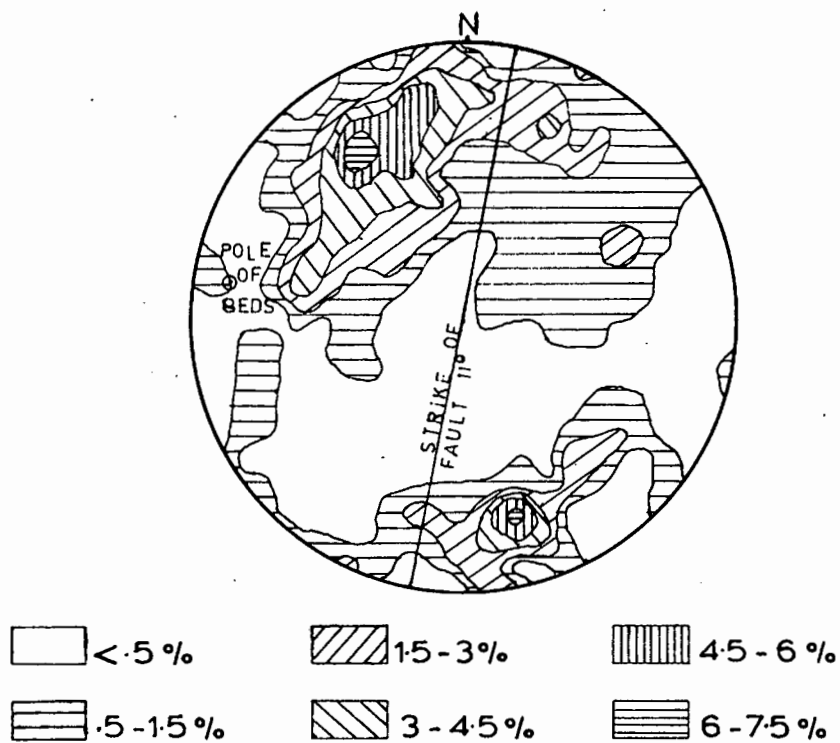


Fig. 7. 200 poles of fracture planes in conglomerate pebbles near the Aruab fault, plotted on a Schmidt net. Lower hemisphere.

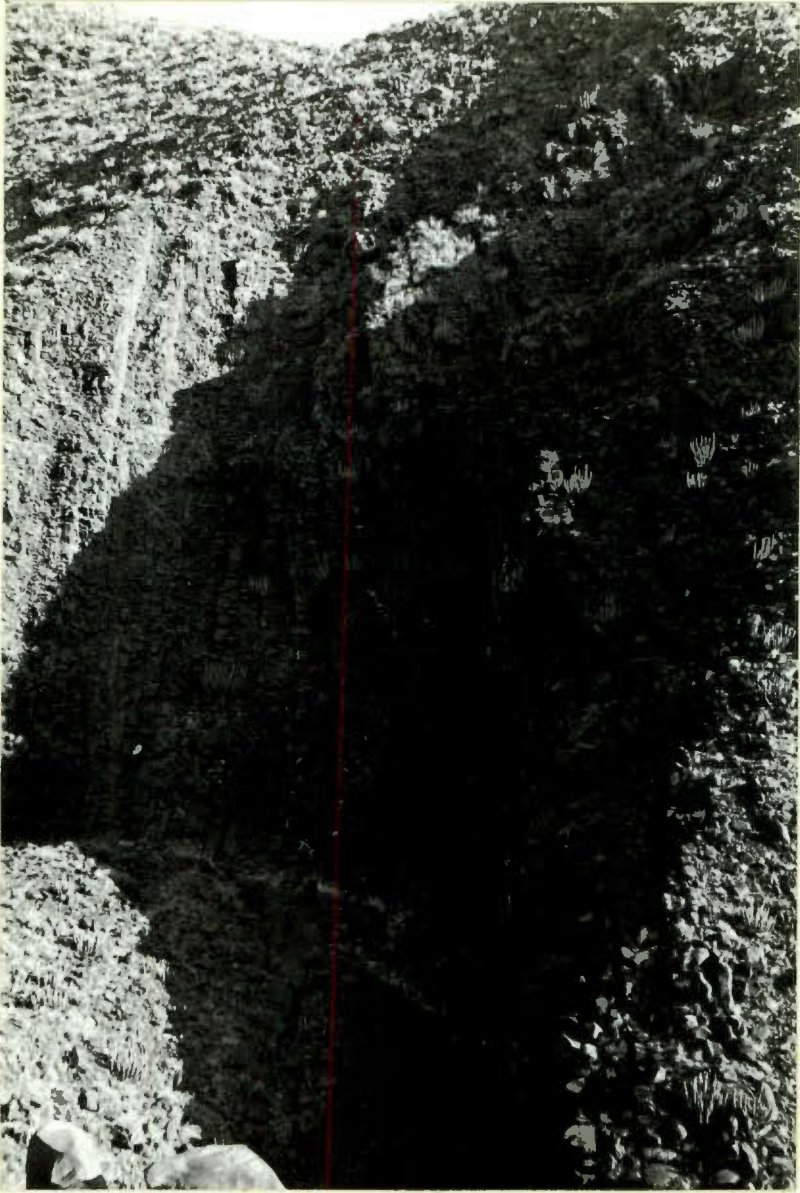


Plate 2
Vertical Auberus sandstone. NW portion of the
farm Aruab.

Figure 6 is a contour map of the poles of 300 joint measurements. Two sets of diagonal joints are prominent and have an acute angle of 77° between them. This is the same for both the western and eastern sections and points to compressive forces from N86E and S26W. There is a very small set of tension joints striking east, and a larger one of release joints with northerly strike. Most are steeply dipping.

(4) Pebble Fractures

On Aruab and Ganaams where faulting cuts through conglomerate (D1,2,3,6, E3,4,5), a few of the pebbles close to the fault have been fractured, the halves slightly displaced and, in some cases, cemented together again along the fractures. In some pebbles the displacement is as much as half an inch. Usually only one pebble is affected but in some cases three or four are broken along the same fracture plane. When only one pebble is affected the fracture plane does not pass into the matrix (Plate 3). Such fractured pebbles are not found beyond 100 ft. from the fault. Figure 7 is a plot of the poles of 200 of these fracture planes from the northern portion of Ganaams (D2). They cluster around two main zones which make trace angles of 46° and 63° with the trace of the fault. There is a slight tendency for a conical concentration of planes. The beds are slightly overturned and have a strike almost parallel to that of the fault.

One purpose of this present study was to determine whether there was any relationship between the positions of these fracture planes and the nearby fault planes. However, consideration of the outcrops in the field and of Figure 7 shows many factors which tend to make any relationship very complex and difficult to determine. Since the conglomerate is poorly sorted and made up of so many different pebble types it must have reacted as a heterogeneous mass during deformation, with the result that the position of the fracture planes varies from pebble to pebble and from place to place. Pebble rotation, either prior to or following fracture plane development, would also be a factor influencing the present position of fracture planes.

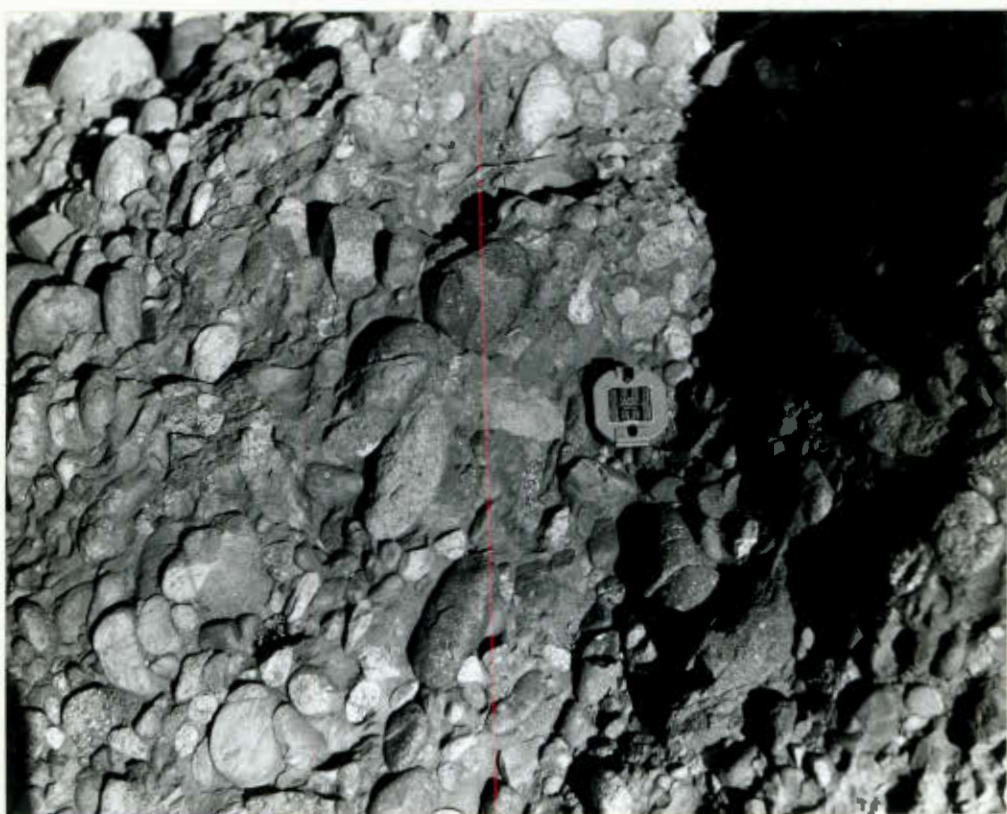


Plate 1

A fractured pebble with displaced halves can be seen just below the compass. A small fracture that passes through the matrix and a pebble can be seen to the left of the compass. This pebble only shows very small displacement. NE portion of the farm Ganaams.

V - SEDIMENTARY PETROGRAPHY

(1) The Conglomerate

Plate 4 shows the typical appearance of conglomerate outcrops on hillsides. The more resistant zones form uneven "bumpy" rounded cliffs.

The thickness of the basal conglomerate varies along its strike, reaching a calculated maximum of 3,300 ft. in the northern portion of Saraus (H3). This decreases northwards in the eastern outcrops, to 3,000 ft. on Blutputz Ost (G2,3) and southwards to 1,500 ft. in the northern portion of Dabis (J6,7). The great thickness of 3,300 ft. and more in the north is due to the lensing out northwards of the sandstone overlying the basal conglomerate. The 1,400 ft. thick conglomerate that overlies this sandstone on Guperas (H5) therefore lies directly on and constitutes part of the basal conglomerate on Chamchawib and in the northern portion of Saraus (H3,4). The sandstone in the eastern outcrop quite often has lenses and beds of conglomerate up to two feet thick, but not in sufficient quantity to form separate mappable conglomerate bands.

In the western outcrop thicknesses are not as great, and also decrease northward. The steeply dipping beds on Barby (E8) total 1,200 ft. This thickness fluctuates westward from 1,300 ft in the western portion of Barby (D9) and 1,100 ft. in the eastern portion of Naus (D8) to 1,350 ft. in the west of Naus (D8). The steeply dipping conglomerate on Aubures (C6) has thinned to 600 ft. and eastwards to a point two miles north-west of the Aruab homestead (D6) there is a further thinning to 270 ft. In the southern portion of Ganaams (C4) the basal conglomerate has a thickness that fluctuates about 500 ft. but this thins to 100 ft. on Ginas (C3).

The conglomerate bands interbedded in the sandstone are wedge-shaped and show a tendency to be thinner the higher up in the succession they are. That on Aruab (D6) is nearly 500 ft. thick while the lowest in the southern portion of Ganaams (C4), the thickest, is 650 ft. The one above it is barely 100 ft. thick (D4). Those west of Ganaams beacon (E3) both have a maximum thickness of 300 ft. but wedge out northwards and the uppermost is only 10 ft. thick on the northern edge of the area (C1).

Plate 5 shows the upper part of a poorly bedded, six-foot breccia band at the base of the basal conglomerate. A few rounded pebbles can be seen among angular fragments of the underlying and nearby basic Sinclair lavas. It is very porous compared with the overlying poorly sorted conglomerate, and calcite infillings can be clearly seen. Usually the change in the degree of roundness from breccia to pebbles that are subrounded to rounded is gradual. The sharp contact between the breccia and the conglomerate shown in this photograph is unusual.

Plate 6 shows how the lowest conglomerate beds fill small depressions in the pre-Auborus topography. Here the pebbles are mainly subangular, with scattered subrounded ones amongst them, while sorting is poor and bedding is medium to thick and inconsistent. The pebbles have been very largely derived from lavas on which the conglomerate lies. Generally by about 20-30 ft. above the contact the degree of roundness of the fragments has noticeably increased and many more rock types appear. Usually pebbles of various types of lavas and sediments appear first. These are accompanied higher up in the succession by granites and gneisses.

The actual unconformity between the basal conglomerate and the pre-Auborus rocks was only rarely seen, but where exposed, the overlying beds were found to have a variable sorting and pebble composition. In most places the upward transition from angular fragments to more rounded pebbles is well demonstrated. However, two and a half miles west-northwest of Dabistafel beacon (J7) a well sorted conglomerate with many different types of well rounded pebbles rests unconformably on older Guperas Series sediments. Granitic and gneissic pebbles are abundant here.

Calcitic infilling of pore spaces is a common feature of the breccia and some subangular conglomerate, but higher up in the succession the sand-size matrix leaves very little pore space and calcitic infillings are rare. The pebble size of these lowermost breccia horizons is usually small compared to that of the overlying conglomerate. In the breccia the inclusions range in size from 2 cm to 15 cm in diameter and lie in an abundant matrix of coarse sand and grit-size material.¹

¹Wentworth's (1922) measures for describing the size distribution of sediments is used here.



Plate 4
Conglomerates on Dabls that dip 3° SE. This is typical of the uneven rounded, buttress - like outcrops of conglomerate on hillsides. The hill is capped with Kubis quartzite. Facing SW.



Plate 5
Breccia below the basal conglomerate. The upper 4 ft. of the 6ft. thick breccia is visible. It contains a few rounded pebbles and much intergranular calcite. Many pebbles in the overlying conglomerate are well rounded and the contact between the two beds is unusually sharp. Two miles NW of Aruab homestead. Facing east, beds dip 27° E.



Plate 6
Lowermost, very poorly sorted beds of the basal conglomerate resting on Sinclair lavas. Most of the pebbles are subangular. Facing SW; beds dip unevenly north. Eastern portion of Naus.



Plate 7

Three boulders associated with a 1 in. thick, inconsistent grit layer (on which the compass is lying) but which penetrate into the underlying fine-grained sandstone. NW portion of the farm Aruab. Beds dip 7° NE.

Grit is interbedded at different levels in the sandstone and in places contains scattered pebbles, cobbles and boulders up to one foot in diameter. These could only have been rolled into position and the depositing currents must thus have been strong. Such large inclusions are also found occasionally in the sandstone associated with only thin gritty beds less than one inch thick (Plate 7).

(a) The Pebbles

By far the greatest number of pebbles in all the conglomerate is of fine and medium grained igneous rocks, most of which are lavas from the Sinclair Formation. The large cobbles and boulders are mainly granite and quartzite but locally large inclusions of the various lava types are also found, usually only of one type in any one locality. Large cobbles of rhyolite occur in the northern portion of Saraus (H4, I4) and large cobbles and boulders of porphyritic basalt on Naus (D8). It is very difficult to assess the total number of different types of pebbles present but an indication can be obtained from Table 1 which is a combination of many observations.

All conglomerate beds have a great variety of pebble types, general poor sorting, and degree of roundness from sub-angular to rounded. Sphericity and rounding are generally better in the larger sizes of pebbles but occasional zones show a good sphericity of all pebbles.

In the lower zones of the basal conglomerate the proportions of the different pebble types vary greatly from place to place. In many outcrops the most frequently occurring pebbles can be traced to underlying or nearby pre-Auborus rocks. Certain areas have an abundance of one pebble type for great thicknesses, as is the case in the northern portion of Saraus (H4), Chamchawib (H3) and Blutputz Ost (G3) where red porphyritic rhyolite is common near the base. It is still common high in the succession but a greater proportion of other pebbles makes it less conspicuous. The phenocrysts in the porphyry are of quartz and pink felspar. The dark porphyritic basalts so common in the south (D8,9) are found to be rare in the southern portion of Ganaams (C4) and the central portion of Saraus (I5). The conglomerate bands in the sandstone all contain these basalts in their pebble crops.

Granites, after their first appearance, increase in quantity upwards to nearly 40% in places, as on Aubures. The height above the base at which granitic and gneissic pebbles appear is very variable. Plate 8, taken two and a half miles south of the Dabis homestead (J7), shows the contact of the basal Auborus conglomerate on steeply dipping purple Sinclair quartzite which is capped by Nama sediments. Here sub-rounded granite and gneiss pebbles occur 40 ft. above the contact. They are up to one foot in diameter and are much larger than the associated pebbles of lava and sediment. The basal beds here have the same purple colour as the quartzite on which they lie, but 20 ft. above the base the colour has changed to red. They contain many pebbles of the underlying quartzite. Three miles east of the Naus homestead (C9) granitic pebbles appear 400 ft. above the base. Here, however, they are of the same size as the other pebbles in the same bed, are very well rounded, and have a good sphericity. Below this the conglomerate is made up of pebbles of the many different types of Sinclair and Nagatis lavas and sediments varying in size from grits to boulders nearly three feet in diameter. The latter are mainly porphyritic basic Sinclair lavas which can be found to outcrop a few miles to the south.

The sorting and roundness of the pebbles is at its best high up in the conglomerate, but the sorting, though variable, is on the whole poor throughout. Plate 9, taken near the top of the basal conglomerate on Naus (D8), shows beds containing many granite and gneiss pebbles and an interbedded sandstone with a limited lateral extent. The fine-grained sandstone matrix in which the pebbles are embedded can clearly be seen here. The pebbles themselves here exhibit a better sphericity than is normal. Generally sphericity is not as well developed even at the top of the conglomerate bands. Plates 10, 11 and 12 show the overall poor sorting with large boulders in a matrix of smaller pebbles. They also illustrate the manner in which small and large pebble and boulder conglomerates are interbedded with each other, and in places with grit and sandstone lenses. Plate 11 shows the uppermost conglomerate on Ganaams (D2) in which sub-rounded and well rounded pebbles and boulders occur in a massive poorly sorted bed.

Von Brunn (1967), who worked on the pre-Nama rocks to the south of the Auborus sediments, was able to identify

Table 1. Pebble types found in the conglomerate.

At least 5 types of sandstone (4, northern portion Dabis).

Banket-like Kunjas conglomerate.

Rare shale.

Several types of granite (4, southern portion Dabis; 5, Barby;

4, Naus; 7, northern portion Dabis).

2 - 3 types of diorite

2 - 3 types of diabase

Many examples of porphyritic and non-porphyritic rhyolite from light

to dark red in colour with rounded and euhedral phenocrysts.

At least 4 types of porphyritic basalt with white, rounded or euhedral

felspar phenocrysts.

Felsite and devitrified tuff.

Brown intermediate amygdaloidal lava with acicular epidote filling the

vesicles. Other rare amygdales with quartz or calcite amygdules.

Several red quartz porphyries.

Epidosite.

Well rounded quartz and jasper pebbles $\frac{1}{2}$ - 2 in. in diameter.

One pebble from Gansams containing much specularite.



Plate 8

Two unconformities are shown in the photograph. Auborus conglomerate on the left rests on steeply dipping Sinclair quartzites. These quartzites are overlain by horizontal Nama sediments. The conglomerates strike N75E and dip 25° NW. View NNE, 2 miles south of Dabis homestead.



Plate 9
A zone in the basal conglomerate consisting of well rounded pebbles in a sandy matrix. A sandstone lense indicates the 13° northward dip. The white material is calcrete which cements the surface rubble where water is close to or reaches the surface. Facing east on the eastern portion of Naus.



Plate 10
Northerly dipping conglomerate on the eastern portion of Naus. The very poor sorting is well shown and boulders more than 1 ft. in diameter are common. Many of these are porphyritic basalt.



Plate 11
Unsorted, massive bed of conglomerate on the Ganaams-Ginas farm boundary. Rounded and sub-angular pebbles and boulders of many types set in a sandy matrix. The largest boulder is nearly 3 ft. across.

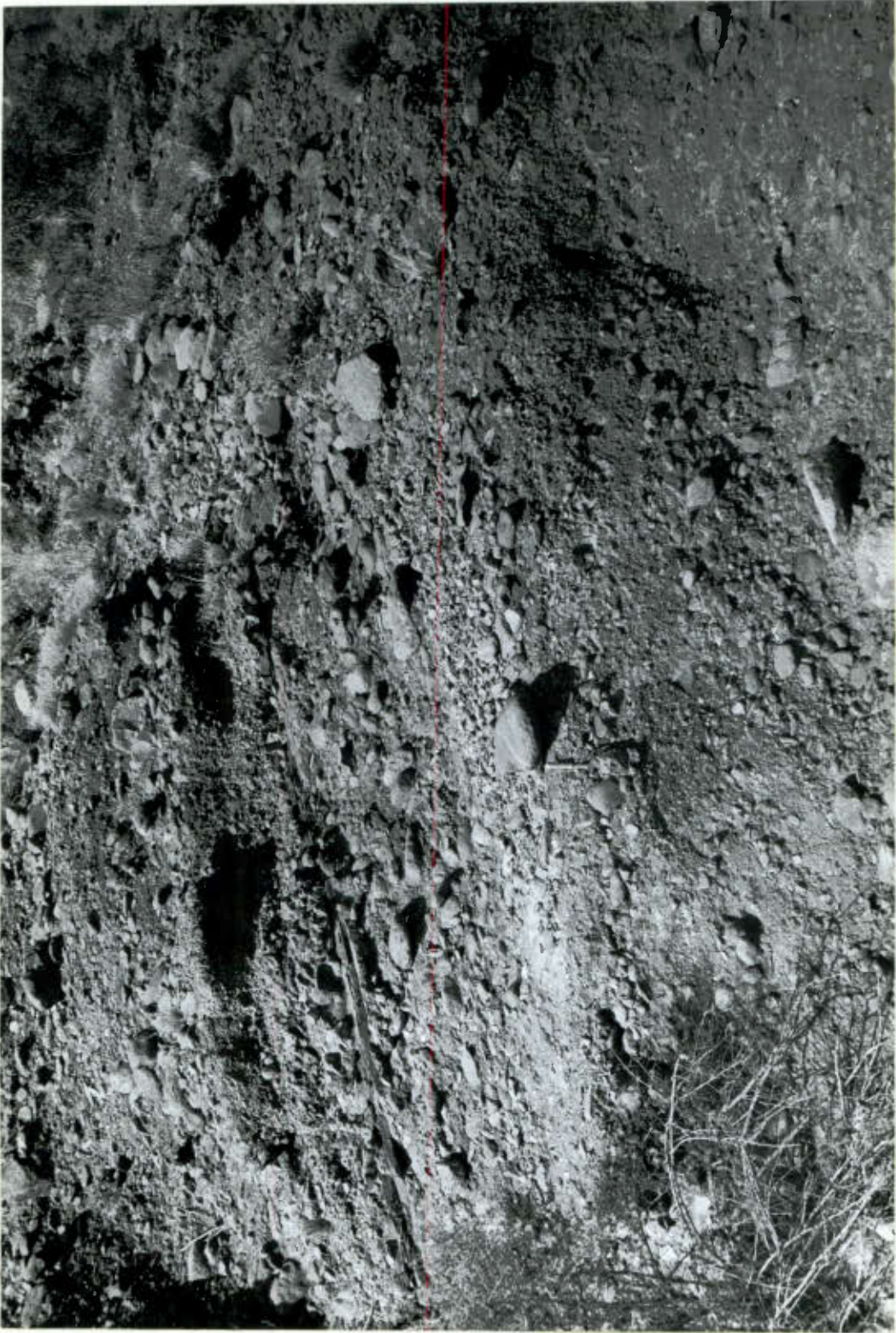


Plate 12
Large and small pebble, cobble, and boulder conglomerates and sand lenses randomly interbedded. The size of loose and embedded pebbles, cobbles and boulders can be gauged from the hammer in the center of the photograph. Facing north on the northern portion of Dabis. Beds dip 7° NW.



Plate 13
An abundant sandy matrix of a small pebble conglomerate. This is in the conglomerate above the shale on Ganazams. The plane of the surface is roughly parallel to the bedding which dips 11° NW, from the top to the bottom of the photograph. Sorting of the pebbles is fairly good.



Plate 14
Two conglomerate beds, very near that in Plate 13, showing different amounts of matrix. That on the left shows poor sorting and rounded and sub-angular pebbles.

Table 2. Some of the pebbles found in the basal conglomerate

Locality	Description	Source area	Distance of deposition site from source	
Northern portion Dabis	Granite	Frisgewaagd	18 miles	SW
	Alaskite	Mooifontein	25 "	SE
	Granite	Nababis	28 "	SW
	Tumwab granite	Gamochas	20 "	S
	Tumwab granite	Gamochas	20 "	S
	Microgranite	Helmeringhausen	11 "	S
	Granite	Sterrafrag	20 "	SE
	Sinclair quartzite	Several localities in south		
	Kunjas conglomerate	Tiras	34 "	SW
Southern portion Dabis	Granite	Korais	20 "	SW
	Alaskite	Mooifontein	20 "	SE
	Granodiorite?	Korais	20 "	SW
	Tumwab granite	Gamochas	16 "	S
	Sinclair basalt	Barby	14 "	ESE
	Sinclair sediment	Several localities in south		
	Nagatis devitrified tuff	Korais	20 "	SW
	Nagatis porphyry?	Korais	20 "	SW
	Sinclair basalt	Several localities		
	Sinclair lava	" "		
	Sinclair grits	" " in south		
	Sinclair quartzite	" " " "		
	Kunjas sediment	Tiras	17 "	SW
	Southern portion Guperas	Gneiss	Tiras area?	32 "
Gneiss		Tiras area?	32 "	SSW
Epidosite		dykes on Rooikam and Witmanshaar	5-10 "	SSW
Porphyritic rhyolites		dykes on Rooikam and Witmanshaar	5-10 "	SSW
Naus		Porphyritic Sinclair basalt	Barby	5 "
	Sinclair porphyry	Barby	5 "	S
	Acid Sinclair lava	Several localities		
	Stratified Sinclair tuff	Barby & others	5 "	S
	Felsite	dyke in Sinclair basalts on Witmanshaar	10 "	ESE
	Nagatis Formation lava	Korais	10 "	S
	Nagatis devitrified tuff	Lovedale, Korais	10 "	S
	Top Sinclair sediments	Witmanshaar	10 "	ESE
	Aubores	Top Sinclair sediments	Witmanshaar	16 "
Barby Sandstone	Quartz porphyry	Gamochas	18 "	S
	Nagatis felsite	Korais	10 "	S

Table 3. Modes of 13 granite pebbles taken from the basal conglomerate.

<u>Specimen No.</u>	<u>A20</u>	<u>A69</u>	<u>A70</u>	<u>A72</u>	<u>A73</u>	<u>A74</u>	<u>A75</u>	<u>A76</u>	<u>A30</u>	<u>A63</u>	<u>A68</u>	<u>A26</u>	<u>A110</u>
Quartz	40.2	40.8	37.1	32.7	28.3	29.5	43.0	39.9	37.0	17.3	35.9	33.8	32.2
K-felspar	0.7	27.5	0.8		1.4	50.2	14.1	1.5	55.5	30.8	5.2	20.9	8.4
Perthite	9.9	1.7	34.4	7.4	52.0	0.3	15.7	46.6	1.8	0.4		17.7	19.0
Plagioclase	39.0	26.2	19.9	49.5	14.5	16.9	26.3	11.4	4.6	43.6	43.9	25.9	34.5
Biotite	4.7	3.5	0.2	0.9	1.1	0.2		0.6			8.1	1.3	3.1
Muscovite	0.2			0.1			0.1						0.9
Chlorite	3.6	0.5	5.7	5.4	1.9	1.3	0.5			4.9	0.5	0.2	0.4
Ore	0.5	0.6	1.1	1.6	0.4	1.3	0.3	0.4	0.2	1.1	5.4		0.8
Calcite	0.5	0.2		2.3		0.1	0.1		0.8	0.2	0.1	0.1	0.5
Topaz												0.2	0.2
Apatite	0.1				0.1	0.1					0.3		
Sphene	0.2		0.1	0.1	0.5	0.1	0.2			0.2			
Epidote	0.5		0.6	0.1		0.2			0.1	1.5	0.6		
Zircon			0.1		0.1								
	100.1	101.0	100.0	100.1	100.3	100.2	100.3	100.4	100.0	100.0	100.0	100.1	100.0

Table 4. Granite Pebbles

Specimen No.	Description	Where Found	Hand Specimen Identification & source
20	Subhedral plagioclase phenocrysts strongly altered; minor perthite and untwinned albite - little altered. Minor biotite and secondary chlorite. Granitic texture.	Southern portion Dabis	Korais Nababis granite 20 mls. SW
26	Subhedral plagioclase, An30, with Carlsbad, albite and pericline twinning. Perthite and microcline, weak alteration of feldspars, K-feldspar most affected. Minor biotite. Granitic texture.	Southern portion Dabis	Moolfontein alaskite 20 mls. SE
30	Euhedral to anhedral crystals of quartz and plagioclase in a groundmass of graphic intergrowths; plagioclase - Carlsbad, albite and pericline twinning. Fine graphic intergrowths around plagioclase crystals due to reaction. Very minor perthite phenocrysts.	Southern portion Dabis	Tumwab granite on Gamochas 16 mls. S
63	Strong alteration of K-feldspar and subhedral plagioclase. Carlsbad and albite twins in plagioclase crystals. Aplitic texture.		unidentified
68	Subhedral zoned, twinned plagioclase phenocrysts with strongly altered central zone. Biotite strongly altered. Granitic texture. Quartz crystals with sutured edges. An 15-30 inwards.	Northern portion Dabis	Starreprag granite 20 mls. SE
69	Aplitic texture of twinned plagioclase, orthoclase and microcline. Microcline hardly altered and plagioclase strongly altered. Strongly altered biotite. Quartz.	Northern portion Dabis	Microgranite intruding metabasalts on Helmeringhausen 11 mls. S
70	Fairly strongly altered twinned plagioclase phenocrysts in a groundmass of fine graphic intergrowths. Very minor, strongly altered K-feldspar phenocrysts	Northern portion Dabis	Tumwab granite Gamochas 20 mls. S
72	Subhedral zoned twinned plagioclase crystals very strongly altered. Much of the quartz is very fine grained, large crystals have sutured edges. Aplitic texture.		unidentified
73	Large anhedral perthite crystals slightly altered. Small subhedral crystals of orthoclase strongly altered. Some plagioclase.	Northern portion Dabis	Nababis granite
74	Anhedral plagioclase phenocrysts in an abundant groundmass of graphic intergrowths. Plagioclase crystals show Carlsbad, albite and pericline twinning. Rare orthoclase phenocrysts. Both feldspars strongly altered. Very small amounts of myrmikite. Plagioclase An28.	Northern portion Dabis	Frisgewaagd granophyric granite 18 mls. SW
75	Anhedral crystals of orthoclase, microcline and perthite. Subhedral-anhedral plagioclase crystals with good Carlsbad, albite and pericline twinning. Slight alteration of plagioclase; coarse and fine perthites. Granitic texture.	Northern portion Dabis	Moolfontein Alaskite
76	Plagioclase crystals subhedral. A few small graphic intergrowths and rare myrmikitic ones. Fine perthite exsolution lamellae. Lines of alteration in the feldspars are parallel to bubble trains in the quartz. Coarse aplitic texture. Plagioclase, Carlsbad and albite twins.	Northern portion Dabis	Tumwab granite 20 mls. S

The composition of all plagioclase, measured from the extinction angles of the albite twin lamellae, lies between An15 and An42.

visually most of the pebbles collected for that purpose (Table 2). A couple of weeks spent in the field with him revealed some of the granites and sediments and many lavas, which are the sources of pebbles found in the conglomerate. He identified 22 pebbles from Dabis (I6,7, J8), 4 from Guperas (D2), 9 from Naus (D8), 1 from Aubures (B7), 1 from the eastern outcrop of Ganaams (D2), and 2 from grit 3,000 ft. up in the sandstone on Barby (D8). It is probable, therefore, that the material was derived from the south and that in some cases (e.g. unsorted boulder conglomerate such as that on Naus) the source must have been close to the present location of the material. It must be pointed out, however, that Sinclair Formation rocks occur extensively to the east and north of the Auborus sediments together with various granites, and the material could have been derived from these areas as well. Von Brunn was unable to identify 21 pebbles of which one was a fine-grained granite, six were gneisses and the rest were fine-grained basic, intermediate and acid igneous rocks, many of which could be dyke material. These could easily have their source amongst the numerous and diversely composed dykes in the pre-Auborus rocks to the south.

Thin sections of 13 granite pebbles were made so as to be able to compare the modes, where possible, to those of von Brunn's (1967) granites and thus identify the pebbles more positively. This, however, was not at all enlightening, since the modes did not correspond, but slides from the Tumuab granite had a similar granophyric texture to the slides of pebbles that were identified as coming from the Tumuab granite. Some showed strong alteration of the feldspars but in the other slides K-feldspars could be seen partially altered to sericite and plagioclase feldspars to coarser grained saussurite. In the strongly altered slides saussuritised grains were counted as plagioclase and sericitised grains as K-feldspar. Table 3 gives the modal analyses of the granite pebbles and Table 4 a general description.

(b) The Matrix

In the conglomerate the matrix is quite variable in the size of its main constituent. It can consist of fine-grained sand, or grit, or small pebbles up to half an inch in diameter. The last two interchange rapidly and randomly

in the same bed and always have the intergranular pore spaces filled with sand. All conglomerate has one of the three types of matrix.

A feature that is shown in places by the upper conglomerate bands is a much higher proportion of red, fine-grained sand matrix which can be seen in Plates 13 and 14, taken near the top of the conglomerate due west of Ganaams beacon (E3). They show a fair sorting of the pebbles in one case and poor sorting in the other.

(2) The Sandstone

Sandstone forms the bulk of the Auborus sediments. The succession on Saraus (I5) reaches 1,350 ft. at its thickest and that on Guperas 2,500 ft. in the southern portion of the farm (G5, H5) and 2,200 ft. in the northern portion (G3, H3). In the three sections DD, CC, and BB in the western outcrop, the sandstones have total thicknesses of 2,500, 3,350 and 5,900 ft. respectively. This shows an increase in the thickness of sandstone northwards. The shale west of Ganaams beacon (E3) is 300 ft. thick and the section AA has a possible 7,400 ft. of fine-grained sandstone and shale.

The sandstone is fine to very fine grained, well consolidated and has an even monotonous red colour which becomes deeper with a decrease in grain size. Throughout nearly the whole sandstone succession bedding is thin to very thin and often laminated. Infrequent massive beds above the shale on Ganaams (D3) have a maximum thickness of 10 ft. Beetz (1922) mentions massive beds up to 20 m thick but these were not confirmed in the field. Randomly in the sequence occur spherical spots of decoloration and occasionally small black spots of ore as well. Bedding planes very often carry mica.

Sedimentary structures are most abundant on the farms Saraus (J5), Guperas (H5), Naus (C7,8, D7,8), Barby (E7,8) and the south-western corner of Aruab (D6,7). The commonest structures are cross-beds, mud cracks and clay pellet impressions. The latter can also be found farther northward on Ganaams (D1,2) and parts of Ginas (C1). Current- and oscillation-ripple marks and parting lineations are present but are generally scarce. The parting lineations

are present but are generally scarce. The parting lineations occur, on the whole, in small isolated patches, with only 2-10 bedding planes marked by them. They are usually in association with other shallow water sedimentary structures such as mud cracks, clay pellets and occasional current or oscillation ripples, and are most abundant two miles east of Grosskopf (D7) in the bed of the Konkiep Rivier. The sandstone on Aubures has a conspicuous lack of sedimentary structures when compared with the rest of the area.

The shale on Ganaams (D3) has abundant ripple marks. Both oscillation and current ripples are present and often two sets are superimposed. In many exposures the current ripples show the internal cross-bedded structure. Mud cracks are absent here.

Other sedimentary structures are very rare. The only specimen of flow casts was found on Naus (D8) (Plate 15). Plate 16 shows a finely and evenly pitted bedding plane, of which only six examples were seen.

(a) Microscopic Characteristics

In thin section no sedimentary calcareous components were found. Clastic grains are the bulk component, often with small amounts of quartz and/or calcite cement. All grains have a very thin and irregular coating of very finely granular hematite. This is also found concentrated in tiny pockets between the grains and in some patches there is sufficient to cement a few grains together (Slide A13). There is a conspicuous lack of any matrix.

Table 5 gives the proportions of the various constituents present in the sandstone. Quartz is the most abundant component, followed by feldspar and rock fragments. Ore is usually more abundant than the heavy minerals but in some cases the situation is reversed. Mica is present in all cases but one, and mostly in smaller quantities than ore; A117 and A125 (siltstone) contain more mica than ore.

Most quartz grains show plain extinction under polarized light. Less than 15 per cent of them show signs of having suffered deformation in the source area. Of these deformed grains those with undulose extinction are commonest. Ruptural shadows in grains are rare and only a very few grains show deformation lamellae. Bubble trains are likewise not often seen.



Plate 15

Flow casts in sandstone just above the basal conglomerate on Naus. Current from left to right.



Plate 16
Strongly pitted bedding plane surface possibly caused by rain. Ganaams-
Arush boundary.

Table 5. The composition of 20 sandstones. Approximately 1,000 counts

Sections A13, A91, A94, A115, A116 are grit and only the sand-size material of the groundmass was counted.

Specimen No.	Quartz	Felapar	Hematite	Rock fragments	Ore	Heavy minerals	Mica	Calcite	Colourless Clay	
A13	479	188	143	115	22	7	16	36	-	1006
A42	493	194	70	121	31	38	13	30	-	990
A43	533	205	126	93	22	15	8	-	-	1002
A44	542	187	123	118	11	5	6	-	-	992
A91	525	181	120	124	23	22	16	-	-	1011
A92	454	206	187	72	41	31	13	-	-	1004
A93	451	214	172	97	31	34	6	-	-	1005
A94	481	213	142	94	25	29	1	24	-	1009
A95	484	238	130	83	24	20	20	6	-	1005
A115	459	189	124	170	26	11	1	19	-	999
A116	464	208	84	144	22	8	-	62	20	1012
A117	428	203	202	89	18	44	28	2	-	1014
A118	394	215	233	63	38	40	12	9	-	1004
A119	432	217	191	64	33	35	15	14	-	1001
A122	423	226	230	50	35	28	10	4	-	1006
A123	480	227	157	96	39		1	-	-	1000
A124	465	185	206	86	39		19	-	-	1000
A125	486	125	278	27	26	8	46	-	-	996
A142	435	249	172	77	16	11	6	25	-	991
A151	495	264	8	162	13	32	4	2	20	1000

Potassic and plagioclase feldspar are present in variable proportions. Orthoclase, microcline and perthite all occur and Figure 8 gives an idea of the composition of the twinned plagioclase grains. Most grains are in the andersine range. Orthoclase and perthite are the commonest K-feldspars. Table 6 shows the K-feldspar/plagioclase proportions, but no trend is revealed.

The state of alteration of the feldspars differs greatly between grains on the same slide. Microcline is usually clear or only very slightly altered but orthoclase shows a complete gradation from only very slightly altered to completely sericitised grains; the strongly altered grains are the most common. Plagioclase may be unaltered or it may be so strongly altered that it becomes difficult to recognise, and a complete gradation between these two states can be found. Perthite is usually either clear or shows partial alteration.

The rock fragments are least abundant in the finest grained sandstone and most abundant and most variable in the grit. The commonest type is strongly altered, fine-grained lava. Several different types of sandstone are distinguishable in the sections, and granite fragments can be recognised in the coarser grades. The latter, however, are usually too coarse to give multimineralic fragments in the fine-grained sandstone and the grits themselves often contain large separate fragments of quartz and feldspar. Metamorphic rock fragments are least abundant. Sections A92 - A95 and All6 contain chert but this makes up less than one per cent of the slides. Felsite is a distinctive rock type in most sections but is not common and it is probably derived from the felspathic dykes and lavas in the Sinclair Formation.

Ore is present in quantities between one and four percent and together with the heavy minerals it makes up between 1.5 percent (Slide A44) and 7.8 percent (Slide All8) of the thin sections. It occurs mainly in two forms, one as a grain with distinct boundaries and the other as a very diffuse grain which in reflected light shows much of the material to be of the same red colour as the intergranular hematite. In some cases ore and heavy minerals are concentrated together in lamellae parallel to the bedding. (Slide A42).

Fig. 8.

Maximum extinction angle of Albite twins for 279 plagioclase grains.

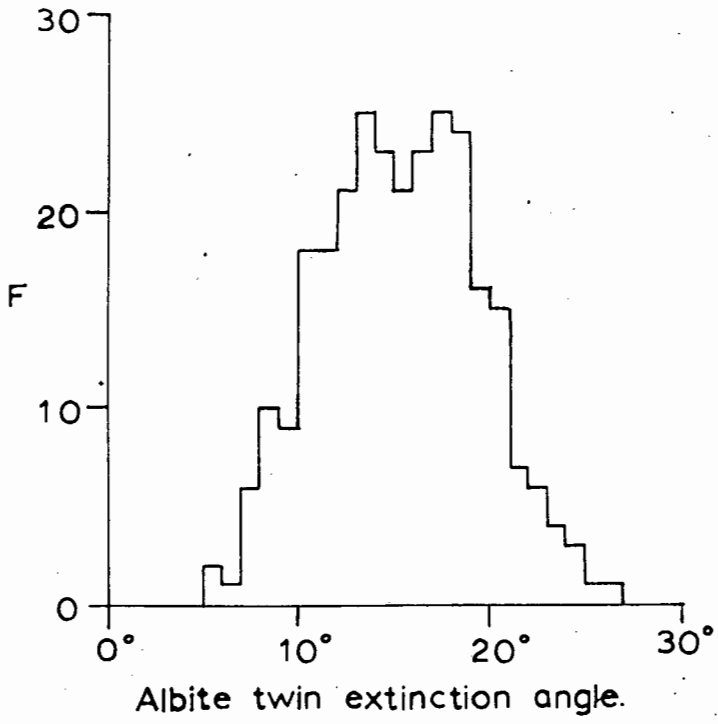


Table 6. Relationship of K-felspar: plagioclase, and muscovite: biotite ratios to mean diameter of the grains in thin section and standard deviation.

Slide No.	K-Felspar: plagioclase	Muscovite: Biotite	mean diameter mm	Standard deviation
A92	34:66	83:17	.071	.032
A119	45:55	54:46	.074	.034
A93	21:79	56:44	.083	.069
A117	12:88	39:61	.083	.044
A95	21:79	49:51	.084	.041
A94	50:50		.087	.036
A142	18:82	66:34	.102	.043
A44	42:58	32:68	.102	.055
A118	35:65	70:30	.108	.107
A42	39:61	37:63	.108	.058
A43	38:62	36:64	.108	.051
A151	41:59		.121	.062
A115	52:48		.194	.406
A13	27:73	51:49	.2	.261
A15		39:61	.205	.211
A91	45:55	65:35	.239	.277
A116	52:48		.454	.485
A122	4:96	66:34		
A124		63:37		
A125	30:70	56:44	+/- .035	

Both muscovite and biotite are present in quantities that vary considerably and apparently randomly. Muscovite is a little more common than biotite in the thin sections. It is usually clear or it may show slight alteration. Biotite on the other hand is rarely unaltered, though unaltered grains do occur along with altered grains in many of the thin sections. The state of alteration ranges from clear biotite to non-pleochroic grains which consist mainly of red fine-grained hematitic ore. These grains are often difficult to recognise as having been biotite. The gradational state of alteration of the different grains is the main aid to identifying them. Their outlines are sharp and they have a similar shape to the partly altered grains. There are few grains of green biotite. Table 6 shows the muscovite/biotite ratio for 100 grains to be in random relation to the standard deviation and arithmetic mean diameter. There is also no relationship between K-felspar/plagioclase and muscovite/biotite ratios.

Calcite is not ubiquitous and on an average forms only two percent of the slides where it is present, although All6 contains more than six percent. It acts as a cement but usually only fills small intergranular pockets. In a very few cases where it is more abundant it encloses clastic grains completely, indicating a pre-consolidation introduction or at least an introduction contemporaneous with consolidation. For the rest it has no tendency at all to surround grains. The larger patches can be optically continuous or can be made up of several crystals.

The proportions of intergranular hematite given in Table 5 are probably higher than the true values because of its being opaque, and to the fact that the film surrounding grains is apparently thicker in inclined section. It forms very thin, irregular coats on all grains but does not act as a cement. Occasional small concentrations look as if they may be cementing a few clastic grains together. This hematite always has the same very fine granular texture irrespective of whether it is in the form of thin grain coatings or small intergranular concentrations.

Colourless clay-size material was only found in sections All6 and Al51, and is noticeably absent in the others. Al51 is a specimen of a two foot thick drab-coloured bed on Aubures (C7) and has very little hematite in it. Very fine crystalline material can be seen between the grains.

In some cases decolored spots also show this material but it seems unlikely to be clay, because X-ray diffraction on very fine-grained samples revealed no clay or only very little. A rock slice of specimen Al26, a shale, showed quartz, feldspar and hematite, but no clay. Four acetone smears of clay-size material, found in 1-3 mm thick lamellae on bedding planes and between mud cracks, were run. One revealed no clay, another a very small mica peak at 10.03A, and the other two gave only small peaks at 14A (chlorite/montmorillonite), 9.8A (mica) and 7A (kaolinite/chlorite). In these the other constituents were again quartz, feldspar and hematite. The conclusion is therefore that there is an overall lack of clay minerals and those present are concentrated in clay-size material that settled on the bedding planes formed by coarser material. But even here clay minerals only constitute a very small percentage of the total.

Table 7 shows the composition of the sandstone, with only the clastic constituents being taken into account. According to Pettijohn's (1957, p.291) classification table, the sandstone varies between arkose and feldspathic sandstone. Figure 9 disregards minor constituents and shows quartz, feldspar and rock fragments recalculated to 100 percent. The quantities of these three constituents do not vary markedly, even in the ground-mass of some of the grit specimens (Sections Al3, A91, Al15, Al16). Al25 (a siltstone) has less feldspar and rock fragments than the sandstone. This is probably due to a longer period of transport of the finer-grained material and consequently a longer period of exposure to chemical and mechanical erosion.

Table 8 indicates that for the grit samples observed, lavas are the commonest larger size rock fragment. There are roughly equal quantities of quartz, feldspar and granite, only small quantities of quartzite and sandstone and even fewer metamorphic rock fragments and chert.

Figure 10 shows histograms of the long diameters of feldspar, quartz and rock fragment grains in 18 thin sections of sandstone and grit. These show a range in size from 0.03 mm to 3.56 mm. The arithmetic mean long diameter varies from 0.071 mm in A92 to 0.454 mm in Al16. The sandstone sections all show a mean diameter in the range of very fine-grained sandstone. The sand size material

Table 7. Composition of 20 sandstones showing clastic constituents only.

Specimen No.	Quartz	Felspar	Rock fragments	Ore	Heavy minerals	Mica
A13	57.9	22.7	13.9	2.7	0.8	1.9
A42	55.3	21.8	13.6	3.5	4.3	1.4
A43	60.6	23.2	10.6	2.5	1.7	0.9
A44	62.3	21.5	13.6	1.3	0.6	0.7
A91	59.0	20.3	13.9	2.6	2.5	1.8
A92	55.5	25.2	8.8	5.0	3.8	1.6
A93	54.1	25.7	11.6	3.7	4.1	0.7
A94	57.1	25.3	10.8	3.0	3.4	0.1
A95	55.6	27.4	9.5	2.8	2.3	2.3
A115	53.7	22.1	19.9	3.0	1.3	0.1
A116	54.9	24.6	17.0	2.6	0.9	-
A117	52.9	25.1	11.0	2.2	5.4	3.6
A118	51.7	28.2	8.4	5.0	5.3	1.6
A119	54.2	27.2	8.1	4.1	4.4	1.9
A122	54.8	29.3	6.5	4.5	3.6	1.3
A123	56.9	26.9	11.4	4.6		0.1
A124	58.6	23.3	10.8	4.9		2.4
A125	67.6	17.4	3.8	3.6	1.1	6.4
A142	54.8	31.4	9.7	2.0	1.4	0.8
A151	51.0	27.2	16.8	1.3	3.3	0.4

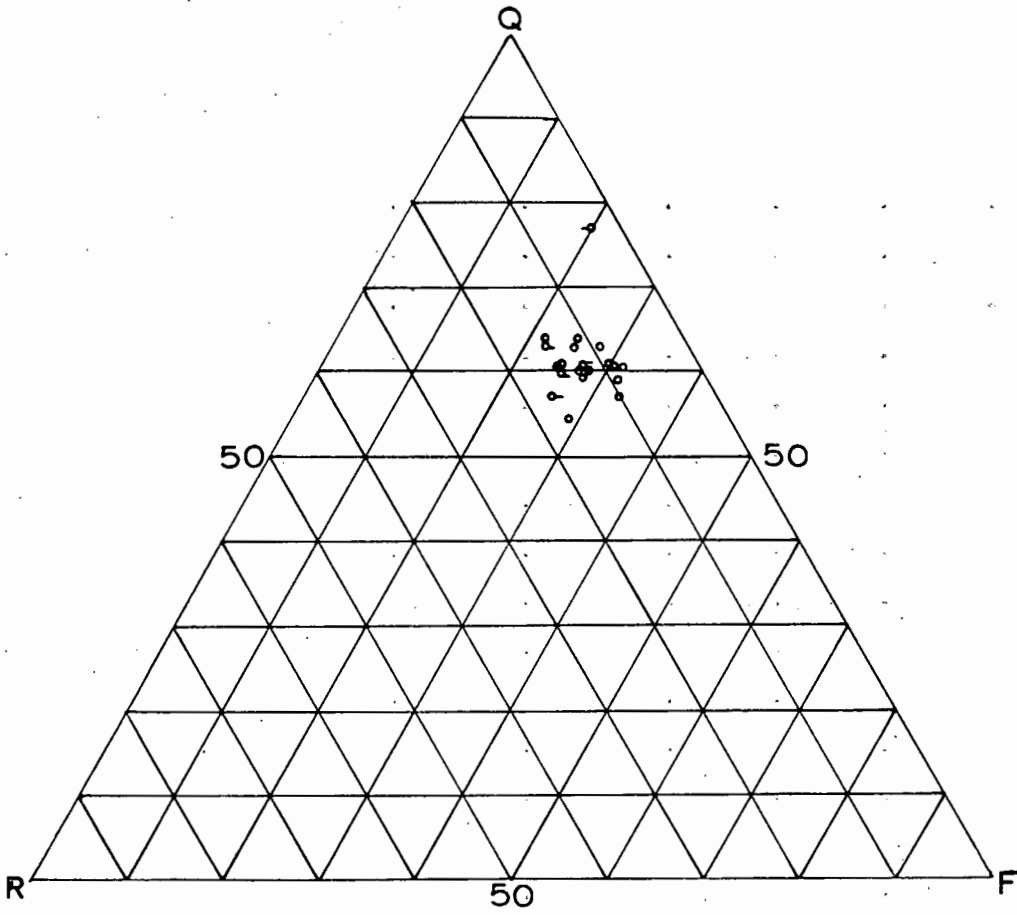


Fig. 9.

Classification chart for 20 samples (main clastic constituents).

• Matrix of grits (4 samples)

• Coarse siltstone

• Sandstone

Q - quartz

F - feldspar

R - rock fragments

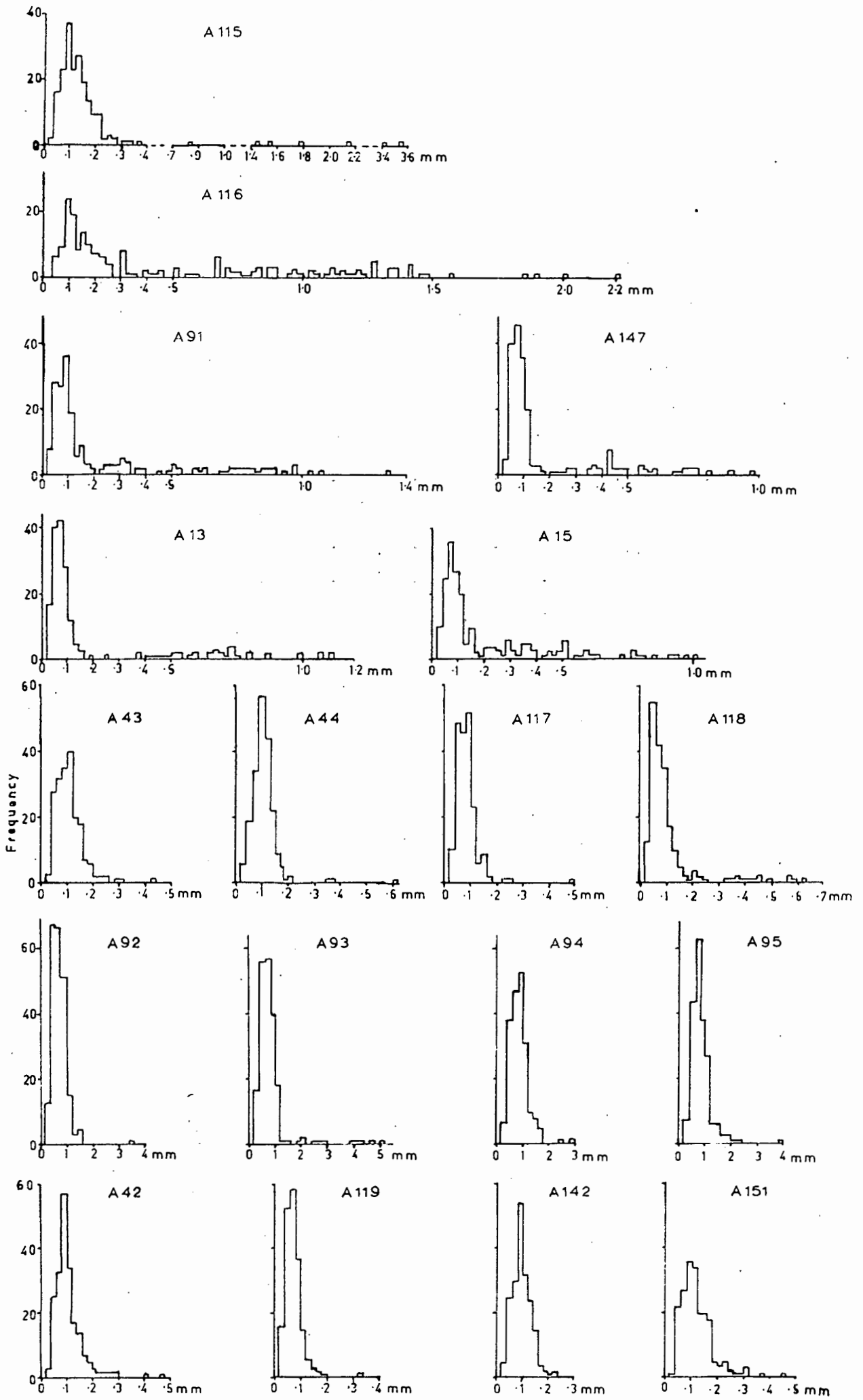


Fig.10. Thin section grain size distribution, long diameter.

Table 9. Arithmetic mean long diameter of 18 thin sections corrected to the equivalent sieve size mean. After Friedman, G.M., (1962, p17).

Specimen No.	Thin section \bar{x} mm	Corrected \bar{x} mm	Thin section standard deviation
A13	.2	.17	.261
A15	.205	.173	.211
A42	.108	.095	.058
A43	.108	.095	.051
A44	.102	.090	.055
A91	.239	.20	.277
A92	.071	.061	.032
A93	.083	.074	.069
A94	.087	.077	.036
A95	.084	.075	.041
A115	.194	.165	.406
A116	.454	.369	.485
A117	.083	.074	.044
A118	.108	.095	.107
A119	.074	.066	.034
A142	.102	.090	.043
A147	.181	.157	.208
A151	.121	.106	.062

Table 10. Sand-size material (up to .4 mm) of grits. Mean long diameter corrected to equivalent sieve size mean.

Specimen No.	Thin section \bar{x} mm	Corrected \bar{x} mm	Thin section standard deviation
A13	.073	.062	.032
A15	.128	.111	.097
A91	.118	.104	.148
A115	.125	.11	.092
A116	.151	.13	.073
A147	.08	.072	.033

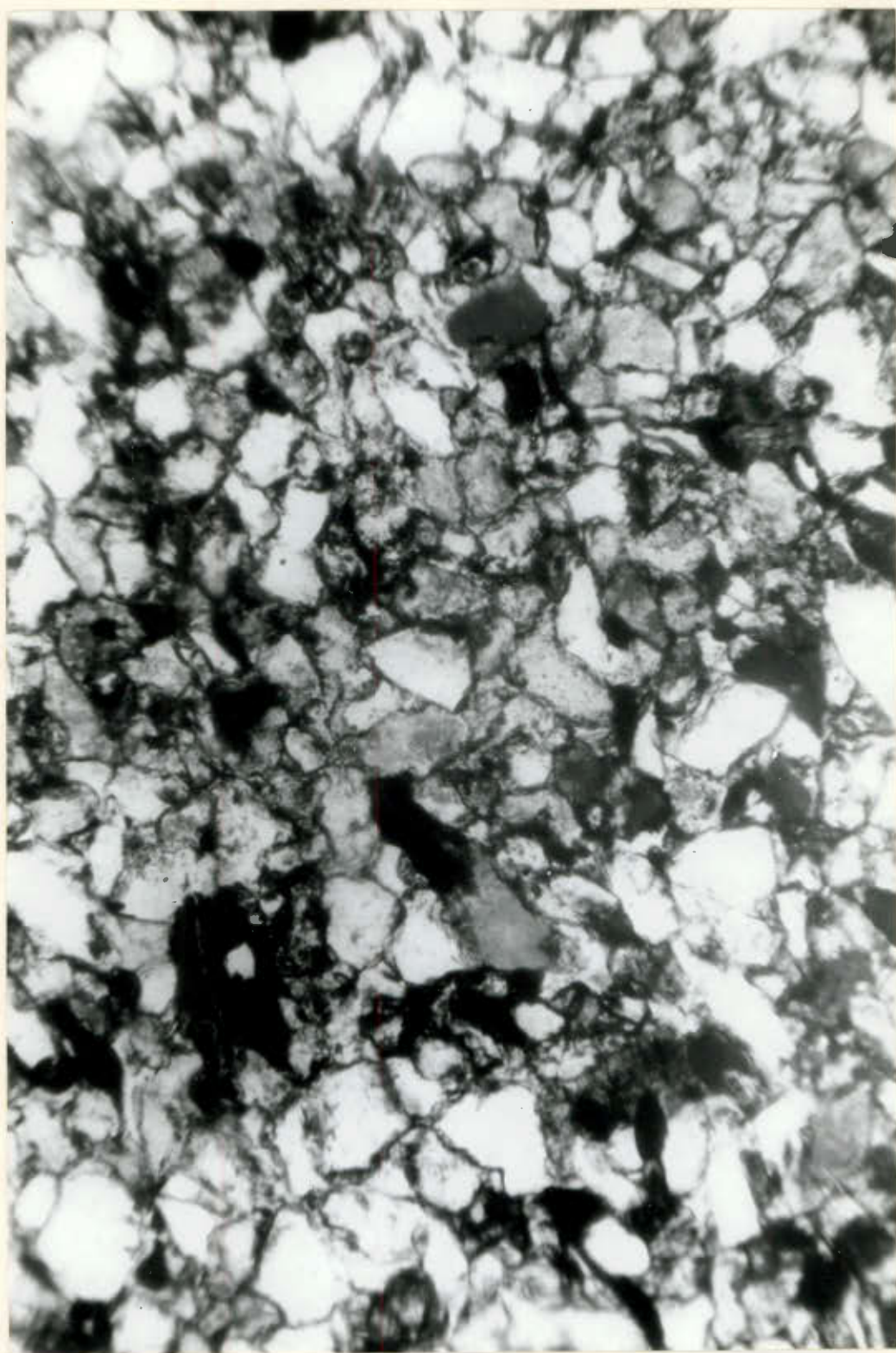


Plate 17

Slide A92, ordinary light, x 120. The section shows good sorting, and a very small grain size. Grain contacts are sutured, compaction is good and the hematite is easily visible as a coating on all the grains. Grains are from angular to sub-rounded. Average grain size, .071 m m.

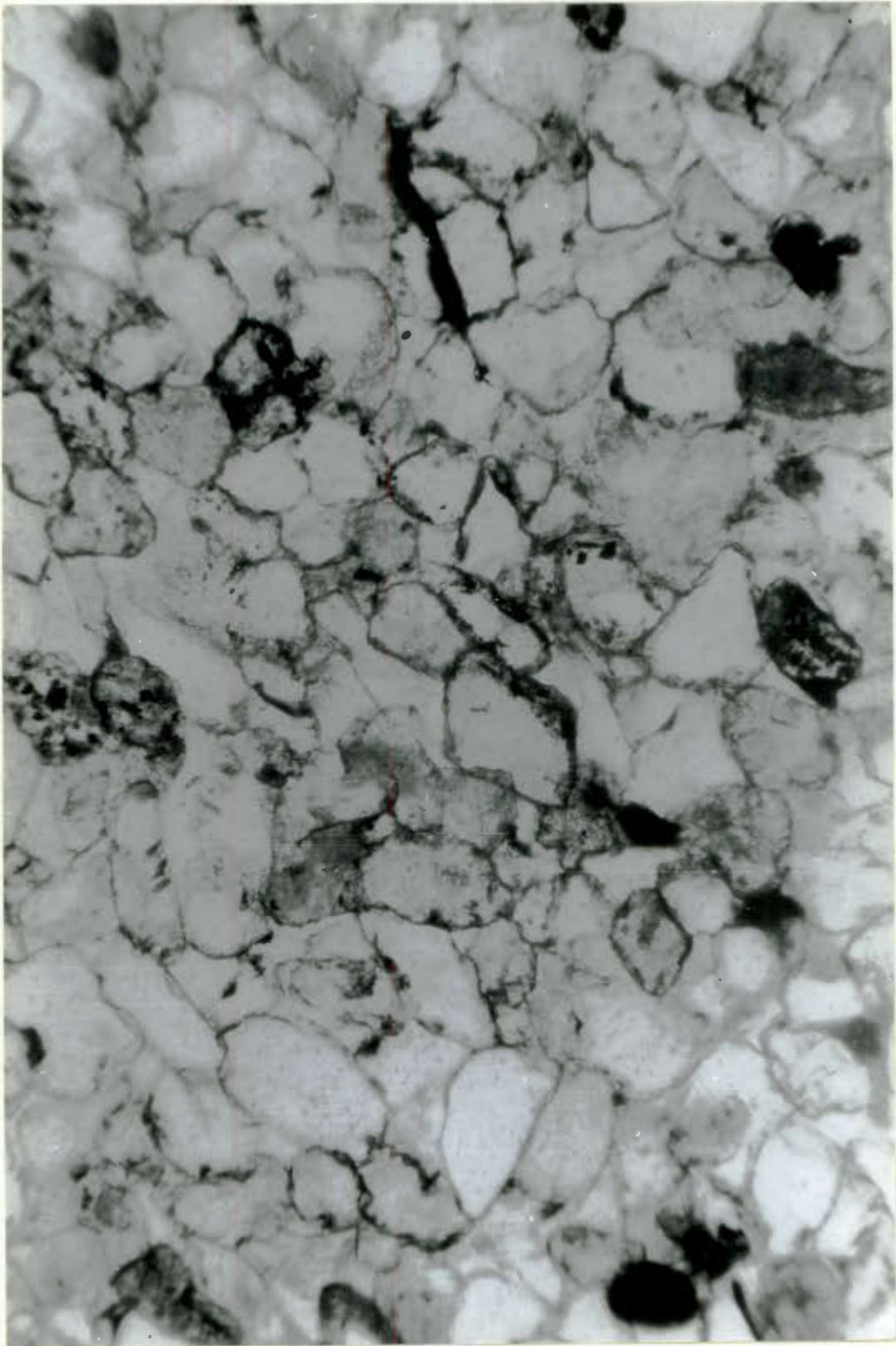


Plate 19

Slide A44, ordinary light, x 120. The section is composed of rounded and well rounded grains that show good sorting. There is a slight sub-parallelism of the long grains and many contacts are sutured. Uncross-bedded sandstone on Naus. Average grain size .102 m m.



Plate 20

Slide A43, ordinary light, x 120. Cross-bedded sandstone on Naus. This shows a strong sub-parallelism of long grains and rounding from sub-angular to sub-rounded. Some grain contacts are concave-convex. The average grain size is .108 m.m. This is one of the largest values for the pure sandstone.



Plate 21

Slide A116, ordinary light x 42. A grit containing grains of quartz and various lavas. Sorting is poor and the matrix grains are angular to sub-angular. As with the other sections there is a notable absence of very fine material.

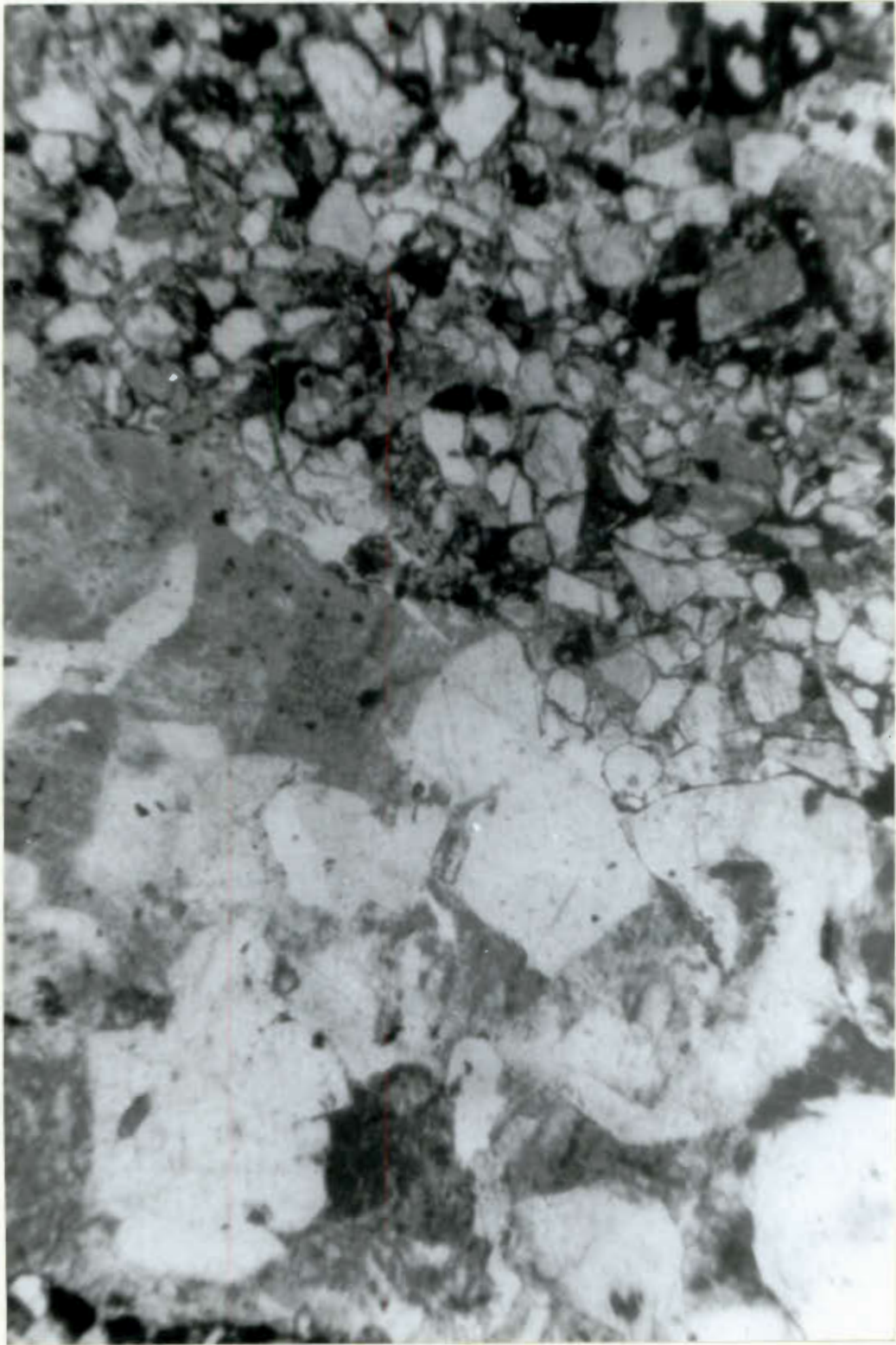


Plate 22

Slide A115, ordinary light, x 42. A large granitic grain set in a matrix of grains that are mainly angular and sub-angular.

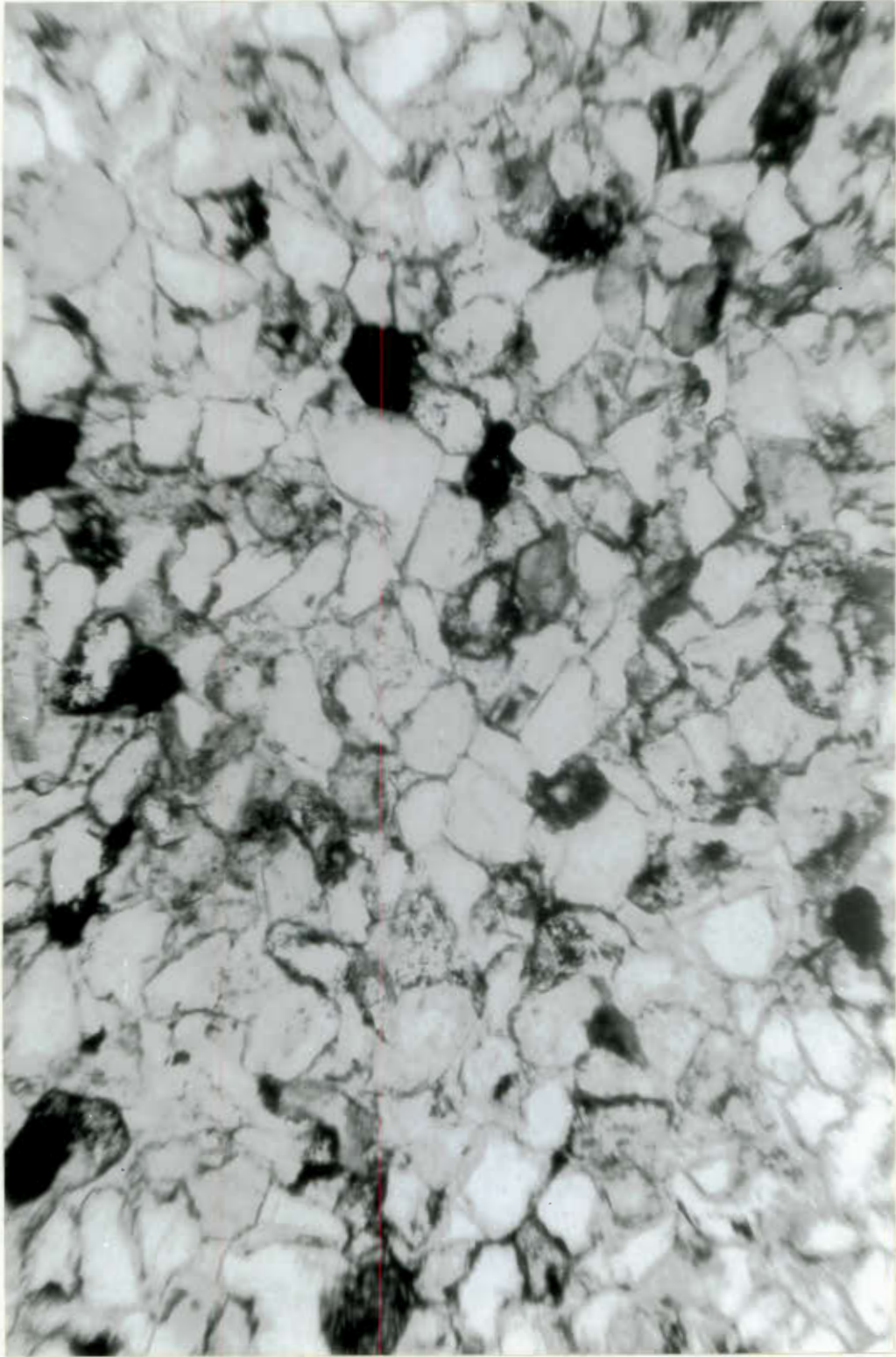


Plate 23
Slide A123, ordinary light, x 120. The grains are
mainly sub-angular. Sorting is good.

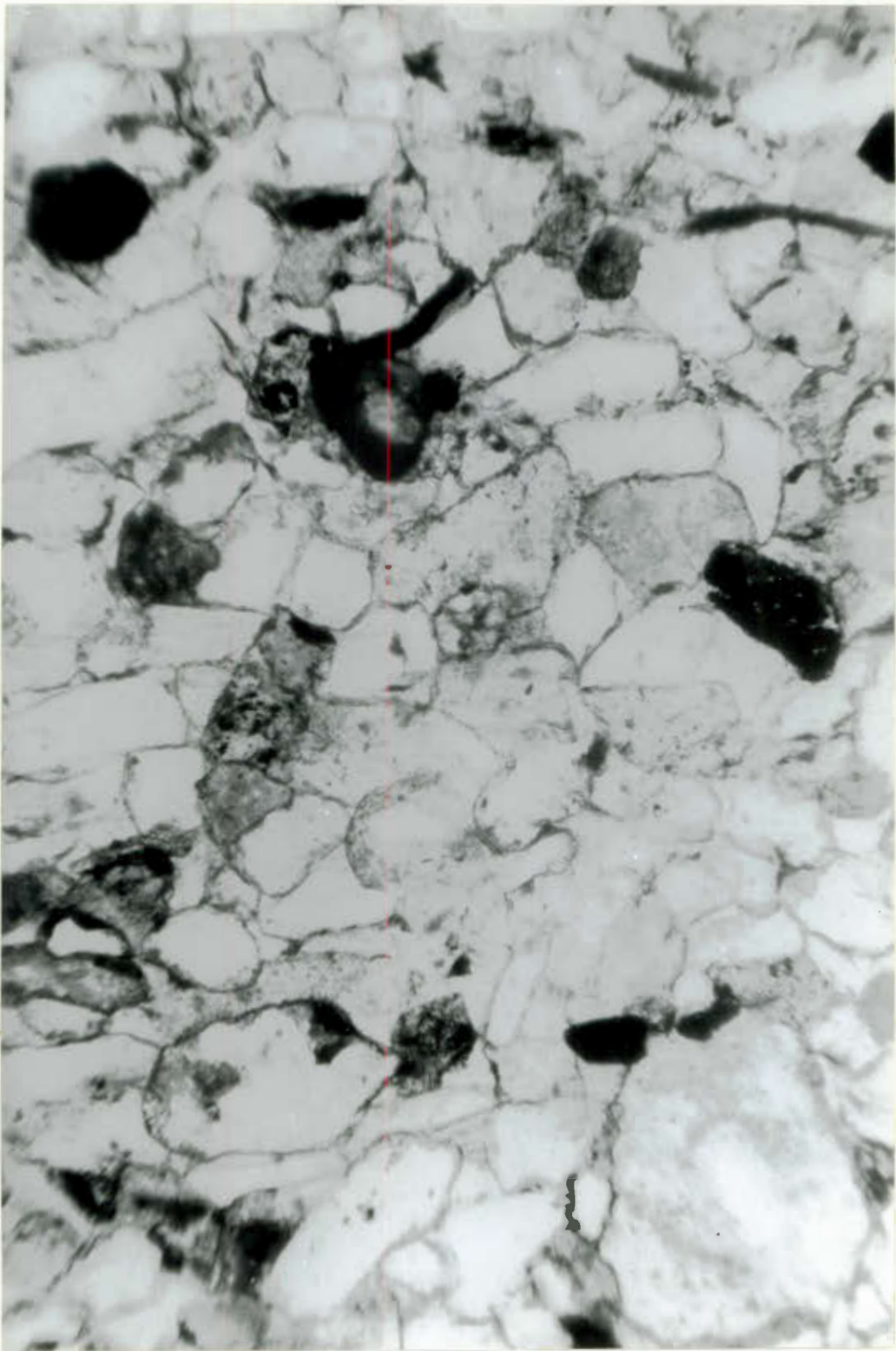


Plate 24

Slide A43, ordinary light, x 120. The grains are mainly sub-rounded. As in plate 19, this slide again shows a good sub-parallelism of long grains. There are a few long and a few concavo-convex grain contacts and a very few sutured.

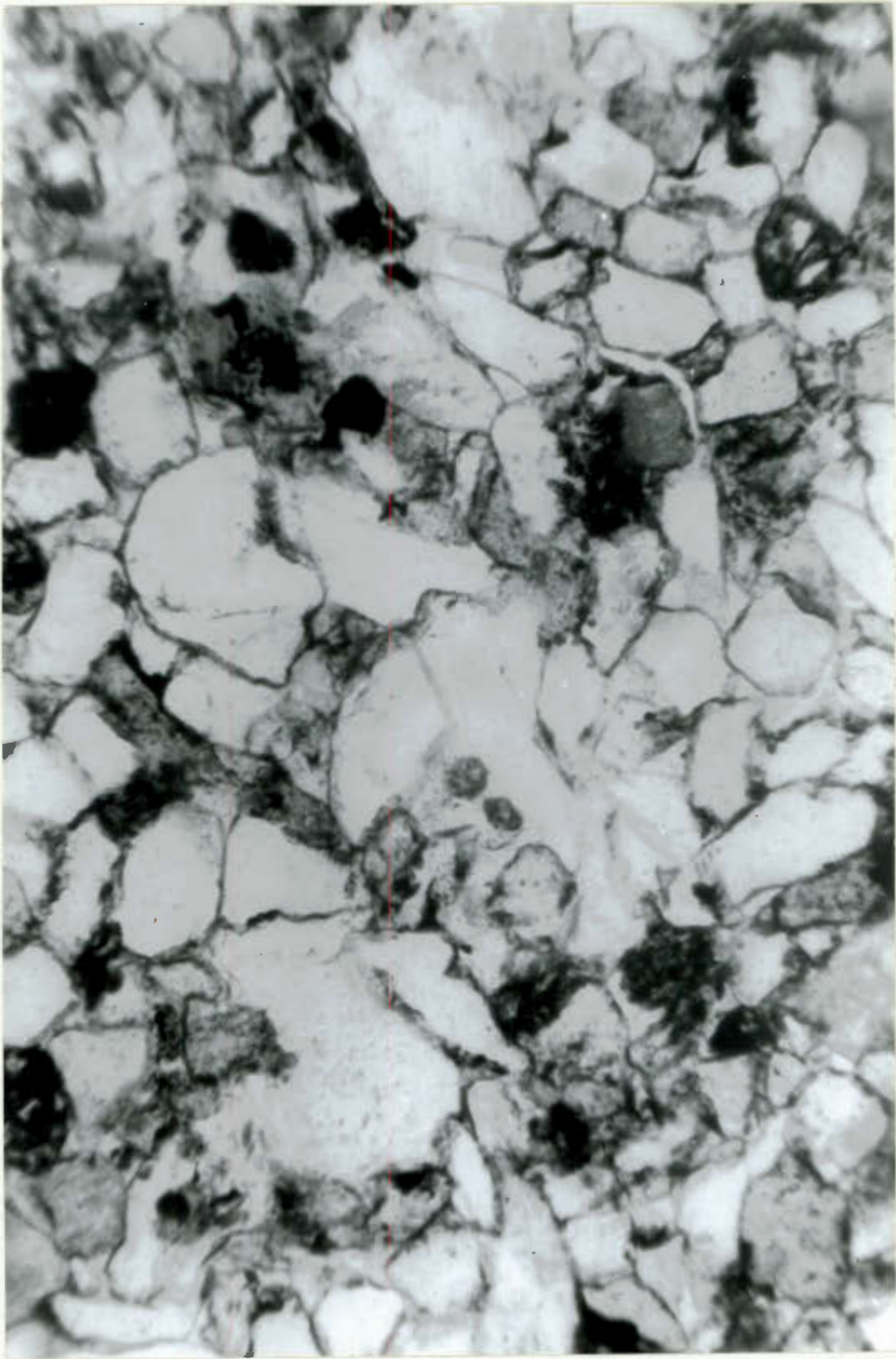


Plate 25

Slide A142 ordinary light, x 120. Two angular grains in the centre of the photograph are embedded in quartz cement and outlined by a thin coat of hematite. Quartz cement is present in other intergranular spaces in the slide.

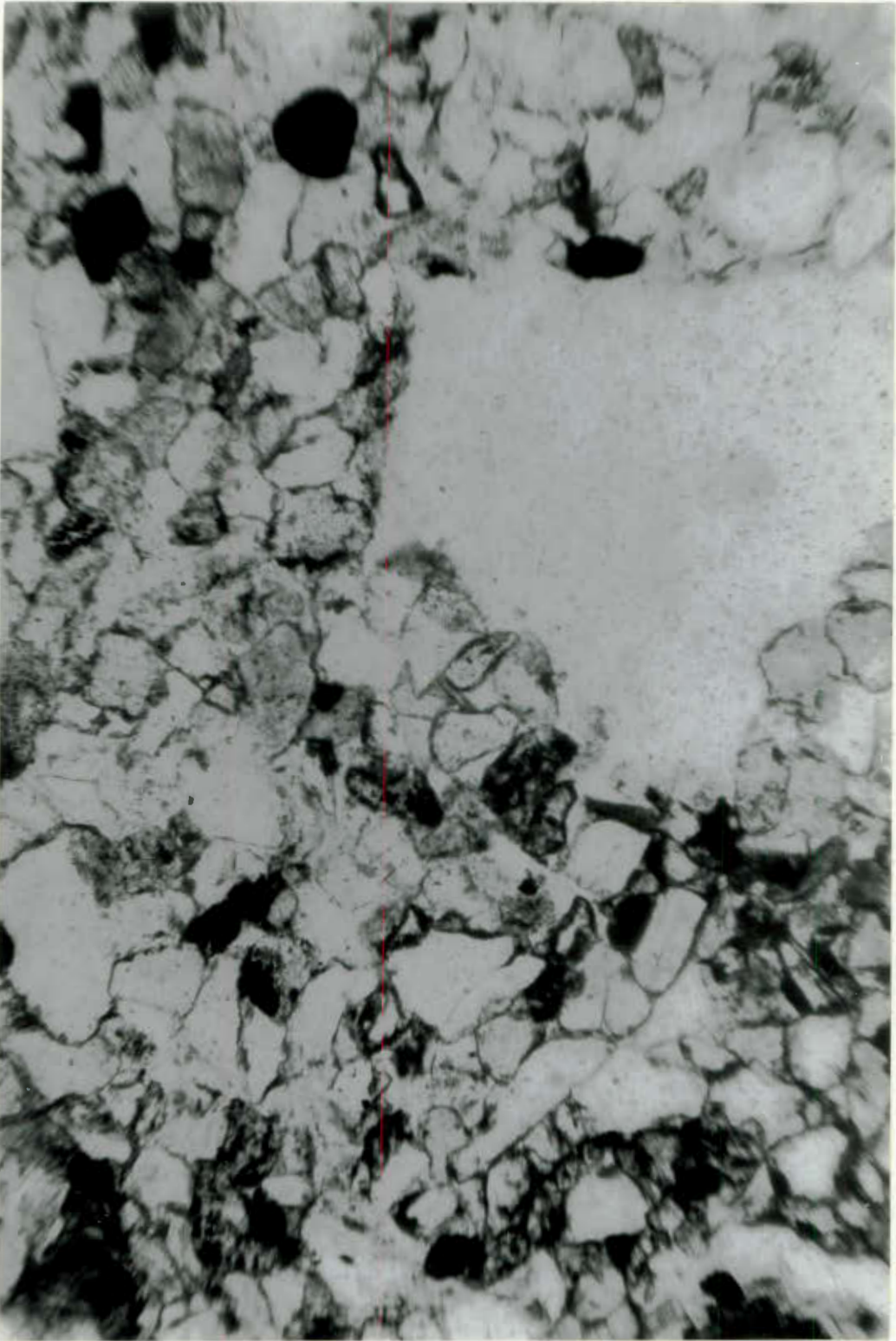


Plate 26

Slide A13, ordinary light, x 120. Strong recrystallization of the large quartz grain has almost engulfed several smaller grains.

(up to 0.4 mm) of the grit has, with exception of A116, a mean diameter below 0.125 mm. Friedman (1962) drew up charts for the correction of thin section grain size dimensions to the equivalent sieve analysis sizes. He found linear relationships between mean, mean deviation and standard deviation but no relationship for skewness or kurtosis. Tables 9 and 10 shows the arithmetic mean long diameter in thin section corrected to the corresponding sieve size mean. The corrected values are all smaller in size than the thin section means and these values are probably very close to the mean intermediate diameter of the grains.

Specimens A94 and A15 are of sandstone lenses interbedded in conglomerate and although the thin section mean diameter, up to 0.4 mm, is 0.128 mm in A15 the histogram has a peak at 0.07 mm. The mean of A94 is 0.087 mm. These values are the same as those for the sandstone. The standard deviation of all the specimens is low, but that of the sandstone especially so, thus indicating very good sorting. Most of the sand-size material, up to 0.4 mm, in the grit also shows very good sorting.

Plates 17-20 show an increase in grain size from a mean in Plate 17 (A92) of 0.071 mm to 0.108 mm in Plate 20 (A43). All show very good sorting and Plate 17 (A92) has a standard deviation of 0.032. Plates 21 (A116) and 22 (A115) show the much poorer sorting of the grit.

There is a variable degree of rounding of sandstone grains from angular to well rounded with good sphericity of some grains. The majority of thin sections show grains that are partially rounded but are nearer sub-angular than sub-rounded. Plates 22, 23, 24, and 19 show a gradation from an angular groundmass in Plate 22 through sub-angular (Plate 23, A123) and sub-angular to sub-rounded (Plate 24, A43) to sub-rounded to rounded (Plate 19). Some grains of quartz and felspar have a very good sphericity and it may well be that the former are second cycle grains. Rock fragments are quite often well rounded.

The grain shape varies largely from roughly equidimensional to long. Often, in sections cut parallel to the bedding, the long grains show a very noticeable sub-parallelism of their long axes. This can be seen in Plates 18, 19, 20 and 24. In other sections there is no tendency to this orientation.

minerals contained by these fragments would eventually become separate clastic grains.

After sieving the samples were washed and dried and a small bromoform separation was carried out so as to determine whether identification of the heavy crop would be hampered in any way by the hematite. It still coloured the grains red and in many cases made identification difficult. Quartz and felspar had also been brought down in considerable quantities with the heavy minerals. Apparently hematite does not always remain coating individual grains after crushing: Dr. A.O. Fuller of the University of Cape Town, at present working on Karroo red beds, does not find any of his heavy mineral grains coated with it (verbal communication). Its persistence after crushing in the present study must therefore be due, in part at least, to the very good compaction of the sandstone, the slight recrystallization that has taken place, and the crystalline state of the hematite itself.

It was therefore necessary to treat the sieved samples with warm dilute HCl until the hematite coatings had dissolved. This process required two washings, and meant that apatite, which is present in many thin sections, was lost. The amounts of quartz and felspar brought down were also greatly reduced. Centrifuging and separation in bromoform then followed. To facilitate identification the samples were run through a Frantz Isodynamic Separator so as to obtain a greater concentration of each type of mineral. Separations were made for every 0.1 amp increase in amperage from 0.2 - 1.5 amps. All these fractions were weighed.

Although ore separated out first, opaque minerals were found in each separation from 0.2 to 1.5 amps and, together with ore, they were the most abundant component of nearly every sample. Garnet followed ore, then a flood of epidote between 0.5 and 0.9 amps characterised most samples. Sample A103 has a conspicuous lack of epidote compared to the others. Zoisite, clinozoisite and tourmaline separated between 0.5 and 1.5 amps and monazite and zircon were the commonest minerals in the fraction that remained after 1.5 amps. 120 grains from each separation were counted. The counts for each separation are so small that bias must be present but the actual process of separation should eliminate this factor to some extent. The large number of counts (2040) for

the whole sample should also reduce bias. The number of attached and loose grains of quartz was also noted. The final results on Table 11 are expressed as a weight percent of the heavy crop. This was obtained by calculating the proportion by weight of each mineral in each separation and totalling the resulting values.

In calculation of the final results care needs to be taken if any one mineral has suffered undue breakage. All garnets are sub-angular and angular and some grains may have been broken. Occasionally long grains of tourmaline and zircon have also suffered breakage, as is easily seen by a rounding of one end and a distinct angularity of the other. The smaller grains of these two minerals as well as grains of epidote, monazite, zoisite and clinozoisite are rarely broken.

The counting of every grain, although introducing error from breakage, eliminates the error of giving large grains too great a frequency in parallel traverse counts where every grain touching the cross hairs is counted. Here grains with a greater volume will have a greater chance of being counted. Volume error is introduced into this study when converting the proportions of each mineral type in the separations into weight proportions. Large grains would have a weight proportion less than that of the true value and small grains greater than that of the true value.

The number of attached and loose grains of quartz was noted, the weight proportions calculated and subtracted from the total sample weight. The total weight of the heavy minerals is expressed as a weight percent of each 500 gram sample at the bottom of Table 11. There is a range from 0.16 - 0.86 weight percent. An idea of the size of the various grains can be obtained from the scale of Figures 11 and 12. At the end of the counting all the separations were again put together and thoroughly mixed for five minutes. Canada balsam slides were then made of each sample.

Ore: only a very small quantity of magnetic ore was removed with the hand magnet. Five samples from separations of 0.2 amp - 0.4 amp were run on the X-ray Diffractometer to determine what type of ore mineral was present. In each case it was found to be α Fe_2O_3 , or specularite. It is probable that all the opaque grains appearing after a certain amperage are something other than specularite, but large samples need to be crushed

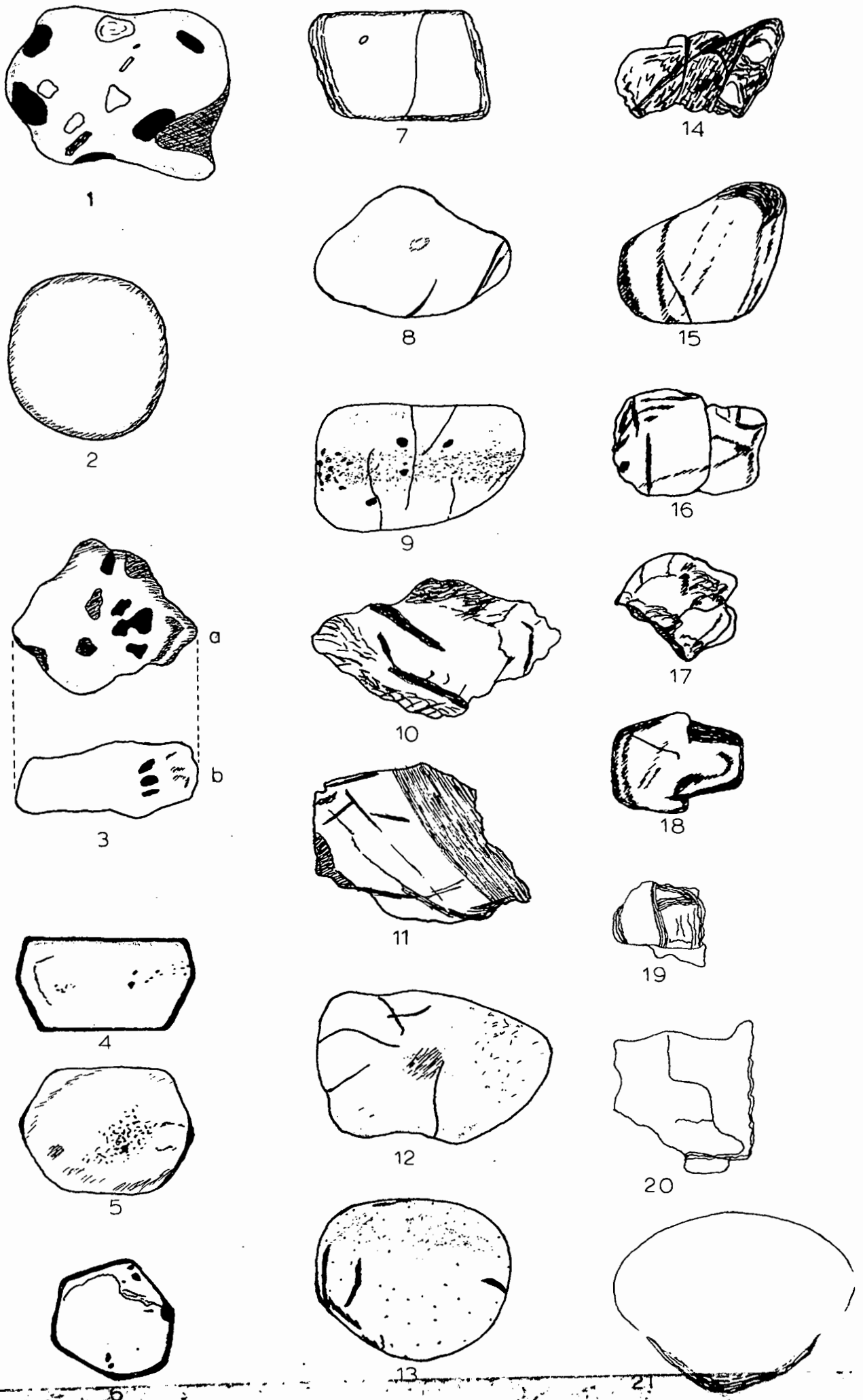


Fig.11—Various grains from the heavy-mineral crop. 1-3 monazite (3, in 3 dimension). 4-9 tourmaline. 10-11 garnet. 12-14 epidote. 15-16 zoisite. 17-18 clinozoisite. 19-21 mica. x 360

Table 11. Heavy mineral composition of 9 sandstones.

Weight percent.

Specimen No.	A16	A45	A49	A99	A100	A101	A102	A103	A104
Ore	9.70	56.3	36.48	72.35	66.05	60.00	47.3	61.35	45.5
Garnet	0.04	0.34	0.04	0.14	6.84	3.03	0.02		0.12
Epidote	82.5	34.39	50.45	19.59	18.13	22.92	41.00	0.80	26.09
Zoisite	4.91		1.93		0.11		0.04		
Clinozoisite	0.37	0.01	0.20	0.20	0.07	0.01	0.04		0.01
Colourless Monazite	0.32	0.82	4.43	3.98	4.26	8.28	7.38	2.22	9.97
Brown Monazite		0.15	0.14	1.08	0.56	0.95	0.71		0.51
Mica	0.12	2.12	0.34	0.77	0.09	1.06	0.03	Tr	0.18
Chlorite		0.05	0.01						
Rutile	0.05		Tr						0.04
Brookite			0.41					1.16	0.38
Hypersthene	Tr		0.01						
Hornblende		0.01							
Fluorite		5.16							
Xenotime	Tr								
Brown Zircon	0.16	0.34							
Lt. Brown Zircon			0.03		0.48		0.95		0.20
Colourless Zircon	0.85	0.07	4.03	0.85	1.10	1.70	2.59	30.48	10.29
Tourmaline	0.52	0.59	1.51	1.09	2.10	2.22	0.51	3.38	6.67
Weight percent of 500gm. sample	0.22	0.35	0.29	0.72	0.86	0.48	0.30	0.16	0.18

Epidote and ore show a good linear antipathetic relationship for specimens A16 - A102, but A103 and A104 have a much greater proportion of ore. There is also a correspondingly greater proportion of tourmaline and zircon in these two samples and in A104 monazite as well.

Table 12. Characteristics of colourless and light brown zircon.

Weight percent of heavy mineral crop,

R = rounded and L = euhedral and
sub-rounded sub-angular

Specimen No.	Inclusions						No Inclusions					
	Non-Zoned		Zoned				Non-Zoned		Zoned			
			Core Zoned		Edge Zoned				Core Zoned		Edge Zoned	
	R	L	R	L	R	L	R	L	R	L	R	L
A16	.16	.20			.16	.07					.16	.10
A45	.03							.01			.03	
A49	.41	.08			.60	.68	.60	.60			1.01	.68
A99	.39					.10	.05				.34	
A100	.45	.18			.23	.09	.09	.05	.05		.32	.14
A101	.09	.19			.28	.09	.28	.28			.47	
A102	.20	.13			.33	.53	.20	.40		.20	.53	1.00
A103	3.59	2.34	.31	.16	5.30	4.84	1.24	1.40	.62	.78	5.30	4.68
A104	.81	1.29			2.74	.32	.48	1.13			1.45	2.25

Table 13. Classification of Tourmalines.

Weight Percent of Heavy Mineral Crop.

✓ Contain Inclusions; R subrounded and well rounded; L Euhedral and angular fragments

Colour											
E	O	A16	A45	A49	A99	A100	A101	A102	A103	A104	
Lt. brown	Brown	R		.23	.15				.15		
		L	.09	.10	.13				.08		
Lt. brown	Rust red-brown	R					.08	.02		.11	
		L		.02				.09		.11	
✓ Lt. brown	Rust red-brown	R	.02	.01							
		L									
Colourless	Lt. brown	R		.04					.08	.11	
		L		.06	✓ .03	.1		.02	.05	.22	
Yellowish brown	V dk. brown	R								.04	
		L				.5					
V lt. brown	Dk. olive green	R	.05				.16		.05	.07	
		L					.24		.15	.18	
✓ V lt. brown	Dk. olive green	R	.02								
		L	.02							.04	
V lt. brown	Green brown	R		.06	.18			.10	.04	.07	
		L		.15	.09		.08	.22	.10	.63	
Lt. brown	Dk. green brown	R	.14	.01						.22	
		L	.07	.09						.81	
Lt. green brown	Dk. green brown	R			.06		.24		.11	.33	
		L			.18	.4	.47		.34	.37	
✓ Lt. green brown	Dk. green brown	R									
		L					.08		.01	.04	
Colourless	Dk. green blue	R		.07							
		L		.16					.01	.04	
Colourless	Lt. green blue	R									
		L				✓ .03			.09	.70	
Colourless	Dk. green brown	R		.19					.16	.33	
		L							.59	.63	
✓ Colourless	Dk. green brown	R		.01					.03		
		L							.09	.04	

Table 13. continued

E	O		A16	A45	A49	A99	A100	A101	A102	A103	A104
Dk grey green	Black	R								.01	
		L								.03	
Green brown	Black	R						.07			
		L									.04
Colourless	Pale pink	R					.1				
		L									
Colourless	Colourless	R		.02							
		L		.02		.09		.07		.03	.18

to provide sufficient material for examination after separation. In the calculations, all opaque minerals have been regarded as being hematite and the S.G. of hematite used throughout.

Tourmaline: certain characteristics were considered during the counting of the tourmaline grains. These were (i) colour differences, (ii) varying pleochroic intensities, (iii) rounding of grains and (iv) presence or absence of inclusions. Shades of green, brown and blue are the commonest while pleochroism varies from colourless, E to black, O. Rare grains are light pink or completely colourless. Grains of the same colour can vary from angular to very well rounded. Where broken grains were encountered only the unbroken edges, if distinguishable, were considered. Euhedral grains were not uncommon. Since tourmaline is so hard (H=7) the well rounded grains are probably second cycle. Inclusions always seem to be limited to a central zone.

Table 13 gives details of 36 different tourmalines, with colour as the main distinguishing feature. Grains with only little colour differences have been grouped together, but these small differences may well be important in distinguishing two different types and one is always conscious of the need of a colour chart to give standard colours to work from. Specimens A103 and A104 have the greatest variety as well as the greatest quantity of tourmaline. Zircon is also far more abundant in these two samples than in any of the others.

Zircon: zircons have been distinguished on colour primarily. The lighter coloured grains have been further distinguished on roundness and angularity, presence or absence of inclusions and bubbles, presence or absence of zoning, and whether this zoning is confined to the core or just to the outer edges. Distinctions can also be made on the form and extent of the zones but this was not done. Although many grains are euhedral a large number are very well rounded and, like the well-rounded tourmaline grains, must be at least second cycle. Inclusions are usually colourless or opaque but occasionally rods of rutile can be recognised. In some grains these are arranged parallel to the C-axis. Larger crystals are sometimes broken.

Garnet: this is faint pink in colour and sub-angular to angular with an appearance of being very broken.

Epidote: epidote is usually rounded to well rounded and grains may be clear, contain tiny speckles or be strongly altered. It varies in colour from strong yellow-green to almost colourless. Pleochroism in all cases is weak.

Zoisite: zoisite is usually rounded to well rounded. Both clear and strongly altered grains are present.

Clinozoisite: clinozoisite may be angular or well rounded and is unaltered.

Monazite: monazite is either colourless or light yellow-brown in colour, is very well rounded, often has a good sphericity and often contains colourless and opaque inclusions and bubbles.

Mica: mica is very variable in size and usually angular but rounded plates can occasionally be seen. During the washing and separating processes much of the mica was lost, giving a paucity in the final result, but Table 5 gives the quantities present in thin section.

Chlorite: chlorite is fairly common in most thin sections but like the micas is uncommon among the separated heavy minerals.

Apatite: in thin section apatite is always well rounded. Its loss due to the use of HCl in the separating process has already been mentioned.

There are also rare grains of rutile, brookite, hypersthene, xenotime, colourless fluorite, and hornblende.

(3) Sedimentary Structures

(a) Cross-bedding and parting lineation

Cross-beds are the commonest structures in the sandstone and are most abundant on the farms Barby (E8), Naus (D8), Aruab(D6,7), Dabis (I6,7,J7), Guperas (H5) and the southern portion of Saraus (I5,6). They have an average thickness of 14 in. but vary from 3 in. to 10 ft. Only one bed of the latter thickness was found, just below the eastern Nama-Auborus contact on the Dabis-Saraus farm boundary (J7) in a sandstone bed in the conglomerate. Several beds about eight feet thick are scattered through the area. Both festoon and tabular cross-beds are present but the former are less common and are found in groups only about 10 ft. thick with

much interbedded, non-cross-bedded sandstone. Good exposures occur half a mile south-east of the Dabis homestead (J7). On Barby (E8) and Naus (D8) the festooned topsets of these cross-beds can be seen on bedding planes in a few places. The southernmost boundary beacon (D8) between these two farms is on a high hill of Auborus sandstone capped by Kuibis quartzite; just below the top of this is a 60 ft. thick bed made up of festoon cross-beds one after the other with no interbedded non-cross-bedded material. Being at the top of a hill this bed has a limited lateral extent, and searching elsewhere did not reveal it again, even on Grosskopf (D7). Plate 27 shows the curved foreset of a cross-bedded unit.

Tabular cross-beds form the majority of cross-beds on Barby (E8), Naus (D8) and Aruab (D6,7). They occur in groups of between two and five, one above the other and have a total thickness of between two and six feet. The lateral extent of one of the largest cross-bedded units on Barby (D8) was measured at 120 ft., but this figure may perhaps be exceeded elsewhere. These cross-bedded units show a very uniform dip of the foresets which may be tangential or non-tangential, and a thinning of the unit towards both ends. On Barby and Naus the groups occur at perpendicular intervals of every 10 - 50 ft., in zones of variable thickness from the base of the sandstone to about 2600 ft. above the base. They often form a small resistant ridge as high as the thickness of the group. Plate 28 shows the lateral extent of a cross-bedded unit and the small ridge that it forms.

Specimen A43 is of the cross-bedded material and A44 of the less weather-resistant, non-cross-bedded material. Examination of the thin sections reveals very little difference indeed. Except for a little less felspar and a few more rock fragments in A44, they show no difference in composition. Their mean grain diameters and standard deviations are very similar. A44 (Plate 19) shows a better overall degree of rounding than A43 (Plates 20 and 24), but both have tangential, concavo-convex, long and sutured grain contacts. There is a sub-parallelism of long grains in both cases, but in A43 it is better developed. This specimen also contains a higher percentage of long grains. This may indicate a better compaction of



Plate 27
Two cross-bedded units in sandstone on SW portion of Aruab. The curved foresets of the lowermost can be seen. Facing south, beds dip 12° west.



Plate 29
Febly and sandy grits containing two cross-bedded units. The fore-sets are only slightly curved. Such cross-beds in coarse grained sediments are usually very limited in extent, and more irregular than this.

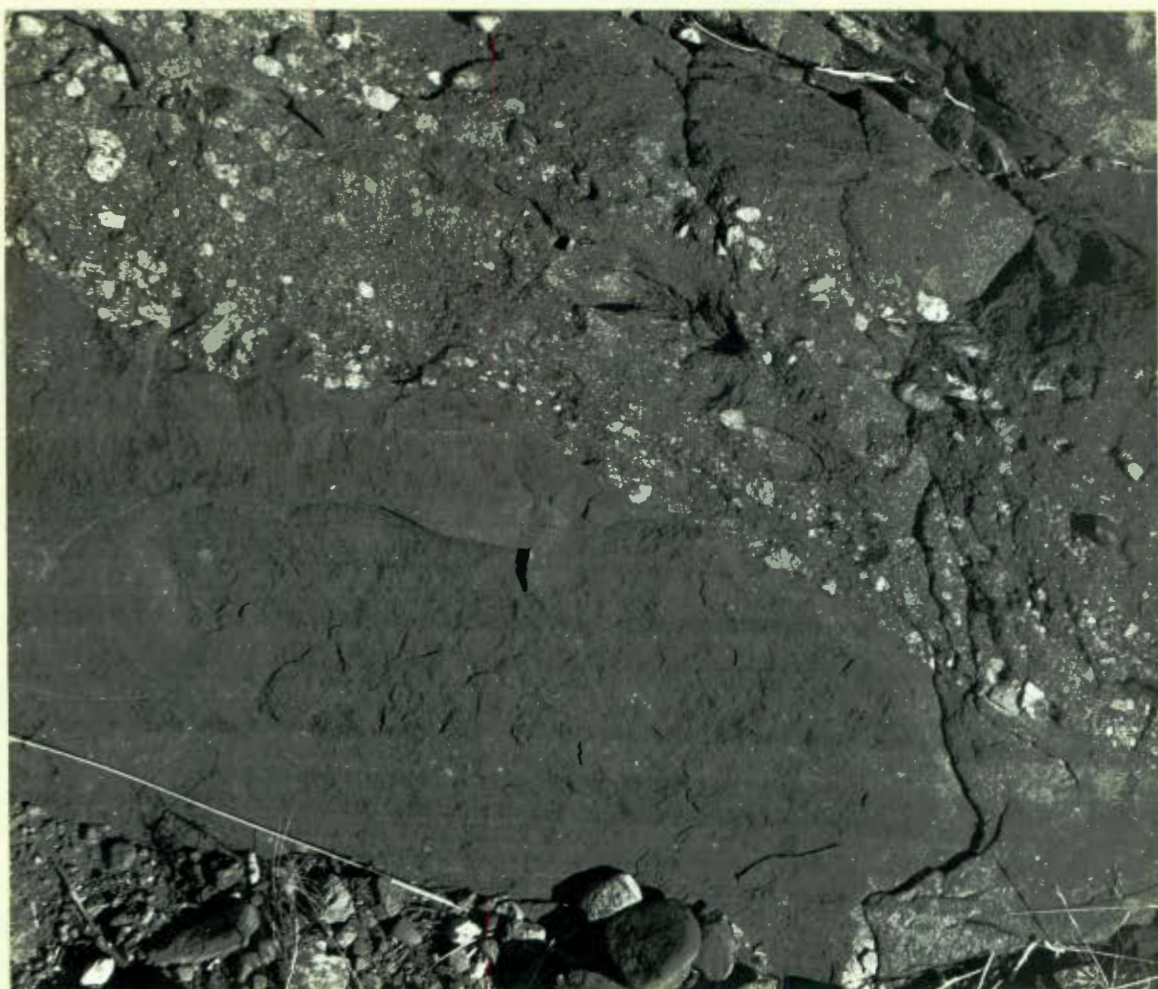


Plate 30
A pebbly grit cutting deep into very thinly bedded
and laminated sandstone.



Plate 31
The uneven base of a conglomeratic grit can be seen
cutting the underlying thinly bedded and laminated
sandstone. Bedding in the grit can also be seen.

Fig. 13. Poles of Cross - beds just west of Aruab beacon.

(200 readings).

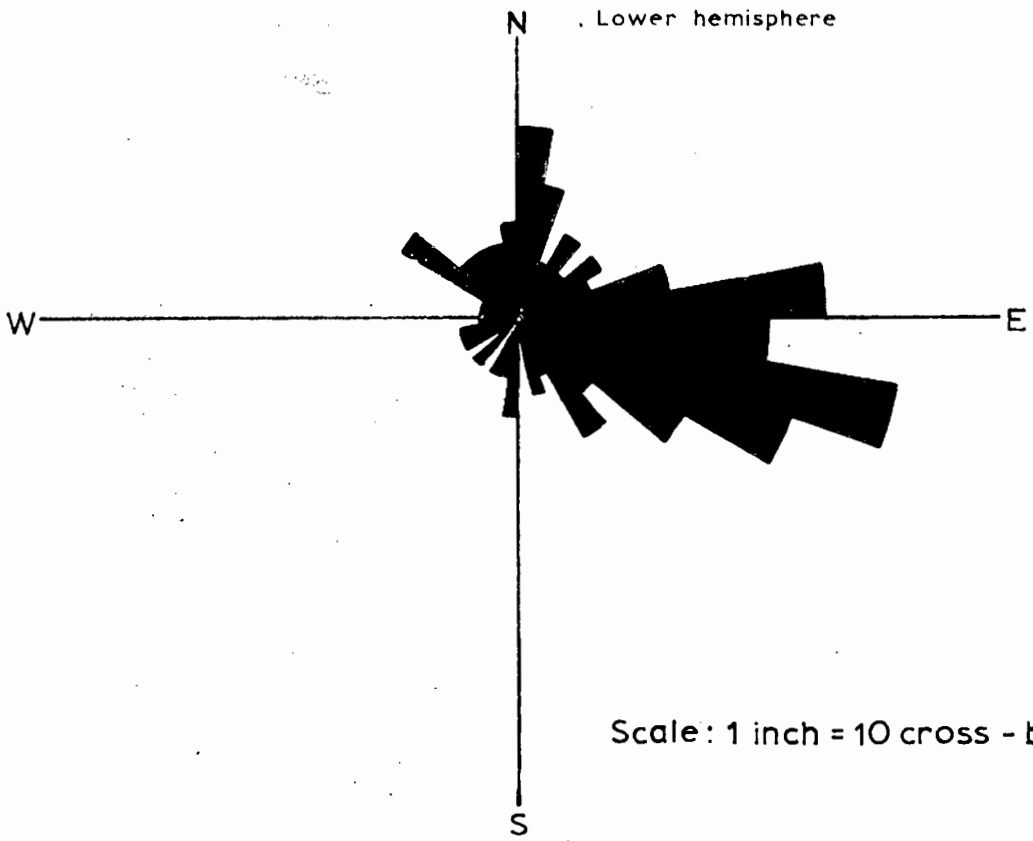


Fig. 14. Poles of Cross-beds on Barby and Naus (138 readings).

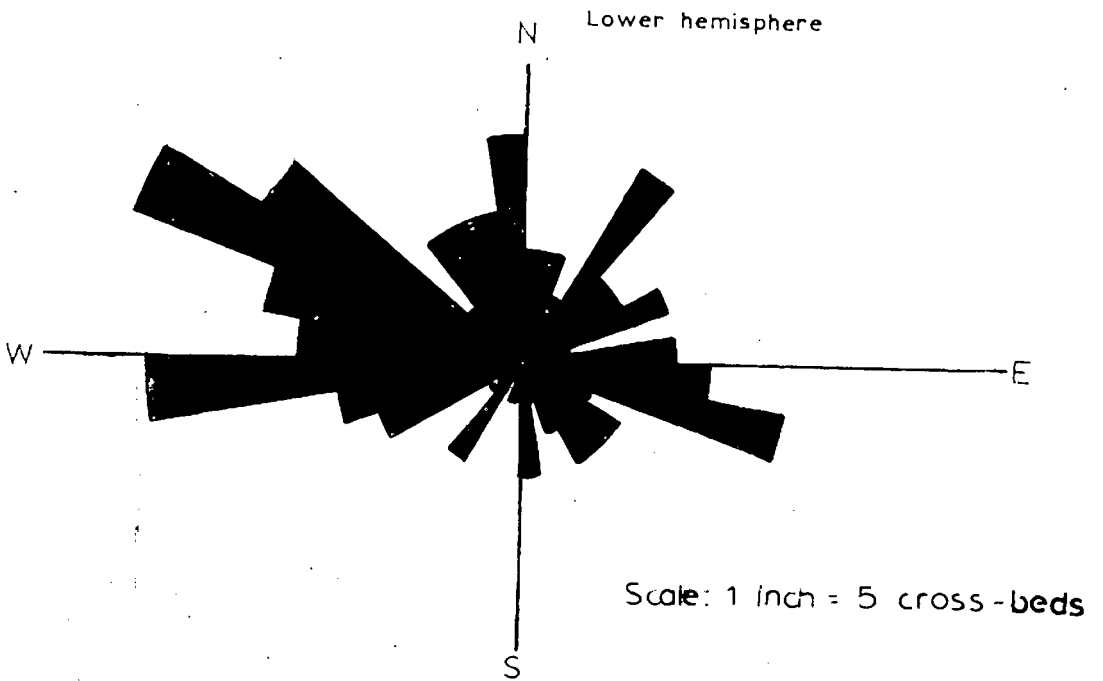
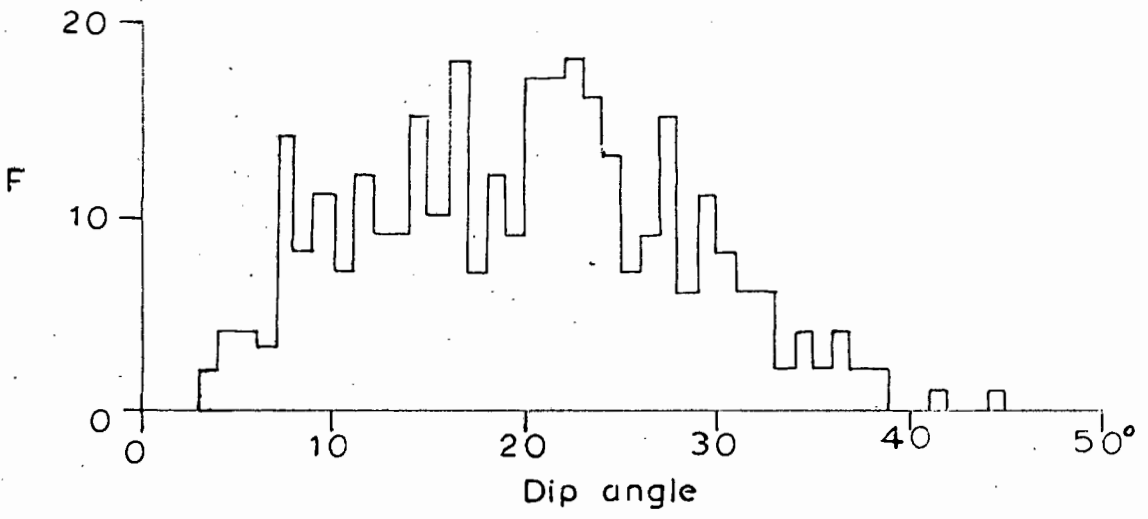


Fig.15. Angle of dip of 338 reorientated cross-beds.



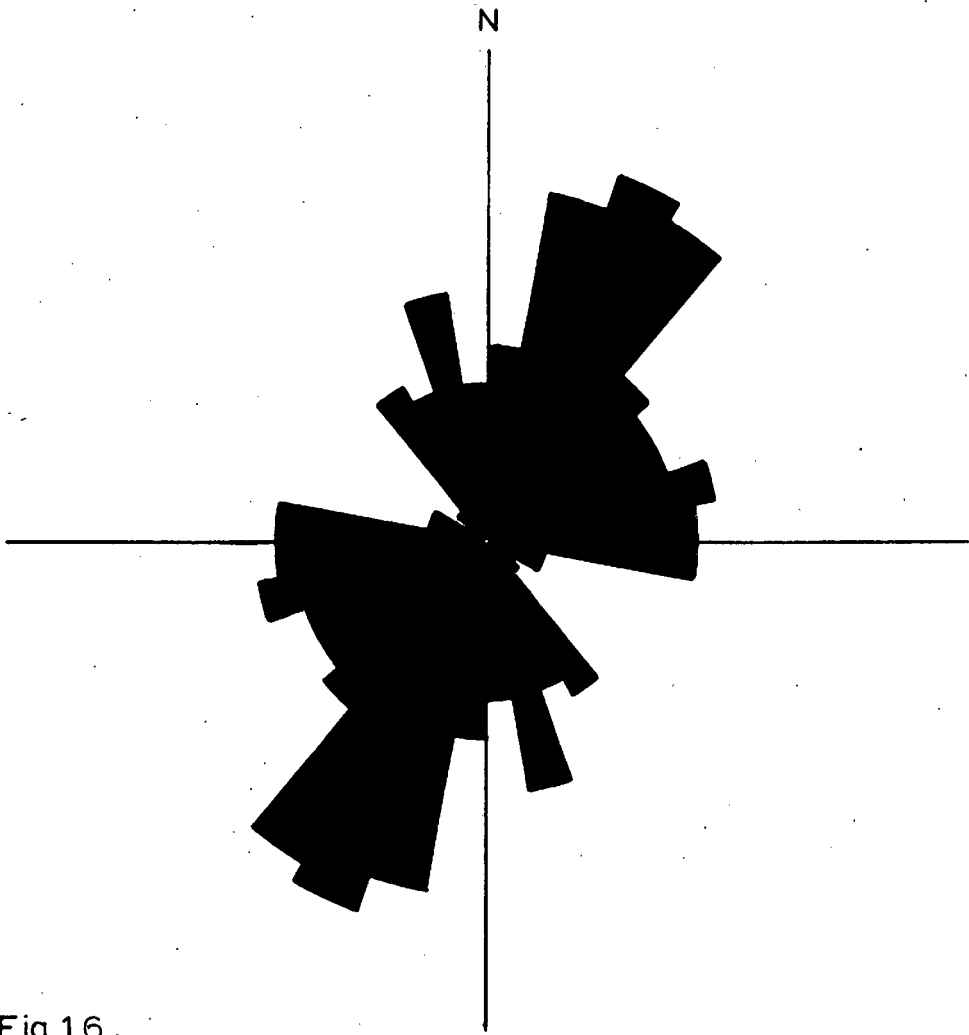


Fig.16.

Current direction as indicated by 178 parting lineation measurements.

the cross-bedded material and this could be the reason why it is more weather resistant.

A few very limited cross-beds can be found in the gritty small-pebble conglomerate and the grit, and often these are more like poorly developed scour-and-fill structures than cross-beds. Most of the conglomerate beds that overlie sandstone beds have even tops (i.e. an even base to the overlying sandstone bed) but eroded footwalls which cut into the underlying, often laminated and thinly laminated sandstone. Plate 29 shows two cross-bedded units in a pebbly grit and Plates 30 and 31 the uneven footwalls of coarse-grained beds overlying finer grained ones.

Figures 13 and 14 show the paleocurrent directions indicated by reorientation of 338 cross-bedding measurements. Both are compiled from measurements made in the western outcrop but give strangely conflicting patterns. The group west of Aruab beacon (E6) (Figure 13) gives a direction of supply from the south-east but on Naus (D8) and Barby (E8) the direction is variable though mainly from the north-west. This is contrary to what one might expect since the underlying conglomerates have many large and small pebbles that can be traced to nearby southerly and south-easterly sources. The cross-beds are not from a limited stratigraphical thickness in either of the two cases and this could introduce error if the direction of supply had changed with time. This may well be the cause of the scatter on Figure 14 but Figure 13 shows a strong main direction of supply and is probably little affected by the change in stratigraphic position of the measurements.

Figure 15 gives an indication of the angle of dip of the cross-beds. Six have a reorientated dip angle of greater than 36° (the maximum angle of dip of undeformed cross-beds, Pettijohn, 1957, p.169) which must be due to deformation. The mean dip angle is 18.4° .

In contrast to the supply directions indicated by the cross-bedding measurements the parting lineations of Figure 16 indicate a current direction orientated south-south-west - north-northeast. The measurements were made mainly in the Konkiep River two miles east of Grosskopf (D7). A few readings were obtained on other parts of Aruab (D6), Ganaams (D4), and Naus (D8). This shows a third direction of supply at right angles to those indicated by the cross-bedding measurements. Together these indicate

various sources for the sandstone material and one would expect from this a lensing **out** of beds away from the source and an interfingering of beds from different supply sources. This was not found to be the case at all and Plates 32, 33, 34 and 35 give an idea of the evenness and consistency of the beds. Figure 10 shows the sandstone to be very well sorted. The grain roundness, as already mentioned, is generally between sub-angular and sub-rounded, **and** for quartz and feldspar to be found in the latter state requires considerable movement. The cross-beds and parting lineations may therefore be due to redistributing currents or meandering streams within a shallow basin of deposition. The numerous laminations, the very thin beds and the lateral persistence of strata seem to indicate frequent inundations by very shallow water. Frequent **cnanges** of the rates of supply and deposition of sediment would account for the thin bedding; currents and varying depth of water would provide for the presence or absence of cross-beds, ripple marks and mud cracks; and periods of quiescence would allow for deposition of the clay-size material which is often seen on bedding planes. The water would have to be shallow enough at all times to preserve the red colour. The conditions were probably similar to those that produce floodplain deposits.

Plates 36 and 37 respectively show parting lineation on a bedding plane and on the foresets of a festoon cross-bed. The lineations in the latter run directly down the dip of the foreset indicating that they are parallel to the current direction. They are due to low ridges of sand particles parallel to the current direction and long axes of grains are found to be parallel to these ridges. Only one other example of a cross-bedded unit with parting lineations on the foresets was found. They are a bedding-plane feature largely and many of the best examples were found in dislodged blocks that had not been exposed to weathering for very long. The lineations in the Konkiep River (D7) bed are associated with numerous ripple-marked and mud-cracked bedding planes which are usually covered by a very thin **layer** of fine clay-size material. Other bedding planes show compressed clay pellets. This association with other shallow-water structures is also found in the other small groups from Naus (D8), Aruab (D6), and Ganaams (D4), and points to a shallow-water origin for parting lineations.

(b) Ripple marks

Ripple marks are far less common than cross-beds, and, as already explained, are often associated with mud cracks and, in places, a few parting lineations. Both current- and oscillation-ripple marks are present and very often two sets are superimposed. Thirty-six current ripple directions were measured, but over a wide area. Their scatter is large, though a small peak indicates a general direction towards the south-east. They are commonest in the thinly laminated shale on Ganaams (D3), where the finely cross-bedded internal structure is often seen. Plate 38, of the shale, shows the superimposition of two sets of ripples. In places in the shale, there occur ripple-marked bedding planes that are followed by very thinly laminated beds about six inches thick whose form follows that of the underlying ripple marks.

Plates 39 and 40 are of ripple marks in the sandstone. Plate 40 shows current-ripple marks that have a small-scale rippling of their foresets. They have a wave-length of four inches and an amplitude of five-sixteenths of an inch. The foreset ripples, which are symmetrical and have a wave-length of three-sixteenths of an inch, only rarely cut the crest of the main ripples and then only very shallowly. Most troughs of these ripples start below the level of the crests of the main ripples. A suggested origin is that the foreset ripples are an erosion feature due to a current of velocity less than that of the current that formed the main ripples. There would thus be a tendency for the wave-length to be shortened.

Ripple indices for 16 measured sets of ripple marks are 4.8, 7.33, 9.14, 9.14, 9.14, 10, 10, 11.6, 12, 12.8, 12.8, 13.5, 14.4, 15.33, 16 and 16. Schwartzbach (1963, p. 65) uses Twenhofel's index value of 15 for separating aeolian from subaqueous current ripples. A value greater than 15 is considered to indicate an aeolian-ripple mark. Potter and Pettijohn (1963, p. 93), however, mention Cornish, Kindle and Bucher as considering large ripple indices characteristic of subaqueous current ripples. This makes the usefulness of the ripple index as a guide to depositional environment rather questionable. The small number of ripple-marked bedding planes dealt with in this study is not sufficient to support either contention. However, ripple marks with superimposed mud cracks must be aqueous

in origin and it is suggested that a further study of these alone may be useful in revealing a limiting value to the ripple index of water-formed ripple marks.

(c) Other structures

Mud cracks are the most common bedding-plane markings and occur fairly regularly in the sandstone on Naus (D8), Barby (E8), Aruab (D7) and the southern portion of Ganaams (D4). They can be found on Dabis (I6), Guperas (H5) and Aubures (B6) in places. They vary in width from one-sixteenth of an inch to over two inches and generally uncracked plates between increase in breadth with an increase in the width of the cracks. Some cracks are superimposed on ripple marks, and though there is some tendency for them to follow the crests of ripples it is not invariable. Plate 41 shows them very closely following the crests of one set of current ripples, and in Plate 42 most of them follow the crests of interference ripples. Relative sizes can be gauged from these two plates as well as from Plates 43, 44 and 45. The last two show the laminae of mud that cover all mud-cracked bedding planes and many ripple-marked bedding planes as well. These are usually very thin but on rare occasions were found to be as much as one-quarter inch thick. Clay-material laminae that are unmarked by structures are generally the thickest.

Plate 46 is of the underside of a dislodged block of sandstone that shows a set of mud cracks, superimposed on ripple marks, which have an exact displaced image depressed into the ripple-marked surface. Only a small portion of the bed from which this block came was exposed - the rest was hidden by talus. The displacement at the two ends of the block is unequal and in situ is in a south west - north east direction. The concave impression is the uppermost. This feature may have been produced by very local displacement at some time during the deformation of the Auborus sediments. It is not shown by the immediately underlying and overlying bedding planes.

Compressed clay pellets are a common feature of many bedding planes all over the area. Their diameter ranges from one-quarter inch to six inches. The larger impressions are rare, however, and average diameters are between one-half and one inch. Plates 47 and 48 give an idea of

the size and concentration of the pellets. Plate 49 shows irregular sand and mud balls that are mud coated and which did not flatten much on compaction. Plate 50 shows what are probably casts of similar sandy mud balls. The cracked surface of the clay-size material can be seen in both cases. Plate 51, taken just north-west of the Aruab homestead (D6), shows two beds made up entirely of compressed clay pellets, one eight inches and the other ten inches thick. This was the only such example found. The pellets are all about one inch in diameter. The even footwall of these beds can be seen as well as the uneven footwall of the overlying coarser grained sandstone. In the interbedded sandstone elongated cavities were filled with, and some still contain, this clayey material. One cavity is spherical and probably had material that was compact enough to resist compression.

Flute casts were only found once. These are shown in Plate 15.

Groove and striation marks are shown in Plate 52. They are somewhat indistinct but were probably caused by current and load action.

The striated surface of the area between large mud cracks is shown in Plate 53. The striations may have been caused by sand-laden wind passing over the still wet surface of the mud which trapped any sand falling on it. This formed uneven ridges of gritty and muddy material parallel to the wind direction. It is difficult to ascribe such a coarse structure in such fine-grained material to subaqueous current action. The similarity of newly formed structures observed on windy days on present-day mud flats was quite striking. The formation of the mud cracks would have followed the formation of the striations. Lineation direction is 163° .

Rain pitting: Plates 16, 54 and 55 are three of about six similar structures found at different places in both outcrop areas. They have a rough, bumpy surface with small, closely spaced mounds between one-sixteenth and one-fifth of an inch high. These may be due to differential compaction, but the overlying beds are undisturbed, hence they may instead have been caused by heavy rain which produced a strongly pitted surface.

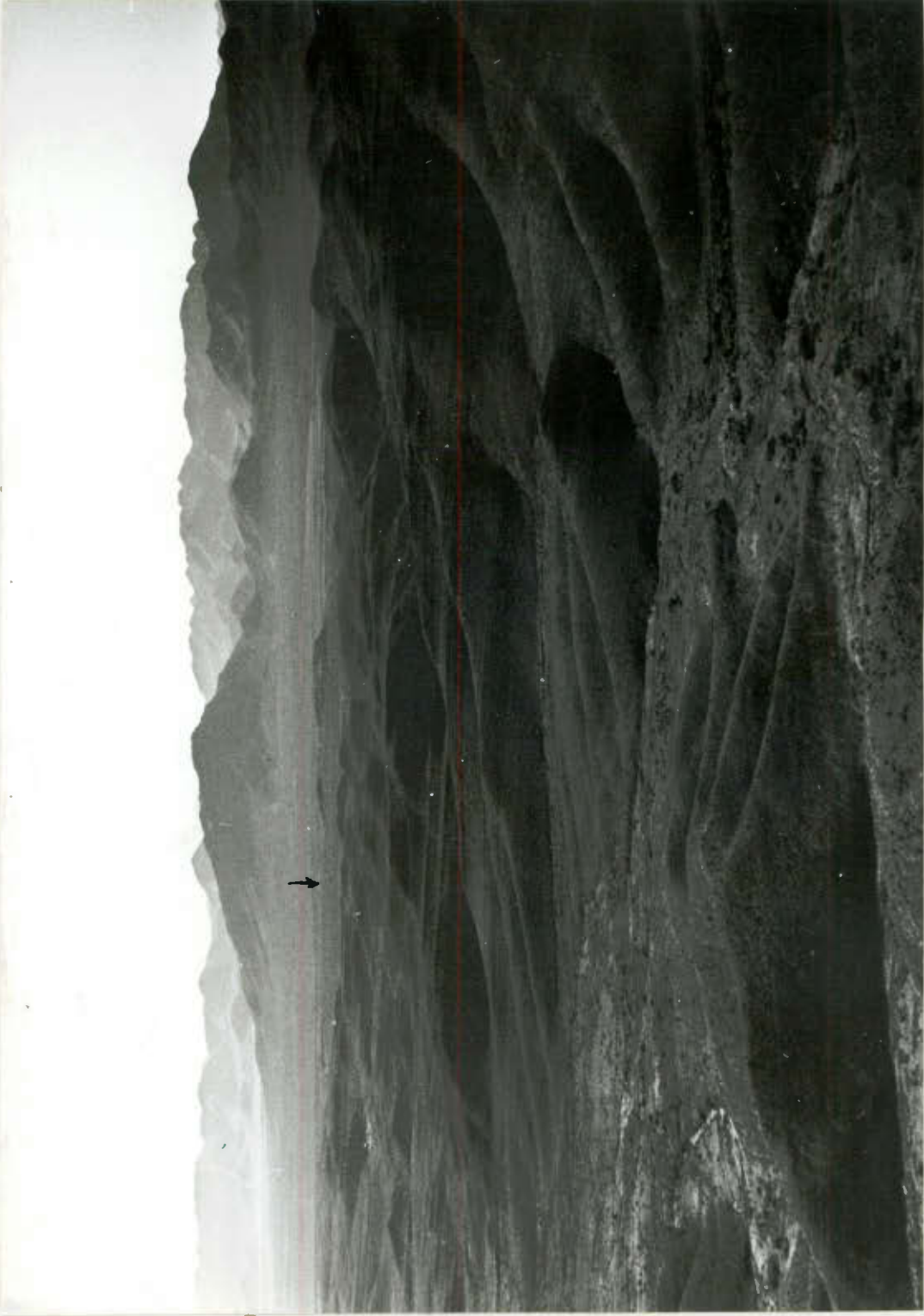


Plate 32

The photograph was taken $1\frac{1}{2}$ miles south of Grosskopf and is a view across the farm Aubures. The arrow indicates the position of the Aubures homestead. Beds can be seen dipping gently north. Thin, white lines of grass in the foreground grow along joint planes.

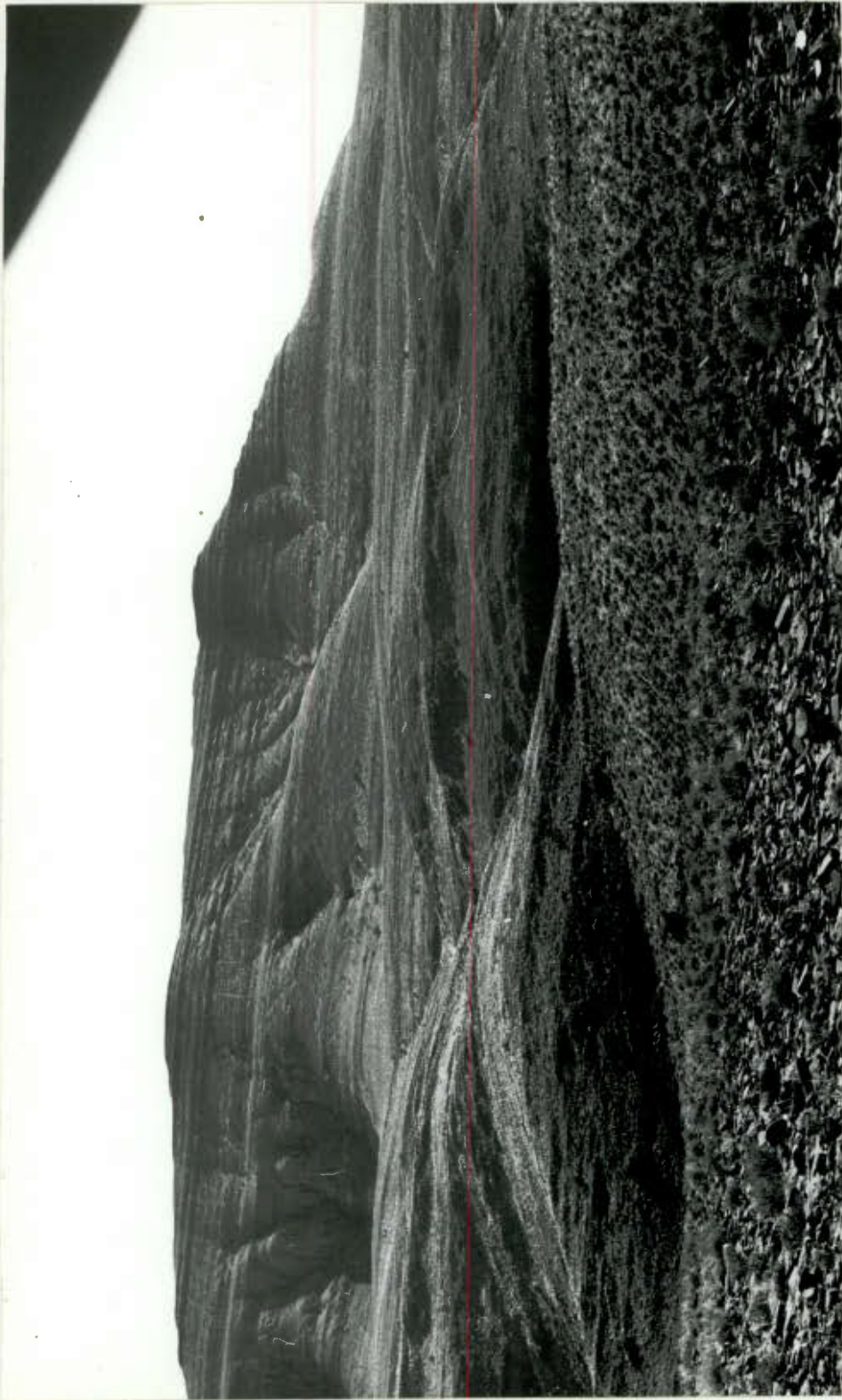


Plate 33
The photograph was taken 1 mile south of Plate 32, faces west, and shows evenly bedded *Auborus* sandstone dipping gently north.



Plate 34

The photograph, taken two miles north of Grosskopf, faces west, and shows strata dipping gently southwards. The lower arrow indicates the position of the Aubures homestead, and the upper the position of Sinclair Mine.



Plate 35
Looking ESE from near Sinclair Mine. It shows the evenness of the bedding which dips gently northwards. The gently sloping pediment of the foreground covers Aurborus conglomerates. The arrow indicates the position of Grosskopf.



Plate 36

A dislodged block of sandstone that shows parting lineations on the bedding plane. The direction of current movement was parallel to the lineations.



Plate 37

A festoon cross bed that shows parting lineations down the dip of the foreset. This shows how they are formed by current action and how they lie parallel to current. Foresets dip towards lower left.

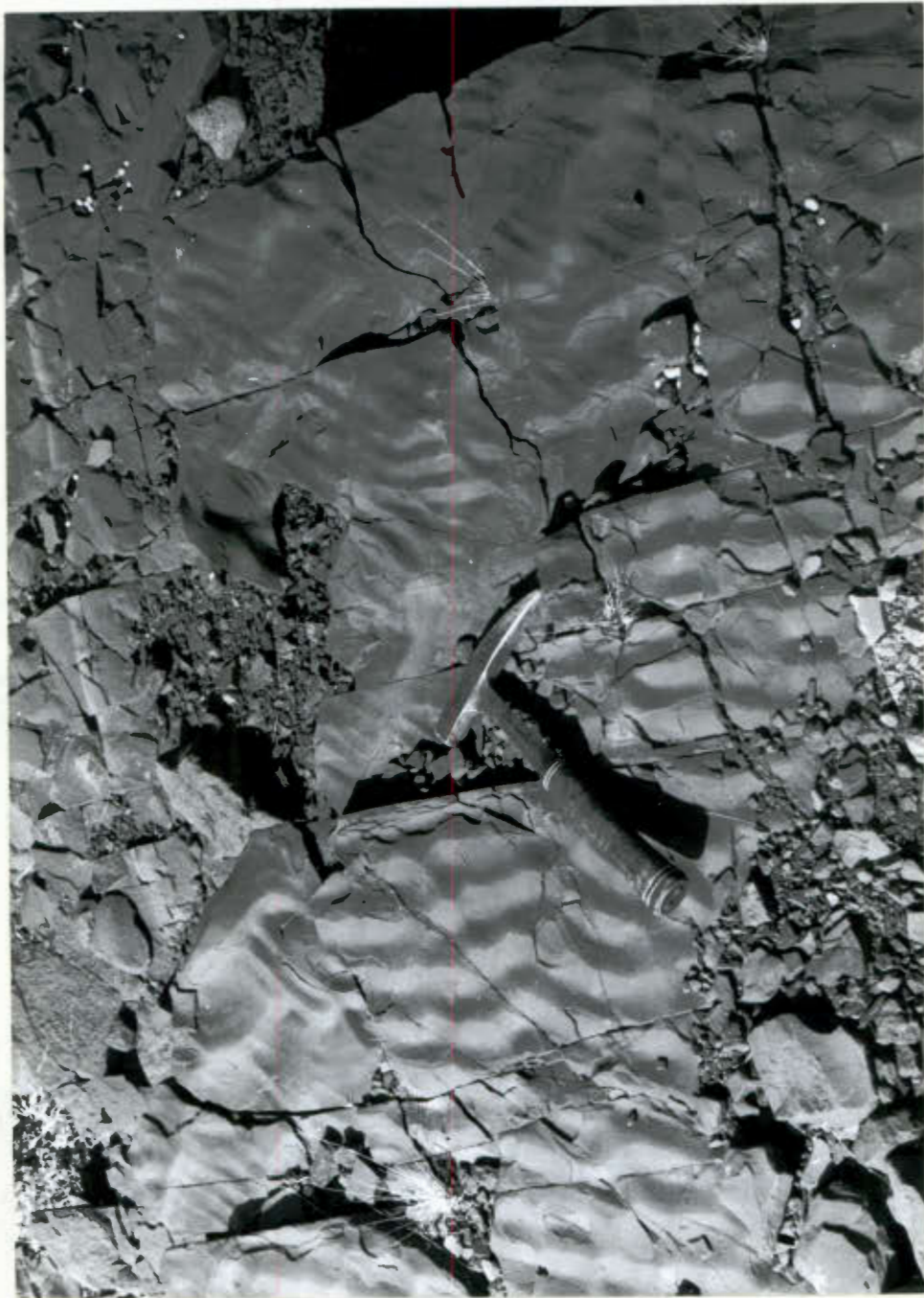


Plate 38

Two sets of interference ripples are shown in this photograph of the shale on Ganansms. Joints are well developed and one in the upper part of the photograph shows a 1 in. thick zone of decolouration. The others, which are far more open, do not show decolouration.



Plate 39

Current and linguoid ripples in a dislodged block of sandstone on ^{SW} portion of Aruab.



Plate 40

Current-ripple marks in sandstone on SW portion of Aruab. These have a wavelength of 4 in. and an amplitude of $\frac{5}{16}$ in. Their foresets have tiny symmetrical longitudinal ripples with a wavelength of $\frac{3}{16}$ in.



Plate 41

Mud cracks following very closely the crests of current ripples. The ripples are covered with a very fine layer of mud. SW portion of Aruab.



Plate 42

Mud cracks roughly following the crests of interference ripples. The ripples are covered with a thin layer of very fine mud. SW portion of Aruab.



Plate 43

An even mosaic of small mud cracks. The laminae of mud can be seen flaking off between the cracks. SW portion of Aruab.



Plate 44

The fine mud between the mud cracks can be seen weathering unevenly. Material similar to this was analysed for clays and iron content. Eastern portion of Naus.



Plate 45

Mud cracks much larger than this are rarely found. The cracks here are wider than those in the previous photographs, and the plates between have a correspondingly larger diameter.



Plate 46

Mud cracks superimposed on current-ripple marks. The cracks have an exact, displaced image depressed into the surface of this dislodged block. The amount of displacement at each end of the block is unequal. SW portion of Aruab.



Plate 47
Clay pellet impressions of various sizes on a bedding plane surface.
SE portion of Guperas.



Plate 48

Bedding plane surfaces that are covered with clay pellet impressions. This is one of the beds in Plate 51. One half mile NW of Aruab homestead.



Plate 49
Sandy clay galls embedded in sandstone. The fine material coating the
galls has cracks similar to mud cracks. Dabis.



Plate 50
Impressions that are probably due to noncompressible clay galls. The fine grained material left in the impressions has cracks similar to mud cracks. Barby.



Plate 51
Two beds made up almost entirely of clay pellets. The sandstone beds overlying these have uneven footwalls and holes that are filled with friable clay-size material. Joints in the sandstone are not visible in the less competent beds. One half mile NW of Aruab homestead. Facing SW, beds dip 10° SE.

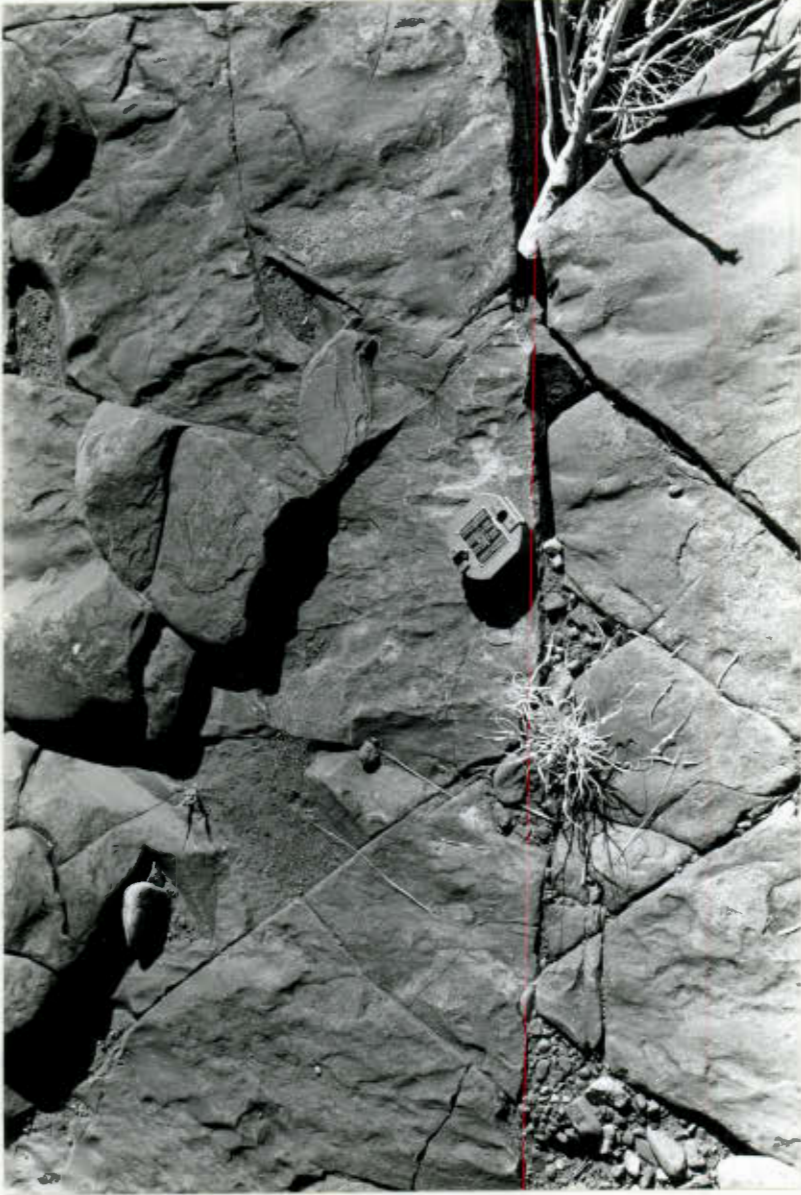


Plate 52
A bedding plane that shows irregular and uneven striations that may be due to current and load action. SW portion of Aruab.



Plate 54
The area between the mud cracks is strongly pitted. The cracks here are 3 in. wide and the area between over 2 ft. across. Smaller cracks criss-cross this area. Central portion of Gansams.



Plate 53

A mud cracked bedding plane that shows uneven, bumpy striations in the fine grained mud between the cracks. This may be due to wind blowing sand over the still wet mud. Central Ganaams-Aruab boundary.

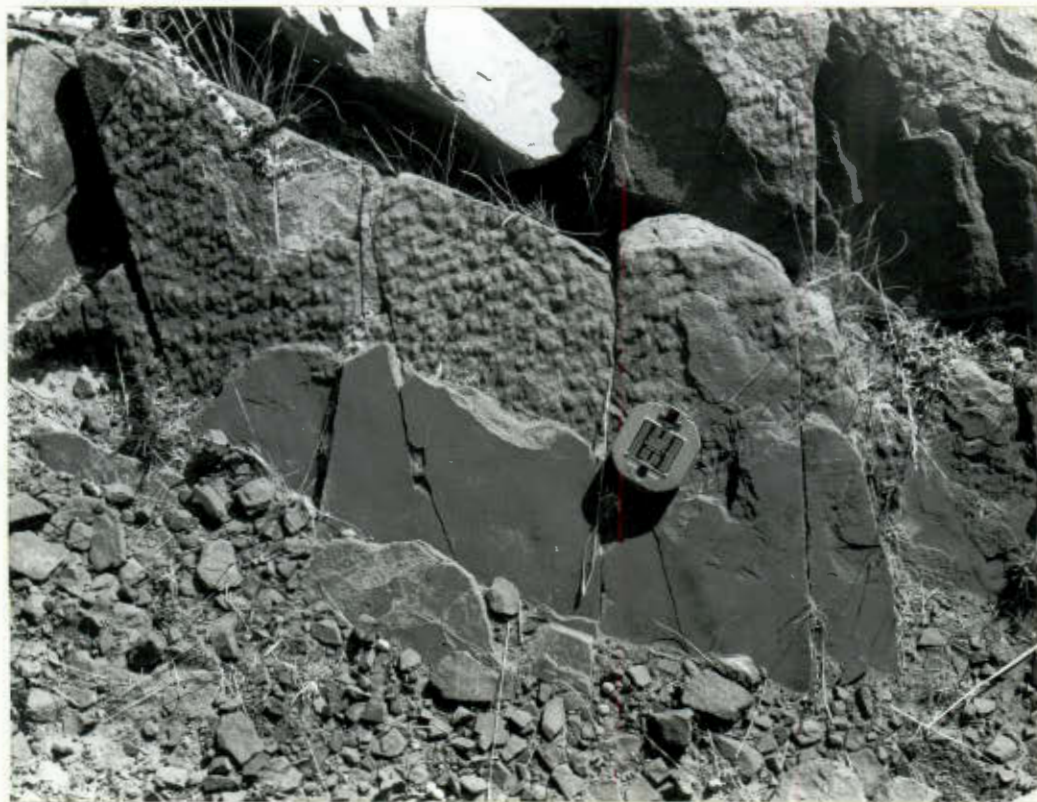


Plate 55

A strongly pitted bedding plane surface that is overlain by a very thin bed with a smooth upper bedding plane. The pits may be due to heavy rain.

VI - THE SHAPE AND NATURE OF THE BASIN

The present-day outcrop of the Auborus sediments is in the form of two wide, parallel, north-south trending bands separated by about 10 miles of Sinclair Formation sediments and lavas. Block faulting in the central region uplifted the Auborus sediments and erosion that followed removed them completely before the start of Nama sedimentation. Prior to deformation, however, the basin must have been roughly pear-shaped with small indentations on Aubures (C5, D5) and possibly Blutputz Ost (G2). The apex of the basin was in the north (C1, D1) - the limit of outcrop here is only two miles further north of the area. The length of the undeformed basin as well as the maximum width was approximately 27 miles.

Nama sediments obscure much of the unconformity of the basal conglomerate on rocks of the Sinclair Formation on Dabis (J7), Saraus (I3, 4, 5, J6) and Chamchawib (H2, I2, 3). The Nama sediments have only undergone slight post-deformational eastward tilting, and faulting has been limited to small rejuvenative movements on a few older faults. Structures in the Auborus strata had therefore been acquired prior to deposition of the Nama sediments, and the present-day limit of outcrop in the eastern section must therefore be approximately the same as in pre-Nama times.

Nama sediments only cap the highest mountains in the central part of the western section. The limits of outcrop here are all below this level and therefore if one extrapolates the dip angles of the basal beds in this section, one concludes that just prior to deposition of the Nama System the basin must have been a little larger, especially on Ginas (B2, 3, C3), the southern portion of Ganaams (C4), the southern portions of Barby (E8) and Naus (C8, D8) and possibly in the southern portion of Sinclair Mine (A7). This extrapolation, however, does not allow for an extension of more than half a mile anywhere to the outcrop limit.

Some of the pebbles in the basal conglomerate can be traced to very nearby sources and this, together with the large boulders and poor sorting of the conglomerate on Naus (D8), points to a very nearby basin edge in the south-west at the start of deposition. The wedge-shaped conglomerates in the western portion of Aruab (D6) and the

southern portion of Ganaams (C4, D4) point to a source of supply from the region of the Hahnenkamm beacon (C4).

The indentation of the basin here must have been present at the time of deposition. The indications in the south and north-west are therefore that, prior to deformation, the basin could not have been very much larger than it is at present and, disregarding the central faulted section, more or less the same shape, that is, essentially pear shaped.

Sedimentation began by the rapid deposition of unsorted subangular conglomerates into a slightly undulating depression in and bounded by sediments and lava of the Sinclair Formation. Breccia below the conglomerate represents the surface rubble that covered the underlying rocks. At this stage sedimentation must have been accompanied in parts by intense marginal uplift of the pre-Auborus rocks, at first very close to the basin edge but later also in areas a little more distant. The result was the production of local unsorted boulder conglomerate, the pebbles of which can readily be traced to nearby sources. On Naus (D8) boulders of Sinclair lava nearly three feet in diameter are found near the base of the basal conglomerate. On Dabis (J8) quartzite boulders from the underlying Sinclair Formation sediments occur at the base of the conglomerate. These are accompanied higher in the succession by granite boulders.

Tectonic uplift was most active in the southern and eastern marginal areas of the basin and was of relatively long duration. It was most intense in the south but there was a general decrease in intensity with time. In the north-west of Ginas (C3) where the basal conglomerate is only 100 ft. thick there seems to have been either very little or no marginal uplift at the time of deposition. Although sorting and roundness are poor here the maximum pebble size does not exceed two inches.

At various stages during deposition of the sandstone small local marginal uplifts caused a sudden increase in the rate of erosion resulting in the deposition of wedge-shaped conglomerates. Examples of these can be found in the sandstone on Ganaams (D2,2,4; C4) and in the western portion of Aruab (D6).

To allow for the deposition of the great thickness of 8,500 ft. of sediment, slow subsidence must have been taking place during deposition. This is not shown by a

thinning of beds towards the edges but by a decrease in dip angle on moving inwards, away from the edges. It must have been very slow and regular to allow for the evenness of bedding units shown in Plates 32, 33, 34 and 35.

The sections in Figures 1 and 2 (Chapter III) indicate a slight asymmetry in the shape of the basin. The deepest portion is nearer the western edge, and from what can be deduced from the now deformed basin the axis trends and plunges in a NNW direction. Thus the sediments thicken from the west and east towards the centre of the basin and are thickest on Ganaams and Ginas. The north-western portion of the basin must therefore have been the deepest. During deposition of the shale (D3) the deepest surface of deposition must have been on Ganaams. Since they lack mud cracks and display almost continuous rippling the shales were probably covered by water most of the time during their deposition.

Post-depositional deformation has taken place but at no time does it seem that the Auborus sediments were deeply buried. There are no overlying pre-deformational rocks, but following deformation Nama System sediments were deposited in the area. However, there are no Schwarzrand or Fish River beds anywhere to the west of the Auborus sediments so the thickness of overlying Nama strata may not have been very great at any time. The compactness of the Auborus sandstone seems to provide contrary evidence but Skolnick (1965) has studied the recrystallization of quartz in quartzite and states that it is not necessary to have great depths for it to occur (p.18). He mentions further variables besides stress that influence recrystallization : time and duration of pressure build-up, temperature, compressive stress, and chemical composition of interstitial fluids. These all act together. The maximum depth of burial of sediments that he studied was 10,000 ft. Therefore, the diagenetic changes that have taken place **in the Auborus** sediments need not have occurred at great depth.

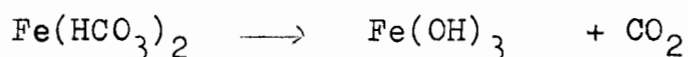
VII - THE PROBLEM OF THE RED COLOUR

A very notable feature of the Auborus sandstone is its even red colour. This only fades slightly in beds that are made up mainly of grit-size grains. All the conglomerates have a sandy or partly sandy matrix and this and the sandstone lenses interbedded in the conglomerate also have the same even red colour. As the sand-grain size decreases a slight increase in the intensity of the colour is noticed so that the shale is the most deeply coloured sediment of all.

The origin and source of the colour of red beds is still very controversial. Krynine (1949) classified red beds into four principal types: Primary, Postdepositional, Secondary and Chemical; however, the problem is to decide with certainty under which heading any one red bed must be placed. Many papers have been written and much experimental work has been done on red beds and the behaviour of iron compounds under various conditions, but no perfect solution for all red beds has yet been found.

If possible, a source for the iron must be established, as a first step. Red beds in the Sinclair sediments have provided a little iron oxide. The cross-beds in the Auborus sandstone seem to indicate a variable direction of supply but the basal conglomerate in the south indicates sources to the south of the area. Lava, both basic and acid, and granite of various types are abundant here and these would provide sufficient iron. The Auborus basin is completely surrounded by Sinclair lava and older granite so that any nearby source would also provide sufficient iron.

The solubility of iron is strongly affected by presence or absence of oxygen and carbon dioxide (Rankama and Sahama, 1950, p.663). Ferrous iron, in the absence of oxygen, dissolves readily in carbonated solutions to give $\text{Fe}(\text{HCO}_3)_2$. Present-day surface waters, however, are poor in ferrous bicarbonate. In the presence of atmospheric oxygen, this decomposes to ferric hydroxide and carbon dioxide:-



Iron is not stable in weathering solutions and since $\text{Fe}(\text{OH})_3$

readily forms colloidal solutions (Rankama and Sahama, 1959, p. 664) some writers have suggested a colloidal transportation of iron (Moore and Maynard, 1929; Castrano and Garrels, 1950; James, 1954). Moore and Maynard (1929) produced ferric oxide hydrosols by hydrolyzing a solution of ferric chloride and by dispersing freshly precipitated $\text{Fe}(\text{OH})_3$ in a solution of ferric chloride. On treatment with dilute solutions of sea salt, both hydrosols were precipitated almost immediately. The inference from this is that if iron were transported as a colloid in river waters it would be precipitated very quickly on entering a saline sea or lake. The conditions in such bodies of water would be alkaline and oxidizing.

Castrano and Garrels (1950) suggest that river solutions with a low pH and carrying much dissolved ferrous iron, enter an ocean in which the sea water is in equilibrium with CaCO_3 . The iron is oxidized and precipitated. The high pH of the sea is at first reduced to an intermediate value by the river water but returns to the high value through the buffering action of the solid CaCO_3 . This cannot be applied in this case because of the general lack of CaCO_3 but it is another suggestion for the transportation and precipitation of iron.

Tomlinson, in 1916, postulated that the red colour and much of the clastic material was derived from soils formed in warm, humid climates. After transportation of the soil the colour would be preserved at the site of deposition, and it would undergo little post-depositional change. He mentions work by Russel (1889) who pointed out that in red soils each sand grain is covered with a brown or red iron ore coat which does not wash off.

In the Auborus Formation no evaporites were found and there is no indication as to the salinity of the basin waters. However, it seems unlikely that the iron ore was deposited chemically in the basin because beds overlying mud cracks have no difference in colour from the underlying beds. If any colloidal or dissolved iron were present it could well be precipitated by saline solutions, but being of a very fine nature, it would be concentrated in the fine-grained sediments and would be lacking in the coarser grades, especially the basal part of any bed. The sand matrix of the conglomerate would be very pale coloured.

Post-depositional movement of the iron could produce a more even colour, but not to the extent shown in the Auborus sediments. It is hence most likely that the red colour is primary and was derived from the source area. It must therefore have been present as a coating on all grains at the time of deposition, giving an even colour which becomes more intense as the grain size decreases.

Freshly precipitated hydroxides of iron absorb considerable amounts of the metals - Cu, Pb, As, Hg, Sb, Bi, Se (Barth 1962, p. 30). X-ray Spectrograph analyses for Pb and As were made of the finest-grained specimens, but no abnormal concentrations of these two elements were found. It is very unlikely that Pb and As would be totally lacking in the transporting solutions and the conclusion must therefore be that iron was not deposited from solution as an hydroxide once it had reached the basin of deposition.

The role of clay as a transporting agent for iron can be ruled out because of the very small amounts of clay found.

Some hematite may have been derived from post-depositional alteration of biotite.

Calcite has been introduced after deposition and the hematite can be seen as a coating around all grains with which the calcite is in contact. However, after this, there has been some movement of hematite because some fractures in calcite crystals, but not all, show a thin line of hematite. Further evidence of this movement is shown by tiny veinlets of hematite in slides Al19, Al22 - 1, 2 and 3, Al24 - 1, 2 and 3 and Al47 - 1, 2 and 3 (Nos. 1 and 2 are perpendicular to bedding and 3 is parallel to it). These veinlets are elongated and tabular in the plane of the bedding and the longest are about 4 mm in length. They all have the same very finely granular texture as the intergranular hematite.

Most red beds elsewhere have amorphous ferric oxide as colouring matter (Twenhofel, 1932), whereas here, as already mentioned, it is crystalline. It may have undergone recrystallization from an amorphous state or it may have been crystalline in the soils in the source area in which case it would remain in this form during transportation and deposition. Since crystalline substances can only form by precipitation of an ion in true solution, and not from precipitated colloids, any colloidal hematite would have to go into solution before being redeposited as crystalline hematite. This would only

occur under oxidizing conditions and since hematite is very insoluble under such conditions the distance of movement must have been very small.

(1) The Occurrence of Decoloration

Some joint planes show a decoloration zone up to one inch thick. These are randomly distributed and there is no macroscopic indication as to why some joints have decoloration zones and others a foot or two away not.

A second type of decoloration of the sandstone is in the form of colourless spots, usually spherical in shape, with diameters from 0.05 mm to 3 in. and with an average size between one-half and one inch. These are post-depositional features as they cut right across bedding planes. Some have one or two concentric green rings, one inside the other; their shape follows the line formed by the limit of the zone of decoloration. These spots do not seem to be limited to any particular zone, but are widespread. Plates 56, 57 and 58 shows the spherical zones of decoloration and Plates 38 and 59 the decolorization along joint planes. Plates 56 and 57 also show the concentric green rings that are found within the spot. In some thin sections of grit decoloration zones can be seen around strongly altered, fine-grained, igneous rock fragments (Plate 60). The spots in the sandstone have no core of this type.

Besides these occurrences, only two other examples of non-red zones were found. One was a two foot thick sandstone bed on Aubures (C7) (sample A151), and the other was in the shale on the Aruab-Ganaams boundary (D4). In this latter case small, irregular, very light green patches about one inch thick and up to six inches long occur randomly through the beds or at intervals in the same bed. Only one one inch thick bed here was a uniform light green colour for its traceable distance of 50 ft. One to two percent of the outcrop is drab coloured.

Table 14 compares five modal analyses of spots with the surrounding pigmented areas.

The disappearance of hematite reveals, in all sections, very fine, interstitial clay-size material in variable quantities but usually less than that of the interstitial hematite of the rest of the section. It is probably obscured

by the hematite in the red rocks. Rock fragments show a decrease in amount, and heavy minerals, mica and calcite (where present) a variable behaviour. All sections, with the exception of A94, show a large drop in the quantity of ore. This is the most marked consistent change, besides the appearance of clay-size materials, and it tallies with work done by Miller and Folk (1955) who found a similar decrease in the quantity of ore in decolored spots in red beds. Robb (1949) found that biotite in green shale associated with red beds did not show alteration, though that in the red beds showed insipient alteration to red hematite between the lamellae. Table 15 shows a slight decrease in the plagioclase content of the spots, again with the exception of A94. However, the change is small in the other four sections and probably not significant for such a small number of samples.

It was at first thought that calcite might in some way affect the colour, as Keller (1929) found an increase in CaCO_3 content in two analyses of spots relative to red beds, but this idea was disregarded after working on samples A158 and A147 which contain no calcite.

Tomlinson (1916, p. 169) mentions W.J. Miller as ascribing similar spots in the red Vernon shale (Silurian, central New York) as being due to reduction by organic particles in the sediment. Although the Auborus Formation is precambrian in age the effect of organic matter cannot be disregarded. However, during the course of the present study no features, either macroscopic or microscopic, were found which indicated the presence of organic matter during deposition.

The grains around which decoloration had taken place were studied in the hope of finding some cause for this phenomenon. All but one of the grains were fragments of very fine-grained igneous rocks and usually strongly altered. The proportions of the constituents vary considerably. Small plagioclase laths are usually the main constituent, followed by chlorite or, in a few cases, epidote. In one case a few plagioclase crystals have an outer zone of perthite. Minor very fine-grained quartz is usually present and in some cases chloritized muscovite or biotite. Ore, sphene, and calcite may be accessory or absent. Epidote is usually accessory but may be absent. Chlorite is always present, but it may be the main constituent or only accessory. One grain was schistose, very fine



Plate 56

Two circular decoloured spots in sandstone. They are about 1 in. in diameter and both show the inner green ring. SW portion of Aruab.



Plate 57

Decoloured spots of various sizes in sandstone. Some show the inner green rings and one shows a green core. SW portion of Aruab.



Plate 58

A decoloured spot 3 in. in diameter. Spots of such a large size are rare. Ganaams.

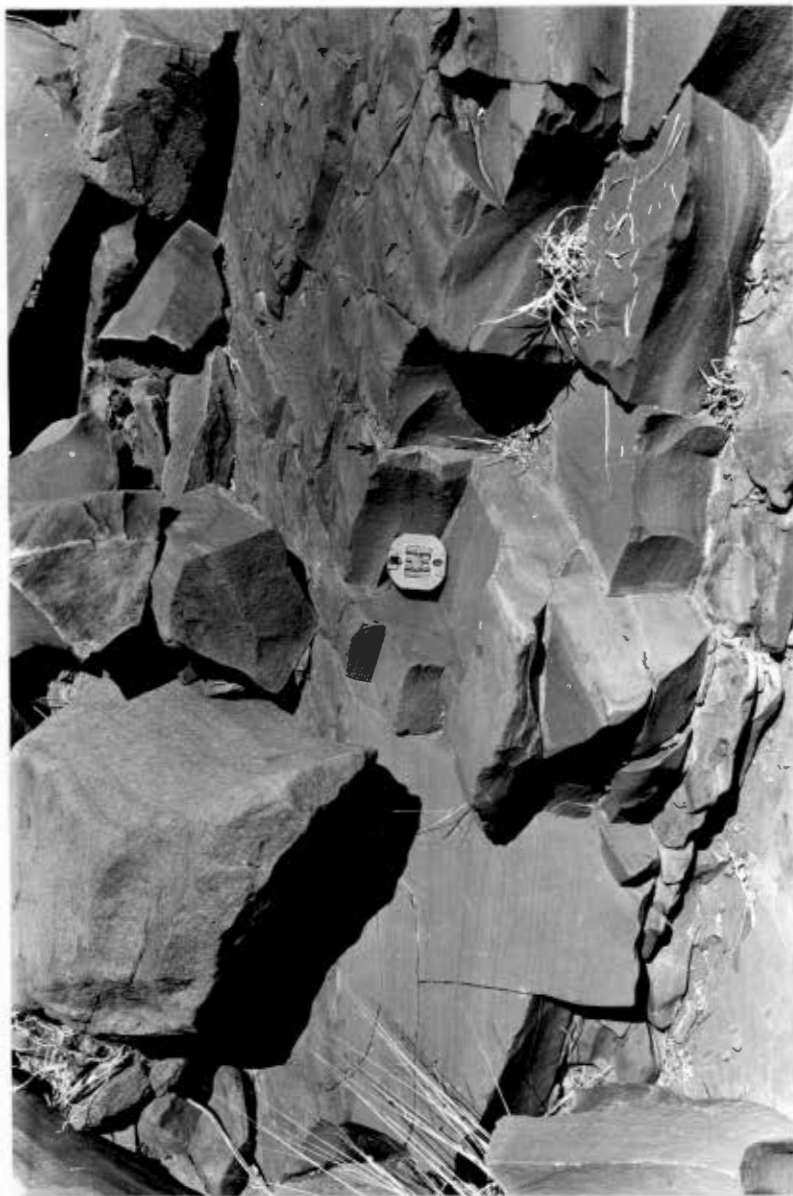


Plate 59
Joints in sandstone. One shows a thick zone of decolouration along its length. The outer edge of this zone is parallel to the joint. Nearby joints do not show any decolouration. The very thin bedding and lamination of the sandstone can be clearly seen. Facing SW, beds dip 8° NW, SW portion of Areaab.

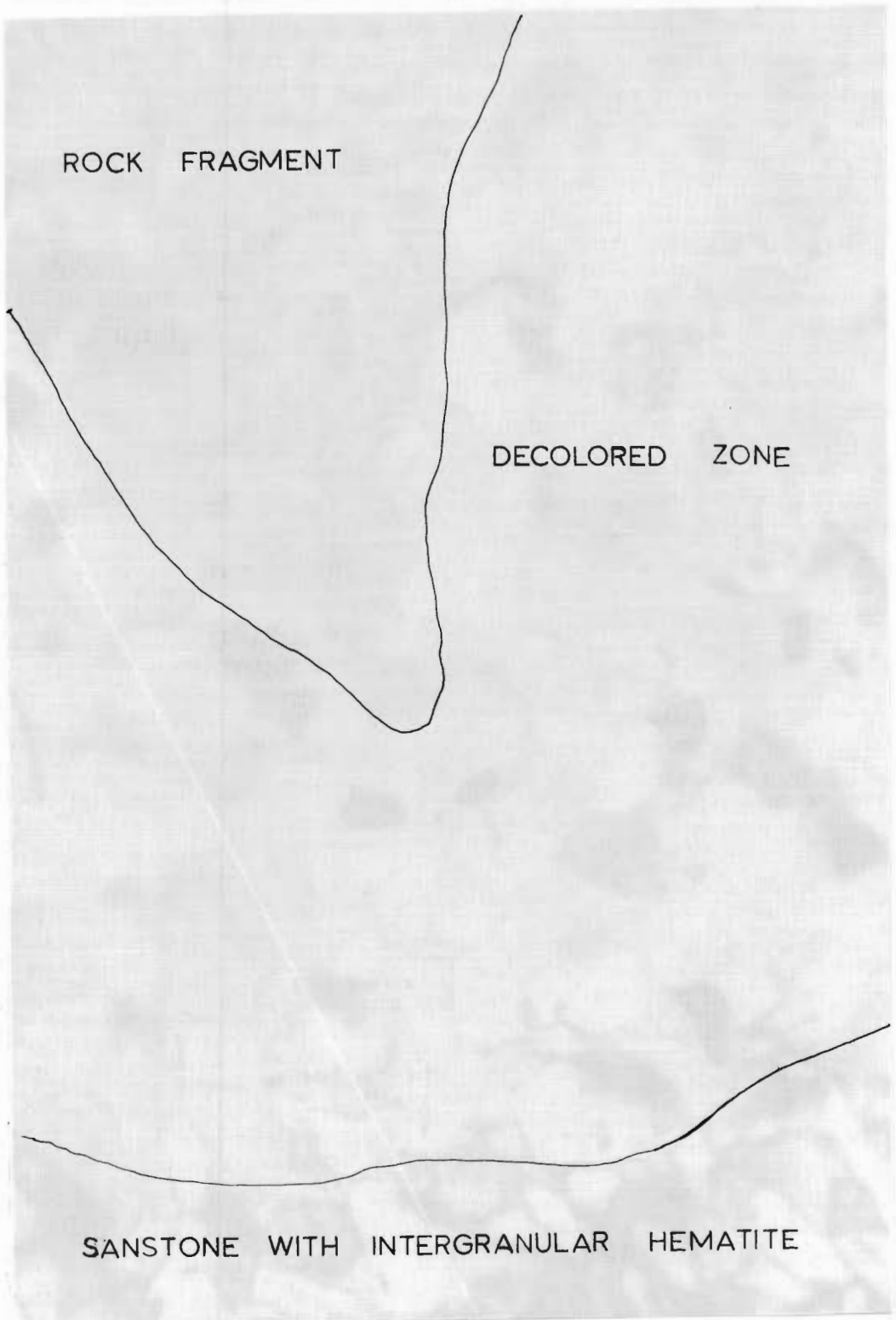


Plate 60

Slide A147, ordinary light, x 120. The zone of decolouration around a rock fragment. The fragment, in the upper left hand corner is fine grained, igneous and partially altered. The darker patches are chlorite. Intergranular hematite at the bottom indicates the edge of the zone which is about .7 mm thick.

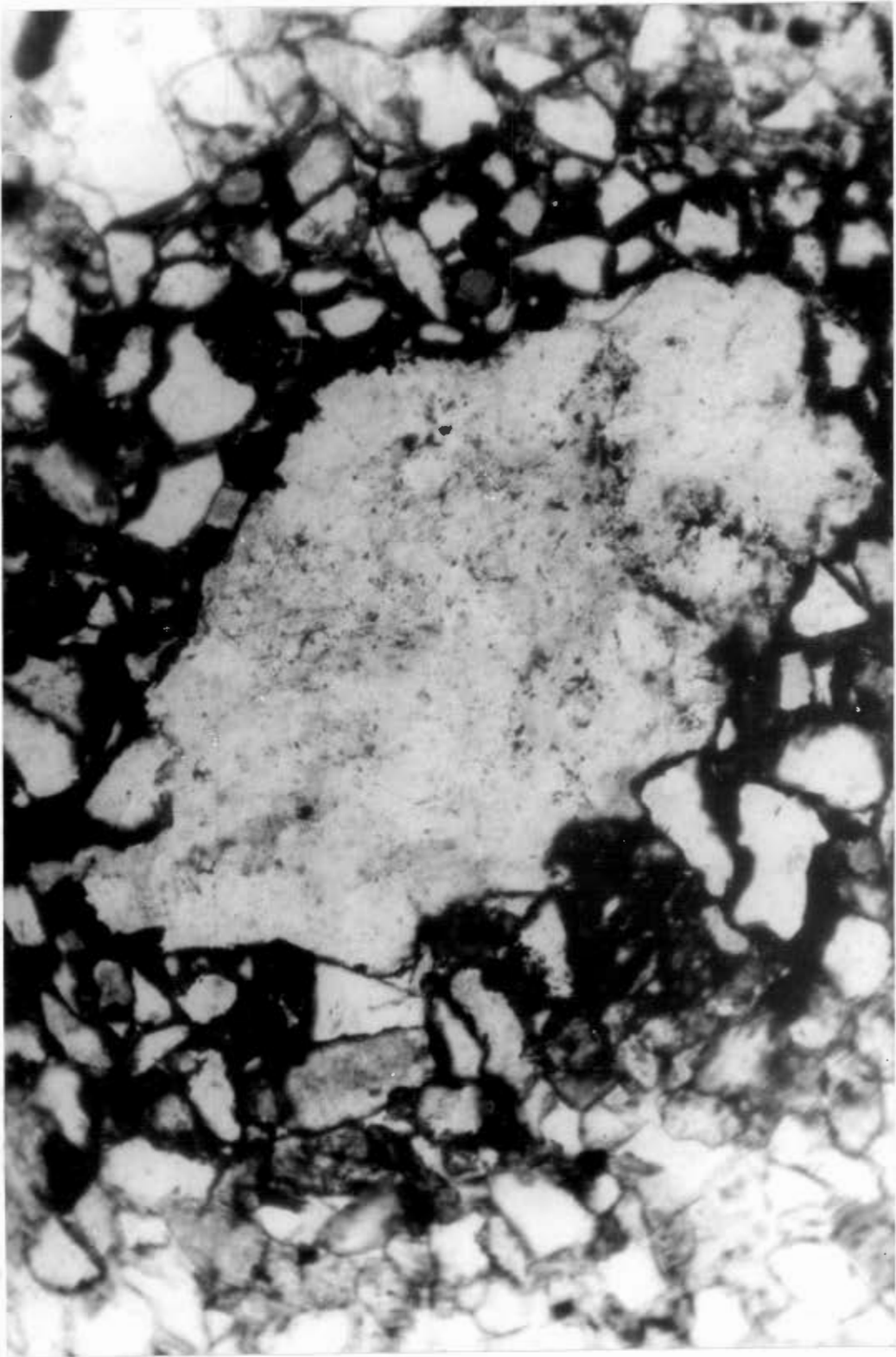


Plate 61
Slide A13, ordinary light, x 120. A fine grained igneous rock fragment that is surrounded by a zone where hematite is concentrated. The normal appearance of the rest of the slide can be seen around the edges of this zone.

Table 14. Modal composition of decoloured spots compared with surrounding red areas. Percent.

Specimen No.	Quartz	Felspar	Hematite	Rock fragments	Ore	Heavy minerals	Mica	Calcite	Colourless Clay
A158 Red	58.9	19.0	7.3	10.3	1.5	1.8	1.0	-	0.4
A158 Spot	62.8	16.6	.2	10.2	0.2	2.4	1.2	-	7.0
A13 Red	47.9	18.8	14.3	11.5	2.2	0.7	1.6	3.6	-
A13 Spot	50.0	18.7	-	11.6	0.7	2.6	2.2	6.6	8.1
A94 Red	48.1	21.3	14.2	9.4	2.5	2.9	0.1	2.4	-
A94 Spot	57.1	22.8	-	3.3	2.4	5.2	0.5	6.8	1.2
A119 Red	43.2	21.7	19.1	6.4	3.3	3.5	1.0	1.4	-
A119 Spot	58.0	17.5	-	7.0	1.0	4.0	1.0	7.0	5.5
A147 Red	55.6	13.2	13.4	12.2	2.2	3.4	0.6	-	-
A147 Spot	66.7	16.4	-	7.0	0.3	3.0	1.7	-	6.3

Table 15. K-felspar: plagioclase ratios of specimens in Table 14.

Specimen No.	K-felspar	Plagioclase
A158 Red	44	56
A158 Spot	48	52
A13 Red	27	73
A13 Spot	30	70
A94 Red	50	50
A94 Spot	39	61
A119 Red	45	55
A119 Spot	49	51
A147 Red	41	59
A147 Spot	53	47

Table 16. Ferrous and ferric iron contents of some Auborus sandstones.

Specimen No.	Fe ₂ O ₃ %	FeO %
A16	3.69	0.64
A45	2.06	0.46
A49	2.27	0.51
A99	2.79	0.56
A104	18.21	0.62
A141	5.02	0.61
A158 Red zone	2.77	0.53
A158 Colourless zone	0.78	0.46
A158 Green ring	0.23	1.03

A141 - very fine grained siltstone.

A104 - clay material scraped from bedding planes.

grained and made up of quartz, chloritized muscovite and minor felspar.

However, the solution does not seem to lie in the microscopic examination of these grains, for other very similar fragments in the same slide have caused no decoloration at all, and still others show strong concentrations of hematite around them (Plate 61). These fragments have a little more ore but are really indistinguishable from the ones that have caused decoloration.

Bubenicek (1964), working on the Lorraine oolitic iron ore minerals, found that diagenetic processes had reduced iron and caused the formation of chlorite. Chemical analyses for ferrous and ferric iron were therefore made for seven samples from the Auborus Formation. One of these was sample A158. Here the red zone, the colourless zone, and the green coloured ring (only easily visible macroscopically) within this zone were analysed. It is possible that the green colour of this green coloured ring is due to chlorite. In the thin section of A158 the edge furthest away from the hematitic material is part of the green coloured ring. Microscopic examination of the slide in ordinary light shows occasional very small, very light yellow contacts between the grains. Chemical analysis was carried out to determine whether there was any large difference in the ferrous/ferric ratios and the iron contents of the green coloured ring and colourless zones of this spot. Ferrous iron was determined by titrating KIO_3 with iodine liberated from ICl solution by ferrous iron (Heisig 1928, Nicholls 1960). Total iron was determined on the X-ray Spectrograph. The results are shown in Table 16.

The values for ferrous iron are a little less than those given by Dorsey (1926) for various red beds. His values range from 0.18 percent to 2.15 percent and average 1 percent for six specimens from the Chugwater and Spearfish formations, Wyoming, the Vernon formation, New York and the Slate Belt of eastern New York and western Vermont. Analyses of green shale and green spots in red beds are also given. A spot in red shale of the Vernon formation gives Fe_2O_3 as 0.0 percent and FeO as 1.19 percent and one in the Slate Belt of eastern New York gives Fe_2O_3 as 1.0 percent and FeO as 1.06 percent. The green shale may or may not show more ferric than ferrous iron, and

Dorsey reaches the conclusion that there is no more iron in red beds than there is in non-red beds. It is only the form in which the iron occurs that determines the colour of the sediment.

Examination of the results from A158 shows that there has been a loss of iron on decoloration. It is the Fe_2O_3 that is mainly affected. In the green ring there has been no loss of iron in relation to the colourless zone, but there has been a reduction of the iron from the ferric to the ferrous state. Bedding planes passing through the spots do not have any effect on them at all so they must be a post-depositional feature. They probably represent small zones in the sediment where reducing conditions both reduce and repel the iron. The most likely stage for this to occur would have been at the time when the hematite veinlets were forming. Recrystallization would have been taking place (whether the original hematite was amorphous or not) from ferric ions to solution. These would thus be able to move away from any material that might repel them, and at the same time they would be available, in their ionic form, for reduction. Overall conditions must have been oxidizing to precipitate hematite. Hematite, as already mentioned, being very stable and insoluble under oxidizing conditions could, therefore, not move far and it may be valid to use the radius of the decolored spots as a guide to the distance which ferric ions can move under oxidizing conditions. It would seem probable that only a very few ferric ions could be in solution at the same time because of the low solubility product of any insoluble substance.

The spots have no relation whatsoever to joint planes. Decoloration on these is considered to be a different problem from that of the spots as it takes place in a more open system. Decoloration of the spots must have taken place in a virtually closed system.

The cause for the reduction and loss of iron still remains undetermined. Chlorite formation may be a possible cause. Koenigsberger and Mueller (Morey and Earl Ingerson, 1937, p. 692) were able to produce a little new chlorite after heating hematite and chlorite in 30 cc of water for 48 hours at 420° with 1.5 gm Na_2O , 1 gm K_2O , 2 gm CO_2 and 0.5 gm Cl_2 . These conditions are unlikely to have been present in the Auborus sediments. One among

many late diagenetic processes is the conversion of clay to illite and chlorite (Fyfe, Turner and Verhoogen 1958, p.215). In this case Fe-chlorite would be formed. However the paucity of clay minerals and the lack of any decoloration zones around the many chlorite fragments and chlorite-containing rock fragments does not really support this view, though it cannot be discarded altogether.

No core grain or mineral was found in any of the spots in the sandstone thin sections.

The presence of specularite as the main ore mineral is, apparently, not unusual. Miller and Folks (1955) found magnetite and ilmenite as their main ore types, but van Houten (1961, p. 103) says that most analyses of the black ferromagnesian grains in red beds give specularite with intergrowths of ilmenite and leucoxene and small remnants of magnetite. The textures are triangular, indicating a cubic host. Some analyses give titaniferous magnetite. The indication therefore is, that the hematite may have been derived from titaniferous magnetite.

VIII - THE CONDITIONS OF DEPOSITION

The poor sorting of the conglomerates and the size of boulders in them point to both rapid erosion and torrential conditions at the start of, and periodically during, deposition. In these early stages the distance of transport was short and burial must have been rapid. Gradually with time however, the duration of transport must have increased as the pebble size diminishes higher up in the basal conglomerate and sorting and roundness improve. New material was also introduced into the basin from sources further afield (e.g. the appearance of granite and gneiss pebbles).

The basal conglomerate is thickest in the southern and eastern portions of the basin and here conditions must have been suitable for a prolonged period to enable these thicknesses to be deposited. There was fairly active uplift and erosion in the source areas, fairly rapid transport but gradually increasing in time of duration as deposition progressed. Then with a gradual change in conditions either in the basin or the source area or both, sandstone began to be deposited in place of conglomerate.

Erosion is dependent on both climate and relief and the greater the relief and the greater the angle of slope, the more rapid erosion will be. Decay, on the other hand, is only dependent on the climate; the hotter and wetter the climate, the more active the process of decay, (Krynine, 1950, p 133). The minerals present in the sedimentary product will be determined by the rate and duration of decay. Since so many rock types, including basic rocks, are present in the source area, hornblende and pyroxene were available. In the sandstone, however, these two minerals are very rare, as appears from the heavy mineral study. Biotite and the feldspars, in the same thin sections, show variable states of decay, and Krynine (1950, p. 158) has ascribed similar features in the Triassic rocks of Connecticut to two foci of erosion acting at the same time at any one place. This indicates both strong erosion and strong chemical weathering; the latter requiring high temperatures and heavy rainfall. He considers that the climate was probably tropical, giving uneven distribution of seasonal heavy rain, similar to savanna type climates

of today (p.158). He points out that 95 percent of the world's red soils are found in warm humid climates where temperatures are about 60°F and rainfall exceeds 40 in. per annum. Krumbein and Sloss (1959, p. 370) give similar figures for red soils, and research by van Houten (1961, p.121) indicates that all fauna and flora preserved in red beds are from warm temperate or sub-tropical climates.

During deposition of the Auborus sandstone, material must have been derived from several sources so as to provide both fresh and weathered felspar. However in all these source regions erosion must have been active long enough to accomplish the almost complete decay of hornblende and pyroxene, as well as to ensure good sorting of the remaining material. Decay must still have been active in the basin itself and redistributing currents must have had some effect on the sorting.

The cross-beds, and the mud cracks and clay pellets, so common in many parts of the sandstone, point to numerous wet and dry periods. The quiet conditions that followed deposition of many beds allowed for the settling of clay-size material onto the bedding planes. This may represent a transition from the wet to the dry season; depositing and redistributing currents cease to be active at the end of the wet season when there are no new introductions of water from the source area, and evaporation begins to take effect. During the deposition of the Auborus sediments, this often led to complete exposure and desiccation, with the formation of mud cracks in the very fine-grained material. Many of these structures have been preserved, but many more were partially destroyed and the resulting flakes redeposited as clay pellets.

In the north-west on Ganaams (D4) and Ginas (D3, C2, 3) the absence of mud cracks and the almost continuous rippling of the shale indicate quieter and probably consistently wet conditions during its deposition. The water depth, however, must have been shallow to maintain the oxidising conditions which would preserve the red colour. Local reducing conditions in the shale on the Auruab-Genaams farm boundary (D4) must have been post-depositional to produce the small, irregularly shaped light green zones.

A warm humid climate almost certainly existed during the deposition of the Auborus sediments, involving more or less seasonal inundation and desiccation. Rapid erosion of the source area would produce the unsorted boulder conglomerates and make available fresh feldspar and biotite, and rapid decay would be possible because of the warm, humid conditions, with seasonal extremes of rainfall. Deposition and burial must have been fairly rapid to preserve the fresh feldspar and biotite, but transport must have been long enough to produce the good sorting of the sandstone. At stages the conditions must have been very similar to those that produce floodplain deposits.

IX - SUMMARY

The basal conglomerate of the Auborus Formation was laid down on Precambrian talus breccias that covered a gently undulating base of sediment and lava of the Sinclair Formation. Nearby, often high, sources supplied pebbles of many types and sizes into an intracratonic basin probably similar in shape to the present-day shape and not much larger. Sandstone was deposited over the conglomerate while slow subsidence was taking place. The sandstone represents a stage of shallow water conditions during which considerable movement of material produced cross-beds and ripple marks and variable rounding, but good sorting, of the clastic grains. Frequent changes in current velocity and rate of deposition of sediment produced the thin bedding and lamination of most of the grit and sandstone (Plate 62). Numerous stages during which there was very little water movement allowed for the deposition of very fine, clay-size material on flat or ripple-marked bedding planes. Exposure and desiccation after this led to the formation of mud cracks. Such exposure must have been very frequent judging by the numerous bedding planes that are covered with clay pellets. The structures therefore indicate a shallow basin that was subjected to repeated inundation and exposure. At times shallow quiet conditions in the north-west allowed for the deposition of red shale. Conglomerate bands of varying thicknesses are interbedded in the sandstone in places.

Throughout deposition, conditions must have been strongly oxidizing to preserve the red colour, but very localised reducing conditions in the shale have produced small light green patches. A warm, humid climate with seasonal extremes of rainfall is deduced as necessary to provide the rapid erosion and rapid decay, required to explain the present-day conditions within the beds.

Diagenetic processes have resulted in the introduction of calcite, the recrystallization of quartz, and the good compaction of the sandstone. A slight movement of the hematite and the development of spherical spots of decoloration have also taken place.



Plate 62

Very thinly bedded and laminated grits with layers of finer grained sandstone. Such pebbles as the one in the photograph are often present in the grits. Central portion of Aruab.

Deformation seemingly took place not long after deposition. At first the upward movement of a long north-trending block began to fold the whole succession on Ganaams (D2), but eventual rupture produced block faulting in the central section. Possible simultaneous inward tilting of the eastern and western edges of the basin produced the respective westward and eastward dips of all the strata. Folding and faulting in the south-east appears to have occurred at the same time. Two sets of later east-trending faults are present in the north-east.

The deformation was followed by a long period of erosion during which the Auborus strata and older rocks were planed down to a very flat or slightly undulating peneplain surface. On this the Kuibis quartzite of the Nama System was deposited. There are no Schwarzrand or Fish River beds anywhere west of the Auborus sediments so the thickness of overlying Nama strata may not have been very great at any time. Slight displacement of Nama beds indicates a little rejuvenated post-Nama movement on some of the larger faults.

X - ACKNOWLEDGEMENTS

The writer would like to thank Profs. H. Martin and J. de Villiers, Dr. A.C. Fuller and Mr. A.R. Newton for guidance and help during the course of the study; the University of Cape Town Geology Department and Precambrian Research Unit for the facilities provided; Mr. J. Willis and Dr. Fuller for running the X-ray traces; his father, Mr. W.T. Miller, and Rev. F.M.M. Haythornthwaite for reading the script; the C.S.I.R. and South West African Geological Survey for financial assistance; and his wife for doing much of the typing and map drawings and helping in many other ways.

XI - REFERENCES

- Barth, T.F.W., 1962, Theoretical Petrology, 2nd Edition, John Wiley and Sons, Inc., New York.
- Barton, P.B., 1959, The Chemical Environment of Ore Deposition and the problem of low-temperature ore Transport, Researches in Geochemistry edited by Abelson, P.H., pp 279-300.
- Beetz, W., 1922, The Konkip Formation on the Borders of the Namib Desert, North of Aus. Trans. Geol. Soc. S. Afr., 25, pp 23-40.
- Billings, M.P., 1957, Structural Geology, 2nd Edition, Prentice-Hall, Inc., Englewood Cliffs, N.J.
- Bubenicek, L., 1964, Etude Sedimentologique du Minerai de fer Oolithique de Lorraine, Devels in Sedimentology. Vol II, pp 113-122.
- Carroll, D., 1958, Clays in the transport of iron, Geochem. et Cosmochem. Acta, 14, p.1.
- Castrano, J.R., and Garrels, R.M., 1950, Experiments on the deposition of iron with special Reference to the Clinton Iron Ore Deposits, Econ.Geol. 45, pp 755-770.
- de Sitter, L.U., 1956, Structural Geology, McGraw-Hill Book Company, Inc., New York.
- Dorsey, G.E., 1926, The Origin of the Colour of Red Beds, Jour. Geol., 34, pp 131-143
- Dunbar, C.O., and Rodgers, J., 1957, Principles of Stratigraphy, John Wiley & Sons, Inc., New York.
- Friedman, G.M., 1962, Comparison of moment measures for sieving and thin section data in sedimentary petrological studies, Jour. Sed. Petrol. 32, pp 15-25.
- Fyfe, W.S., Turner, F.J., and Verhoogen, J., 1958, Metamorphic Reactions and metamorphic Facies, Geol. Soc.Amer.Mem. 73.
- Heisig, G.B., 1928, Volumetric determination of Ferrous ion by means of KIO_3 , Jour. Amer. Chem.Soc. 50, pp 1687-1691.
- James, H.L., 1954, Sedimentary Facies of Iron-Formation, Econ.Geol. 49 pp 235-293.
- Keller, W.D., 1929, Experimental work on Red Bed bleaching, Amer.Jour.Sci. 18, pp 65-70.

- Kerr, P.F., 1959, Optical Mineralogy, 3rd Edition, McGraw-Hill Book Company, Inc., New York.
- Koen, G.M., 1955, Heavy minerals as an aid to the correlation of sediments of the Karroo System in the Northern Part of the Union of South Africa, Trans.Geol.Soc, S.Afr., 57.
- Krumbein, W.C., and Sloss, L.L., 1959, Stratigraphy and sedimentation, W.H. Freeman and Company, San Francisco.
- Krumbein, W.C., and Pettijohn, J.F., 1938, Manual of sedimentary Petrography, D. Appleton-Centuary Company, Inc., New York.
- Krynine, P.D., 1946, The Tourmaline Group in Sediments, Jour.Geol.54, pp 65-87.
- _____ 1949, The Origin of red beds, N.Y. Acad.Sci. Trans., series II, 2, pp 60-68.
- _____ 1950, Petrology, Stratigraphy and Origin of the Triassic Sedimentary Rocks of Connecticut. State of Connecticut. State Geological and Natural History Survey.Bull.73.
- Miller, D.N., and Folk, R.L., 1955, Occurrence of detrital magnetite and ilmenite in red sediments; New approval to the significance of red beds, Bull.Amer. Assoc. Petrol. Geol. 39, pp 338-345.
- Moore, E.S., and Maynard, J.E., 1929, Solution, Transportation and Precipitation of Iron and Silica, Econ. Geol. 24, pp 272-303, 365-402, 506-527.
- Morey, G.W., and Earl Ingerson, 1937, The Pneumatolytic and Hydrothermal alteration and Synthesis of silicates, Econ.Geol. 32, pp 607-761.
- Moss, A.J., 1963, The physical nature of common sandy and pebbly deposits, Pt.II, Amer. Jour. Sci. 261, pp 297-343.
- Nicholls, G.D., 1960, Techniques in Sedimentary Geochemistry; (2) Determination of Ferrous Iron contents of Carbonaceous Shales, Jour. Sed.Petrol. 30, pp 603-612.
- Pettijohn, F.T., 1957, Sedimentary Rocks, 2nd Edition, Harper and Brothers, New York.
- Potter, P.E., and Pettijohn, F.J., 1963, Paleocurrents and Basin Analysis, Springer-Verlag, Berlin.
- Rankama, K., and Sahama, Th.G., 1950, Geochemistry, University of Chicago Press.
- Rittenhouse, G., 1950, Detrital mineralogy, Subsurface Geologic methods edited by L.W. Le Roy, Colo.School of mines, Golden Colo, pp 116-139.

- Robb, G.L., 1949, Red bed coloration, Jour. Sed.Petrol.
19, pp 99-103.
- Russell, I.C., 1889, Subaerial Decay of Rocks, U.S. Geol.
Surv. Bull.52.
- Schwarzbach, M., 1963, Climates of the Past, D.van Nostrand
Company, Ltd.
- Skolnick, H., 1965, The Quartzite Problem, Jour.Sed.Petrol.
35, pp 12-21.
- Tomlinson, C.W., 1916, The Origin of Red Beds, Pts.I and II,
Jour. Geol.24, pp 153-179, 238-253.
- Twenhofel, W.H., 1932, Treatise on Sedimentation, 2nd Edition,
Baltimore: Williams and Wilkins Co.
- _____, and Tyler, S.A., 1941, Methods of study of
sediments, McGraw-Hill Book Co., Inc., New York.
- Turckian, K.K., and Wedepohl, K.H., 1961, Distribution of
the elements in some major units of the Earth's crust.
Geol.Soc., Amer.Bull. 72, pp 175-192.
- van Houten, F.B., 1961, Climatic Significance of Red Beds,
Descriptive Paleoclimatology, edited by Nairn A.E.M.,
pp 89-139 , Interscience Publishers.
- von Brunn, V., 1967, Acid and Basic Igneous Rock Associations,
west of Helmeringhausen, South West Africa, Ph.D.Thesis
in preparation, Univ. of C.T., Cape Town.
- Wentworth, C.K., 1922, A scale of grade and class terms for
clastic sediments, Jour.Geol. 30, pp 377-392.
- Williams, H., Turner, F.J., and Gilbert, C.M., 1958,
Petrography, W.H. Freeman and Co., San Francisco.
- Winchell, A.M., 1959, Elements of Optical Mineralogy,
Pts.II and III, John Wiley and Sons, Inc., New York.